

**Woods Hole  
Oceanographic  
Institution**



---

**Monthly Atmospheric and Oceanographic Surface Fields  
for the Western North Atlantic:  
December, 1986 – April, 1989**

by

Michael J. Caruso, Sandipa Singh, Kathryn A. Kelly and Bo Qiu

April 1995

**Technical Report**

Funding was provided by the National Oceanic and Atmospheric Administration under Contract No. NA16RC0468-01 and by the National Aeronautic Space Administration under Contract No. NAGW-1666.

• Approved for public release; distribution unlimited.

---

WHOI-95-05

Monthly Atmospheric and Oceanographic Surface Fields  
for the Western North Atlantic:  
December, 1986 - April, 1989

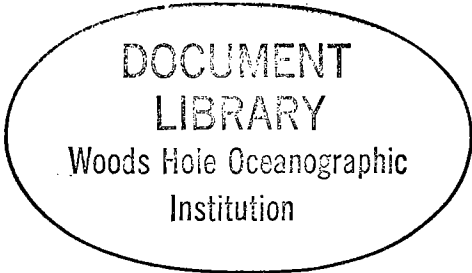
by

Michael J. Caruso, Sandipa Singh, Kathryn A. Kelly and Bo Qiu

Woods Hole Oceanographic Institution  
Woods Hole, Massachusetts 02543

April 1995

Technical Report



Funding was provided by the National Oceanic and Atmospheric Administration under Contract No. NA16RC0468-01 and by the National Aeronautic Space Administration under Contract No. NAGW-1666.

Reproduction in whole or in part is permitted for any purpose of the United States Government. This report should be cited as Woods Hole Oceanog. Inst. Tech. Rept., WHOI-95-05.

Approved for public release; distribution unlimited.

Approved for Distribution:

A handwritten signature in cursive script, appearing to read "Philip L. Richardson".

Philip L. Richardson, Chair  
Department of Physical Oceanography





# Contents

<b>1 Introduction</b>	<b>1</b>
<b>2 Atmospheric Fields</b>	<b>2</b>
<b>3 Oceanographic Fields</b>	<b>3</b>
<b>4 Comparison of ECMWF and Model Net Surface Heat Flux</b>	<b>4</b>
<b>Appendix: Monthly maps</b>	<b>9</b>



# 1 Introduction

Atmospheric and oceanographic fields for the western North Atlantic Ocean from various sources were assembled to study the upper ocean heat budget in the vicinity of the Gulf Stream. Atmospheric fields include the surface heat fluxes and 1000 mb winds from the European Centre for Medium-range Weather Forecasting (ECMWF). Oceanographic fields included the sea surface height (SSH) from the Geosat radar altimeter and sea surface temperature (SST) from the AVHRR radiometer. The fields used in the heat budget analysis were averages over two-week periods, at intervals of one week. The same raw data set was used for the fields shown here, but the averages were computed over a month. All of the fields were interpolated to the model grid, which was 1/2-degree resolution in latitude by 1 degree in longitude.

Geostrophic velocities, derived from the SSH fields, and SST were assimilated into an oceanic mixed layer model forced by the wind stress to obtain estimates of the net surface heat flux as the residual of the upper ocean heat budget. The mixed layer model was forced by wind stress computed from the ECMWF winds. Assimilation was done using a Kalman filter on both the temperature tendency and the temperature of the mixed layer, as described by Kelly and Qiu (1995a). The error in temperature tendency was used to derive a new surface heat flux estimate. The agreement between the time series of spatially averaged surface flux and that obtained from the ECMWF atmospheric model was surprisingly good. The temporally averaged surface flux estimates from the mixed layer model were in good agreement with the Bunker climatological values, except in February and March, when the model mixed layer shoaled more rapidly than expected from climatology.

The heat budget of the mixed layer was analyzed to determine the importance of temperature advection relative to eddy diffusion and vertical entrainment, as de-

scribed by Kelly and Qiu (1995b).

The atmospheric fields are described in section 2 and the oceanographic fields are described in section 3. Section 4 contains a comparison of the heat fluxes and the monthly mean fields are presented in the appendix.

## 2 Atmospheric Fields

The mixed layer model was forced by wind stress and the surface heat flux. The surface wind data used to calculate the wind stress fields are the twice-daily 1000 mb wind vectors from ECMWF, with horizontal resolution of  $2.5^\circ \times 2.5^\circ$ . Wind vectors were converted to surface wind stress using the bulk aerodynamic formulae proposed by Trenberth et al. (1990), then averaged temporally and finally interpolated to the model grid.

The fluxes were available by component, short wave solar radiation, latent heat flux, sensible heat flux and outgoing longwave radiation, as cumulative values over two six-hour periods per day. To estimate the daily-averaged short wave solar radiation from the available values, we first estimated the clear-sky radiation values and inferred the (average) cloud cover from the 6-hour-accumulated data from ECMWF, as described in Qiu and Kelly (1993). The short wave radiation was the only ECMWF flux that was actually used in the mixed layer model; it was needed to estimate the vertical entrainment. The modified short wave radiation was combined with the other fluxes to obtain the net surface heat flux. The ECMWF estimates of net surface heat flux were used to test and tune the prognostic model, and for comparison with the surface flux estimates.

### 3 Oceanographic Fields

The sea surface height (SSH) data were derived from the Geosat altimeter, which had a repeat cycle of 17 days, using the new orbits and water vapor corrections (GEM-T2; Cheney et al., 1991). To eliminate the geoid, which dominates the altimetric height profiles, we computed and subtracted the mean altimetric sea surface from collinear profiles. Subtracting the temporal mean sea surface also removes the temporal mean topography due to ocean currents. Mean sea surface topography profiles relative to the geoid were then synthesized using the method of Kelly and Gille (1990), as modified by Qiu et al. (1991), and added back to the residual heights to obtain total SSH profiles. In this method, the Gulf Stream is modeled using a Gaussian velocity profile; the large SSH anomalies created by a narrow jet meandering far from its mean position are exploited to estimate the center position and magnitude of the Gaussian. The single jet model was revised to include recirculation as in Qiu (1992). Details of the computation of the mean SSH are contained in Qiu (1994), along with a comparison of the synthesized mean with the mean dynamic height from climatological data. The absolute surface height data were objectively mapped to the model grid.

To obtain the SST maps, we used AVHRR data and the optimal average method of Chelton and Schlax (1991), which is an extension of the usual optimal estimate to temporal averages of the data. The AVHRR data were weekly averages, which were initially processed by National Oceanic and Atmospheric Administration (NOAA) using the multichannel SST (MCSST) algorithm and then interpolated to an 18 km by 18 km grid at the Rosenstiel School of Marine and Atmospheric Science (RSMAS). The SST data were temporally averaged and then interpolated to the model grid. The optimal average method gives an error map, which was used in the data assimilation



of Kelly and Qiu (1995a), but it is not shown here to save space. The spatially averaged SST estimated errors (figure 1) show periods of extensive cloud cover (e.g., December 1987–January 1988), which gave errors that were nearly a factor of two larger than errors for times with clear skies (September 1988 and March 1989).

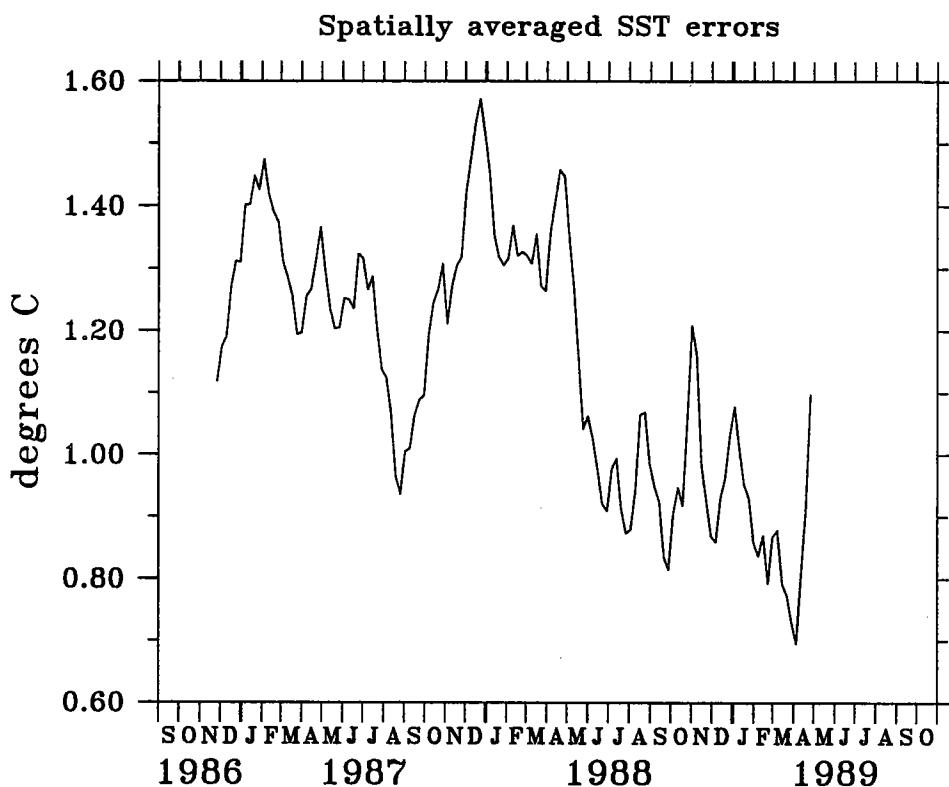


Figure 1: Spatially averaged SST errors from the optimal estimates. Weekly averages of AVHRR data were optimally averaged with an averaging interval of two weeks to reduce random errors and those from cloud cover gaps. The error estimates varied by nearly a factor of two, both temporally and spatially.

#### 4 Comparison of ECMWF and Model Net Surface Heat Flux

Two estimates of the net surface heat flux are shown in this report: the ECMWF model estimates and the estimates derived from assimilating winds and satellite data into the mixed layer model. Spatially averaged values of these two quantities agree

rather well (figure 2, after Kelly and Qiu, 1995b); however, the details of these fields differ substantially. In part, this is due to the way in which the heat fluxes were estimated, as a linear combination of empirical modes derived from the weekly differences in ocean temperature (Kelly and Qiu, 1995a). In general, the mixed layer model fluxes tend to be more positive (atmosphere heating the ocean) than those from ECMWF. Also, the mixed layer model fluxes become positive earlier in the year (March, as opposed to April–May), relative to the ECMWF fluxes. This latter problem is associated with a tendency for the mixed layer depth to shoal too early in the year, relative to climatology.

Near the end of the time series (December 1988–March 1989), the two heat flux estimates differ substantially in spatial structure. During this period, winds are consistently strong, particularly the eastward winds in the northeast part of the region, where the temperature gradients from the Gulf Stream are also anomalously strong. This combination results in an unusually large cooling term (0.5 degree per day) from advection by the Ekman transport. The ocean temperature does not show a correspondingly large drop; thus, a large positive heat flux is inferred as the residual of the upper ocean heat balance near the Grand Banks. Although the magnitude of this positive flux clearly appears too large, particularly in the winter, the mean annual net surface flux from the Bunker climatology (Isemer and Hasse, 1987) is positive near the Grand Banks. In contrast, the ECMWF annual net flux is negative in this region.

That Ekman transport is responsible for this excessive cooling can be seen by examining the maps from December 1987, when winds were again strong, but the net flux estimate does not become positive. This is undoubtedly due to the weak ocean temperature gradients during that period, which did not produce the strong advection term. The temperature gradients were not the result of a weak Gulf Stream, but

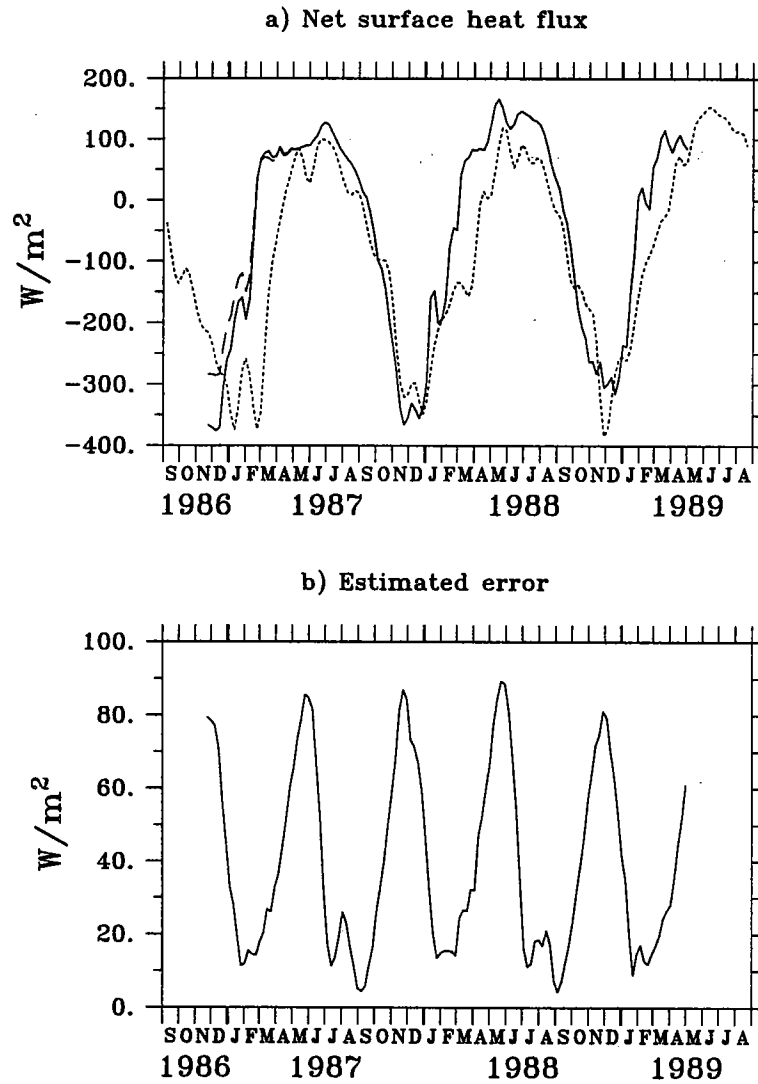


Figure 2: Net surface flux estimates from the mixed layer model and from ECMWF. (a) Spatially averaged estimates of the net surface flux from the Kalman filter (solid line), ECMWF (dotted line) and climatological (dashed line) and (b) an error estimate for the Kalman filter estimate. The larger (more negative) fluxes in the fall of 1986 resulted from initializing the model with the November 1987 mixed layer depth, rather than with a climatological estimate.

were due to the lack of available SST data, which forced the ocean temperature estimate to resemble the climatological mean. In addition, large values of the estimated temperature error (Figure 1) caused the Kalman filter to damp the adjustment to the flux estimate, resulting in a weaker response. These cooling episodes, as well as the tendency for the heat flux estimates to be too positive on average, suggest that the wind stress may be too large. Mestas-Nuñez et al. (1994) have suggested that using the 1000 mb winds, in place of 10-m winds, may produce wind stresses which are as much as 50% too large. A simple reduction in magnitude of the wind stress was attempted, but it did not eliminate the overall positive bias of the fluxes, and it underestimated the mixed layer depth.

#### *Acknowledgments*

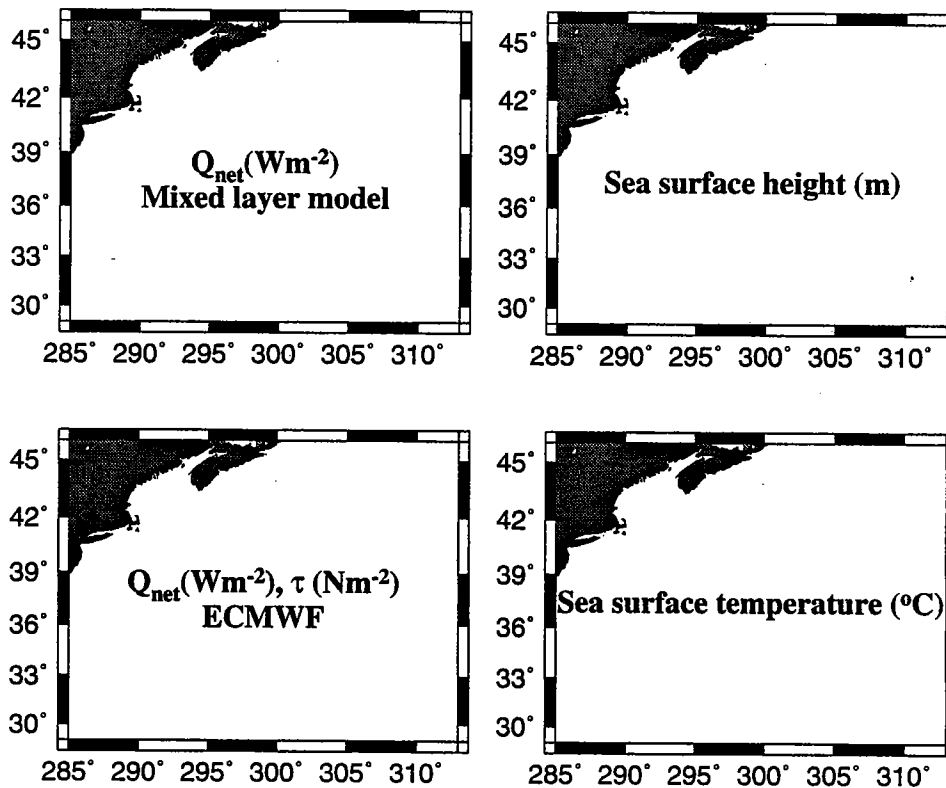
Geosat altimeter data were obtained on CD-ROM from the NOAA National Oceanographic Data Center. AVHRR data were provided by the NASA Physical Oceanography Distributed Active Archive Center (PODAAC) at the Jet Propulsion Laboratory/California Institute of Technology. The wind fields and surface heat flux estimates were derived from ECMWF/WCRP Level III-A data from the Global Atmospheric Data Archive, supplied by the European Centre for Medium-range Weather Forecasting and the National Center for Atmospheric Research. This research was supported by the National Oceanic and Atmospheric Administration through the Atlantic Climate Change Program under contract NA16RC0468-01 and by the National Aeronautics and Space Administration under contract NAGW-1666.

## References

- Chelton, D.B., and M.G. Schlax, 1991. Estimation of time-averaged chlorophyll concentration from irregularly spaced satellite observations, *J. Geophys. Res.*, **96**, 14,669–14,692.
- Cheney, R.E., W.J. Emery, B.J. Haines, and F. Wentz, 1991. Recent improvements in Geosat altimeter data, *EOS Trans. AGU*, **72**, 577.
- Isemer, H.-J., and L. Hasse, 1987. The Bunker Climate Atlas of the North Atlantic Ocean, Vol. 2: Air-sea interactions. Springer-Verlag, 252 pp.
- Kelly, K.A., and S.T. Gille, 1990. Gulf Stream surface transport and statistics at 69 W from the GEOSAT altimeter, *J. Geophys. Res.* **95**, 3149–3161.
- Kelly, K. A., and B. Qiu, 1995a. Heat flux estimates for the North Atlantic, Part I: assimilation of satellite data into a mixed layer model, *J. Phys. Oceanogr.*, in press.
- Kelly, K. A., and B. Qiu, 1995b. Heat flux estimates for the North Atlantic, Part II: the upper ocean heat budget, *J. Phys. Oceanogr.*, in press.
- Mestas-Nuñez, A. M., D. B. Chelton, M. H. Freilich, and J. G. Richman, 1994. An evaluation of ECMWF-based climatological wind stress fields, *J. Phys. Oceanogr.*, **24**, 1532–1549.
- Qiu, B., 1992. Recirculation and seasonal change of the Kuroshio from altimetry observations, *J. Geophys. Res.*, **97**, 17,801–17,811.
- Qiu, B., 1994. Determining the mean Gulf Stream and its recirculations through combining hydrographic and altimetric data, *J. Geophys. Res.*, **99**, 951-962.
- Qiu, B., and K.A. Kelly, 1993. Upper-ocean heat balance in the Kuroshio Extension region, *J. Phys. Oceanogr.*, **23**, 2027–2041.
- Qiu, B., K.A. Kelly and T.M. Joyce, 1991. Mean circulation and variability of the Kuroshio Extension from Geosat altimetry data. *J. Geophys. Res.*, **96**, 18,491–18,507.
- Trenberth, K.E., W.G. Large, and J.G. Olson, 1990. The mean annual cycle in global wind stress, *J. Phys. Oceanogr.*, **20**, 1742–1760.
- Wessel, P. and W.H.F. Smith, 1991. Free software helps map and display data, *EOS Trans. Amer. Geophys. U.*, **72**, 441,445-446.

## Appendix: Monthly maps

Monthly means of heat flux  $Q_{net}$ , wind stress  $\tau$ , sea surface height SSH and sea surface temperature SST are presented. The plots are positioned so that  $Q_{net}$  and  $\tau$  are on the left hand page and SSH and SST are on the right hand page. The plots were generated using the GMT plotting package developed by Wessel and Smith (1991).



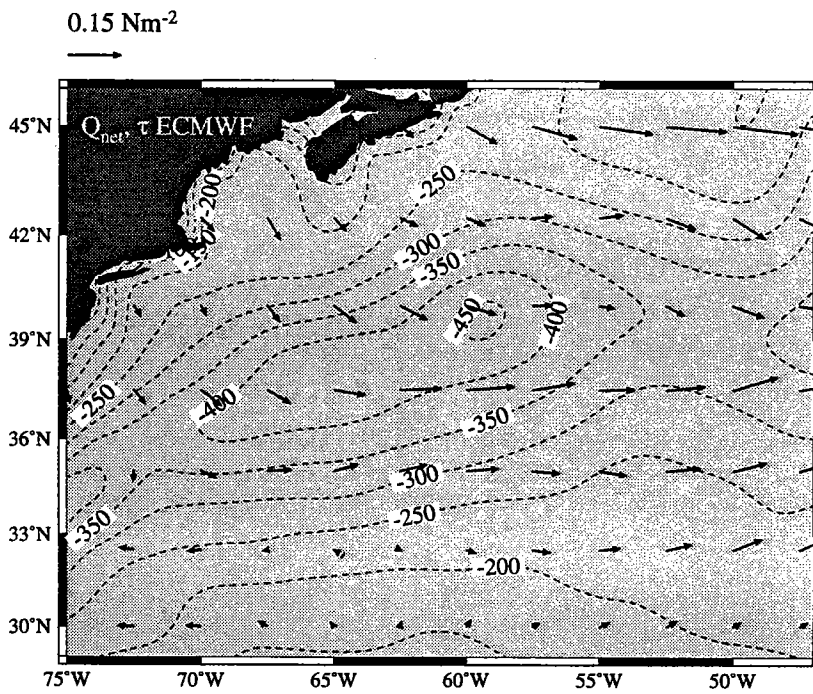
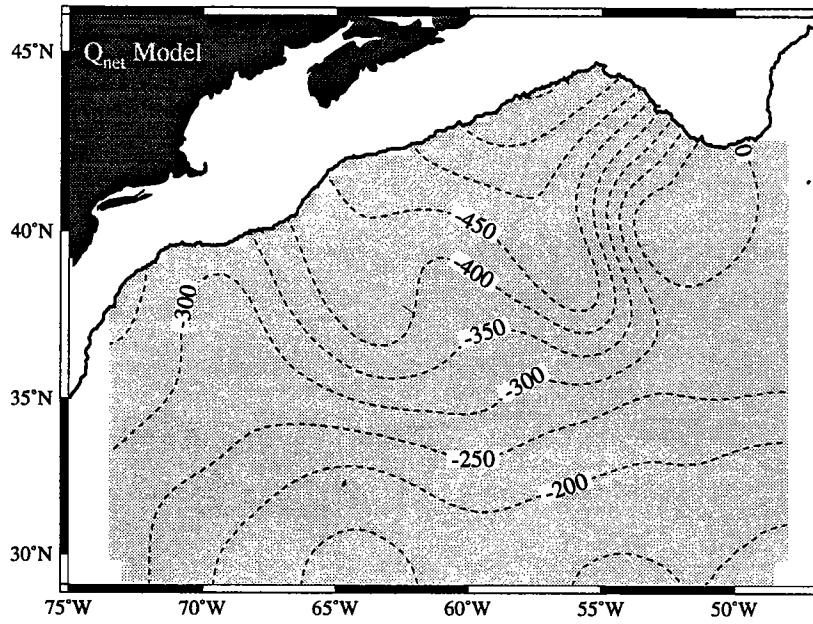


Figure 3: December 1986

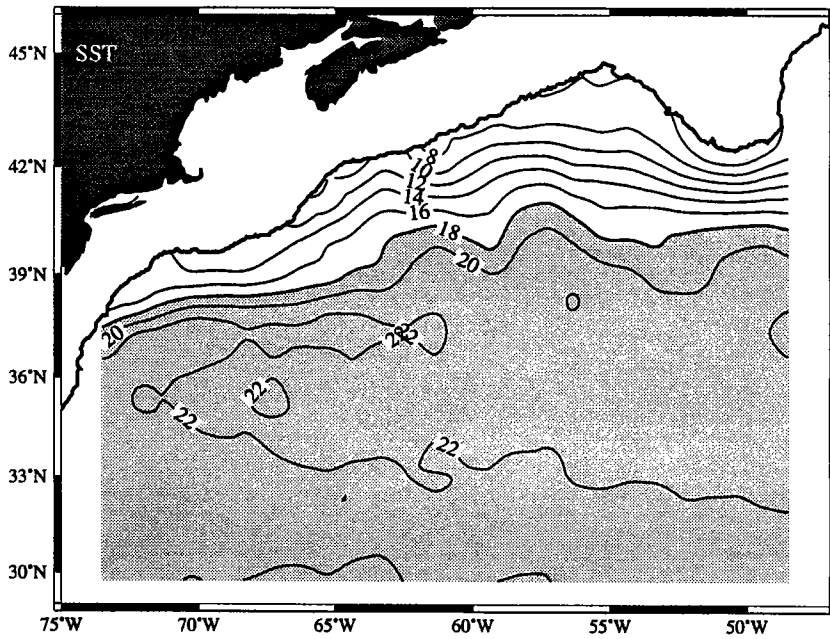
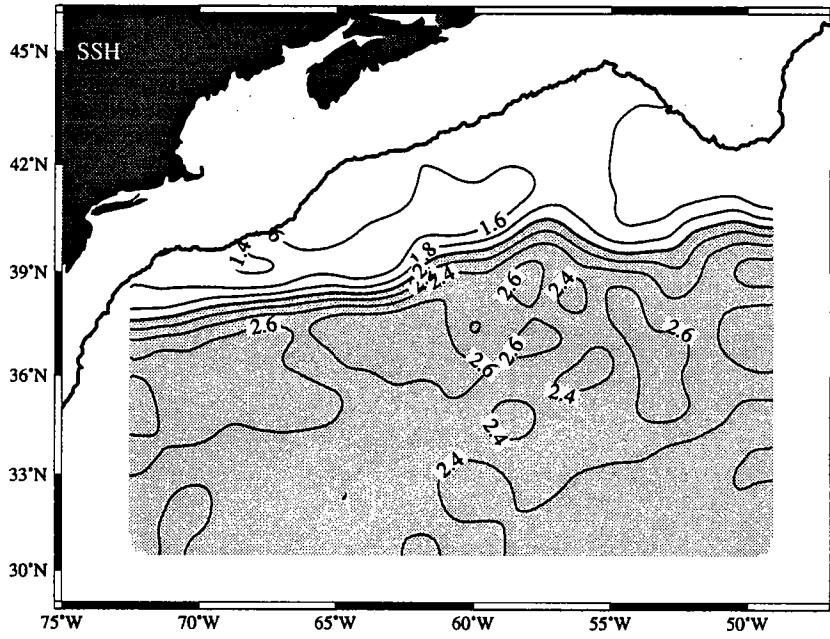


Figure 4: December 1986



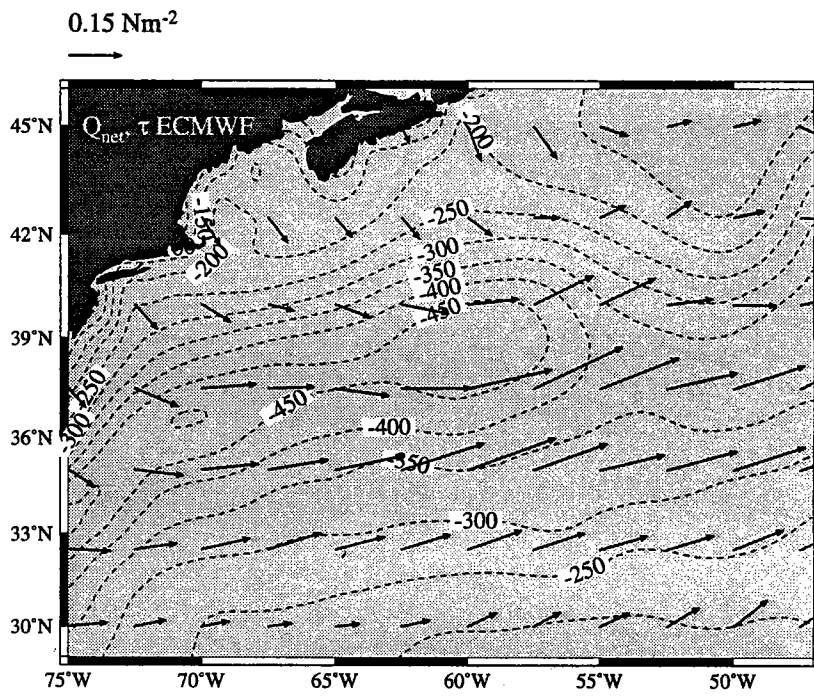
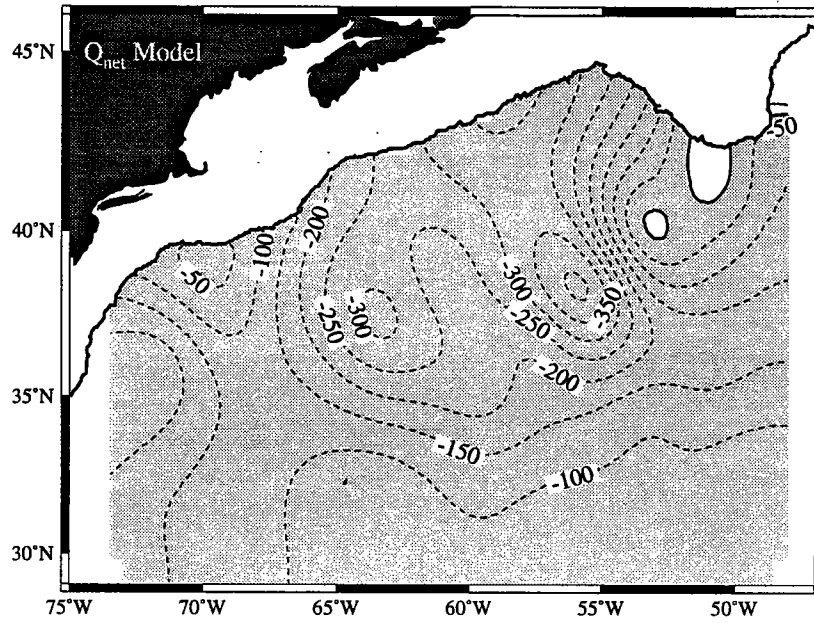


Figure 5: January 1987

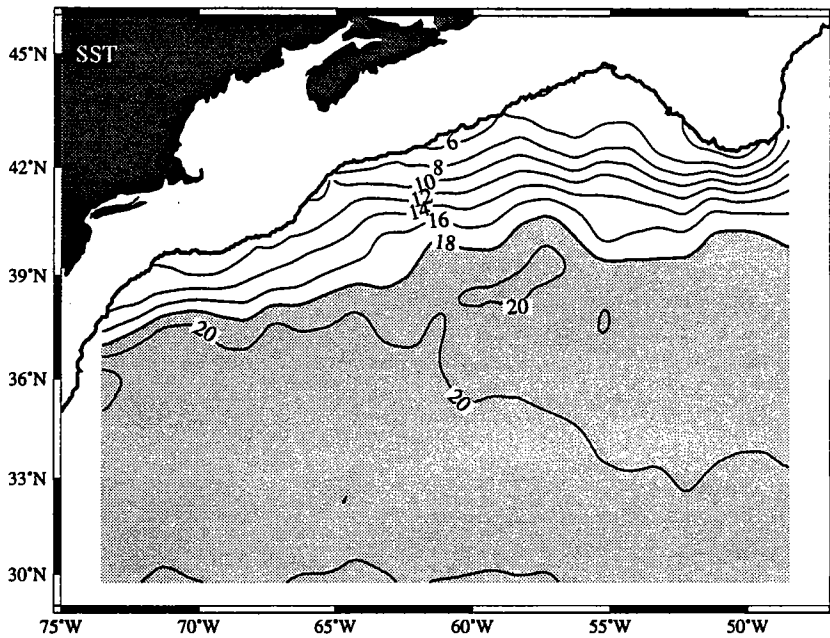
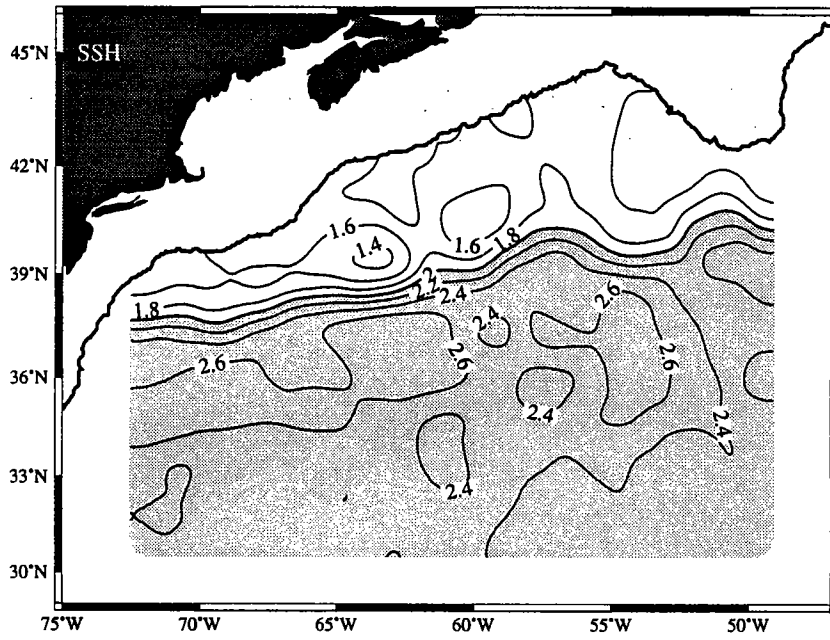


Figure 6: January 1987

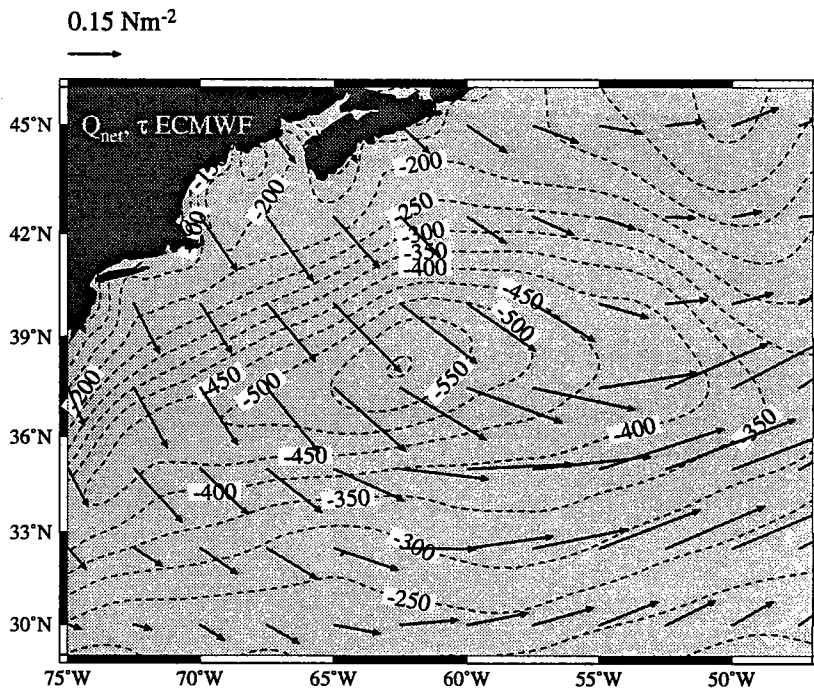
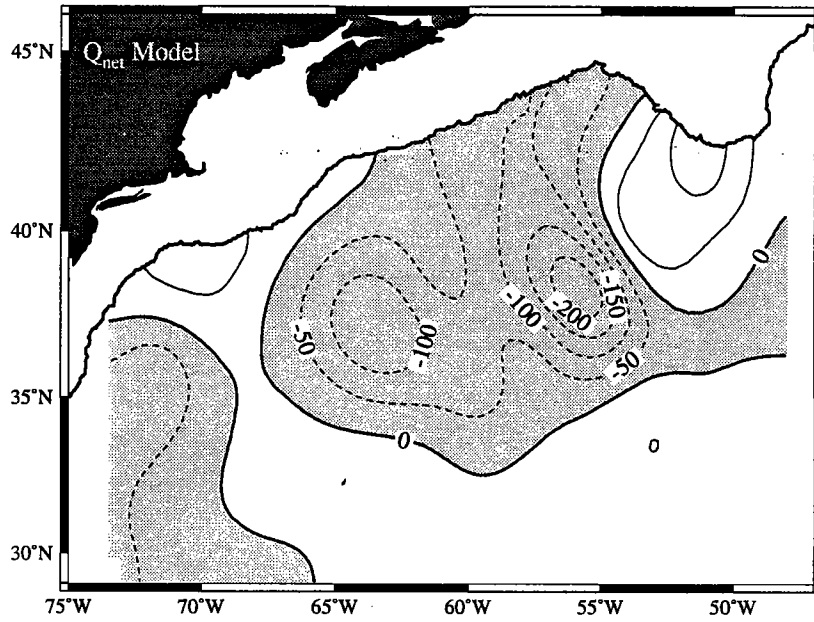


Figure 7: February 1987

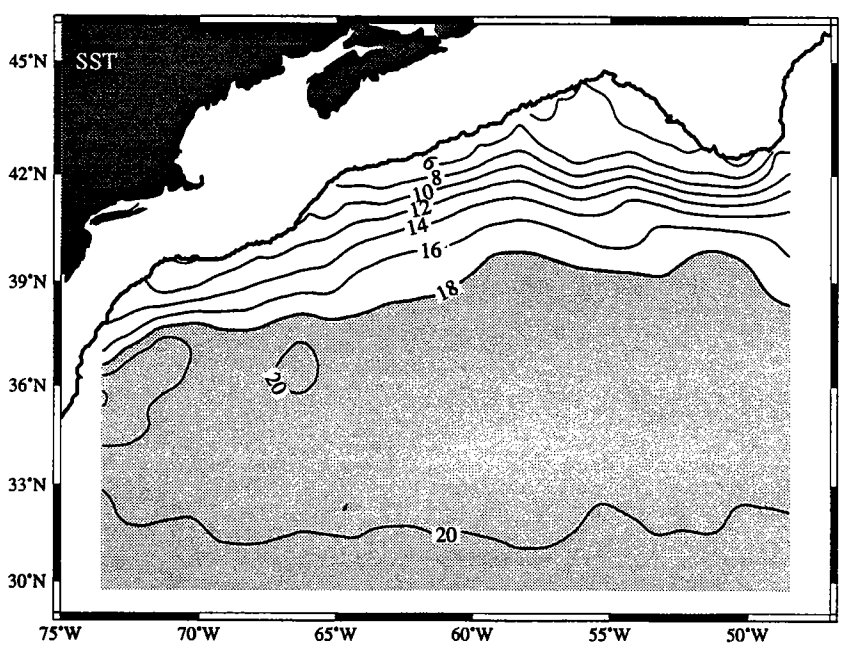
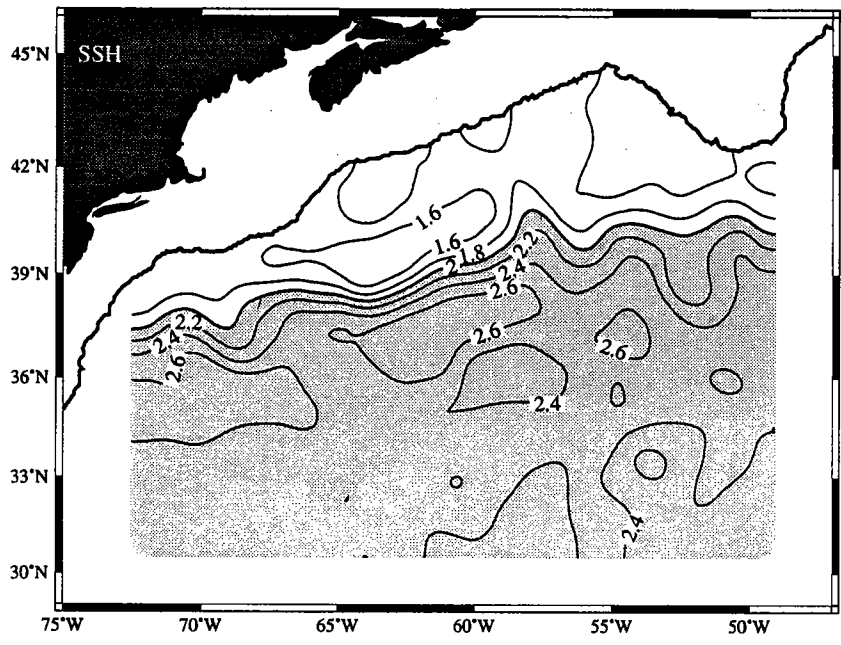


Figure 8: February 1987

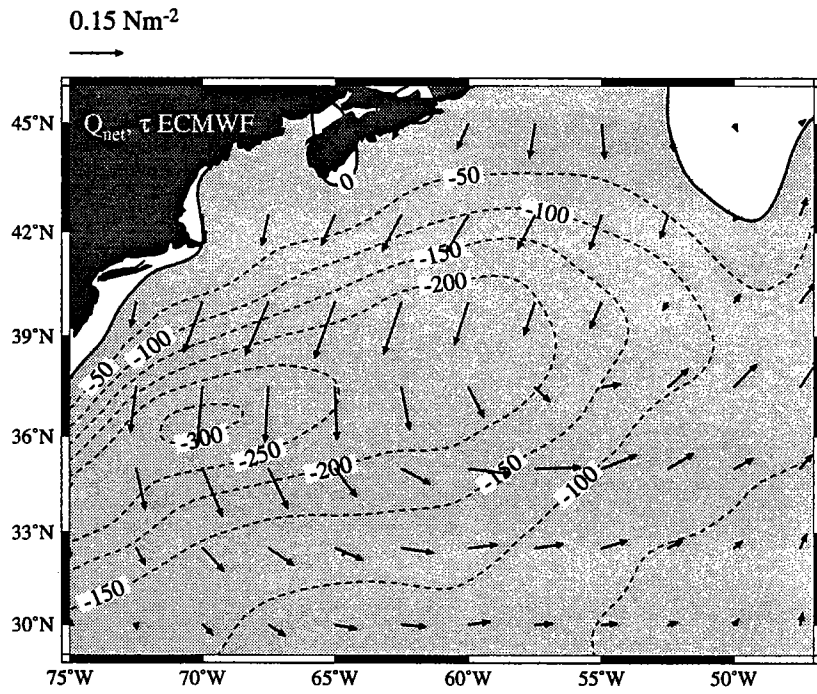
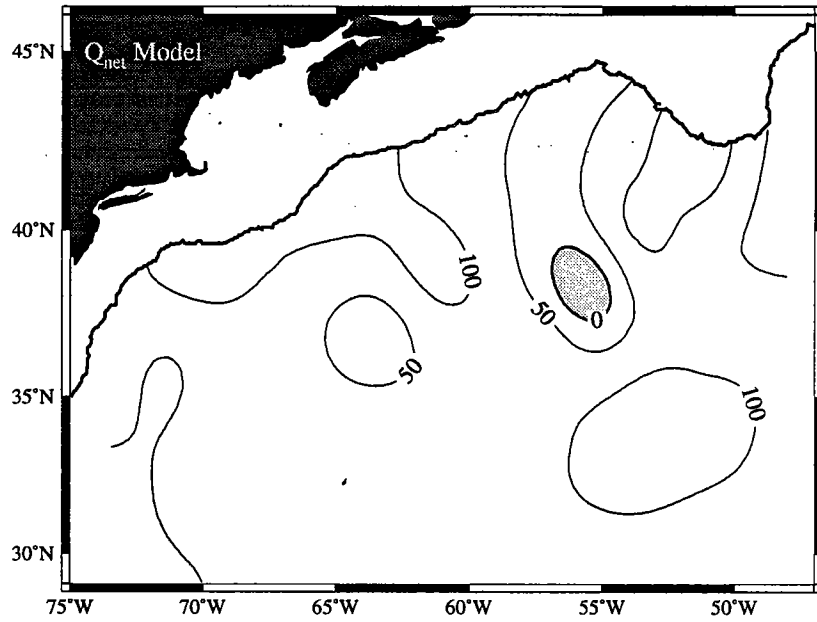


Figure 9: March 1987

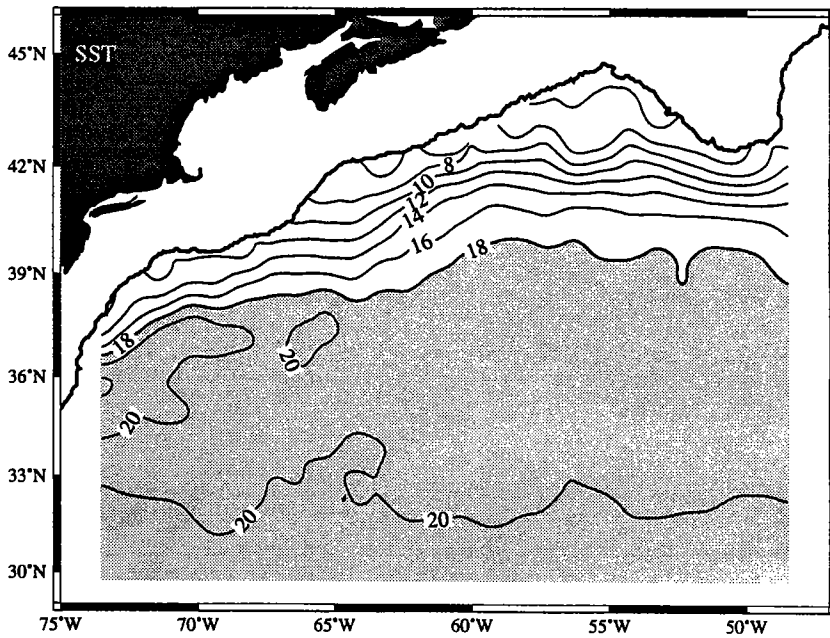
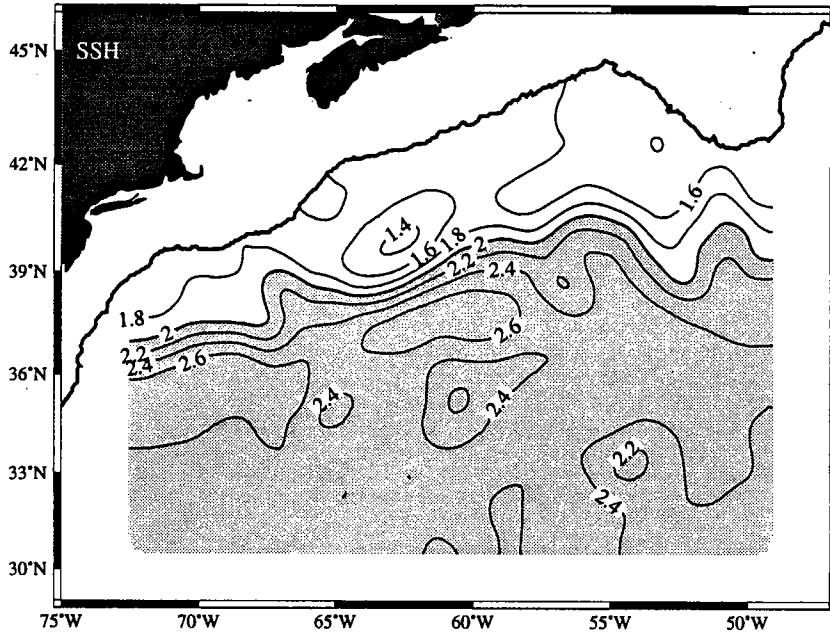


Figure 10: March 1987

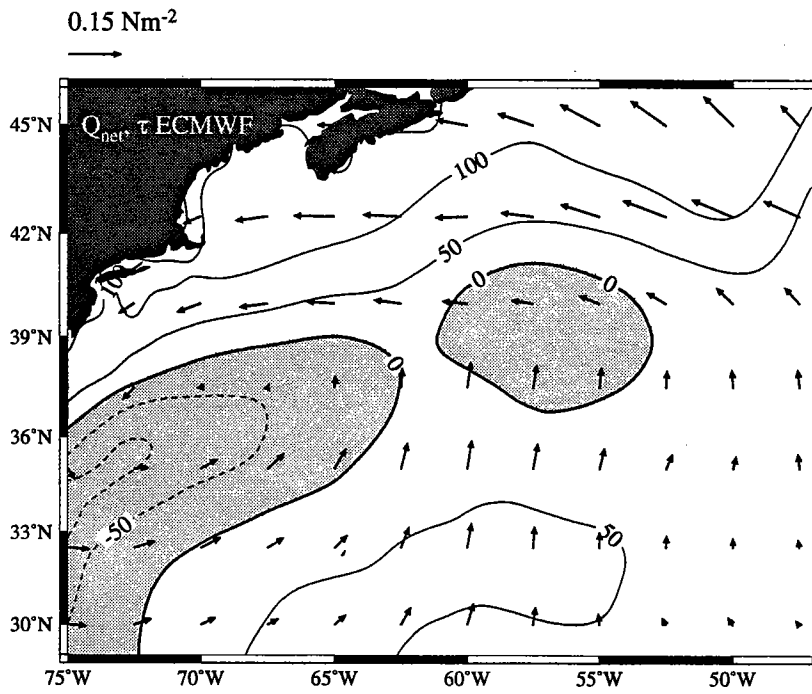
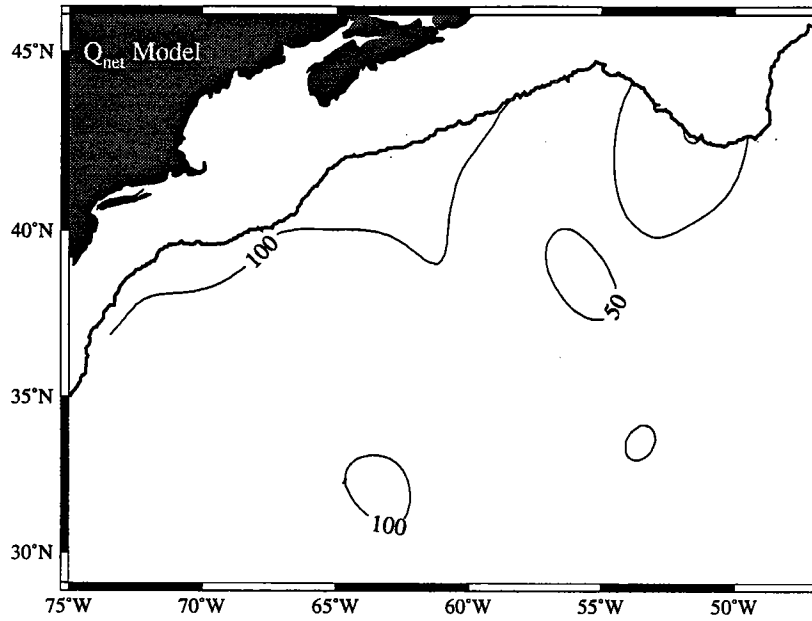


Figure 11: April 1987

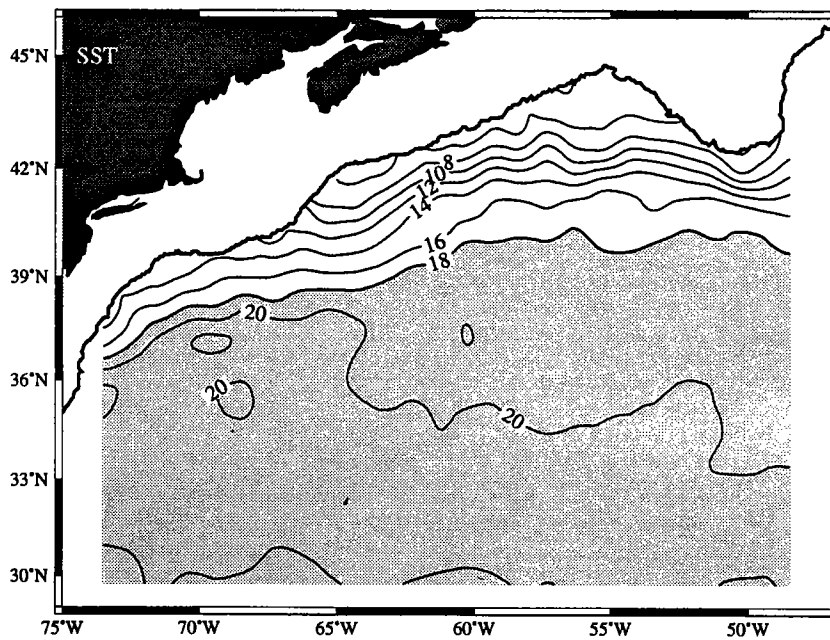
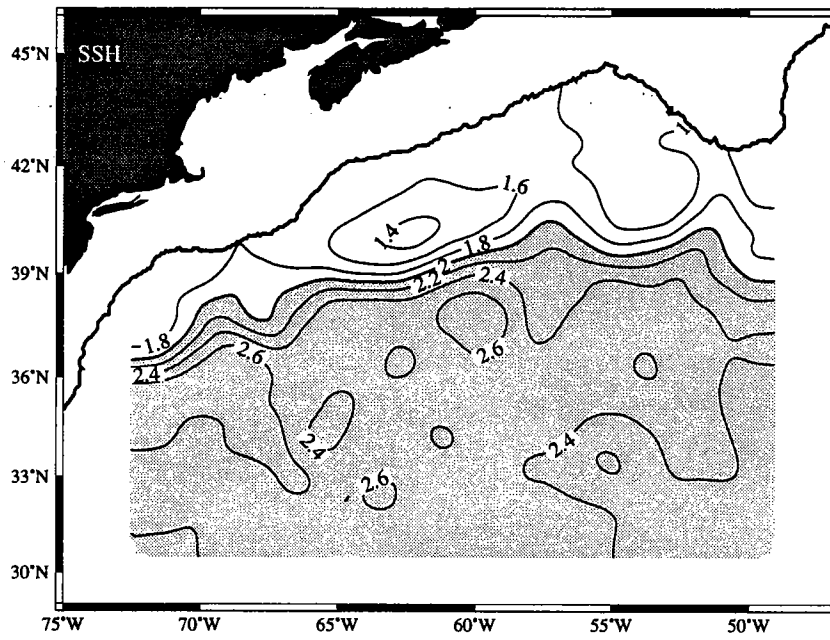


Figure 12: April 1987



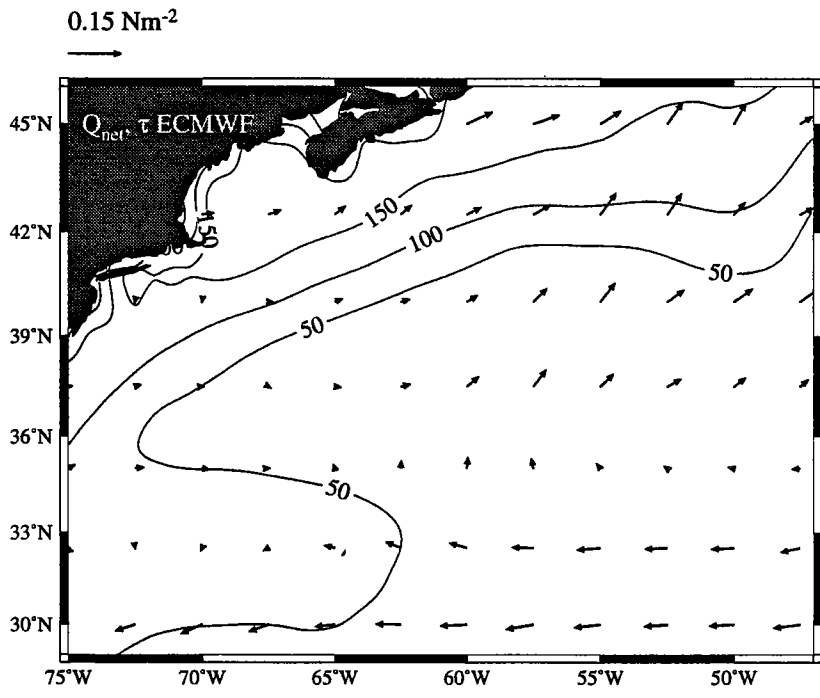
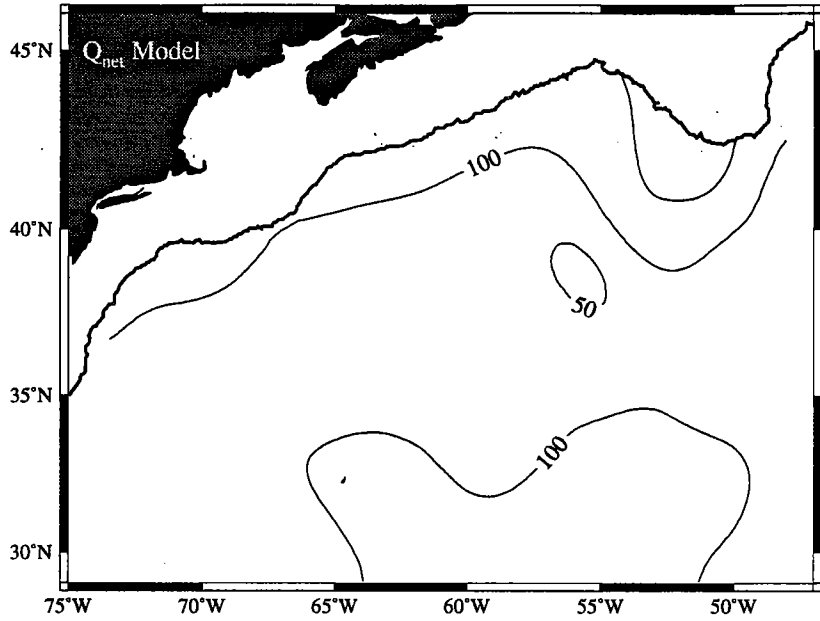


Figure 13: May 1987

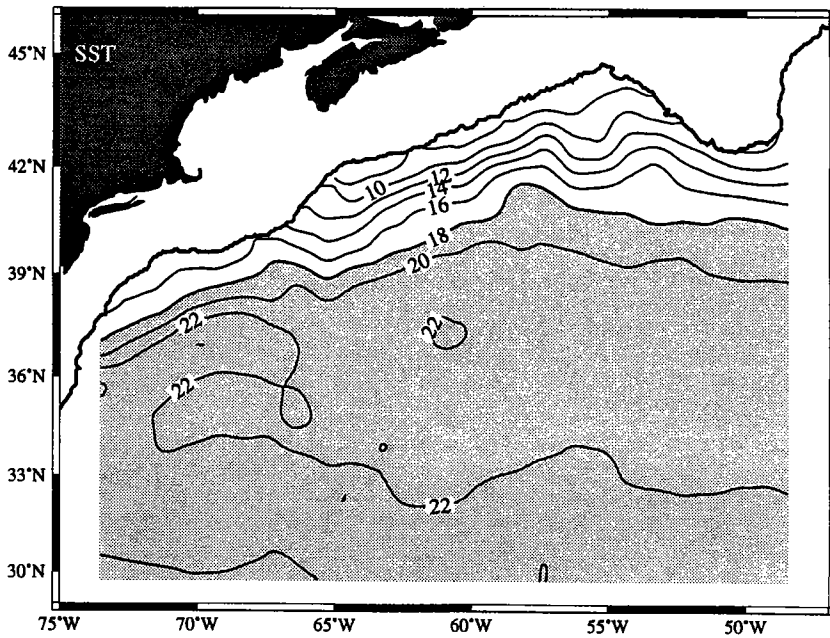
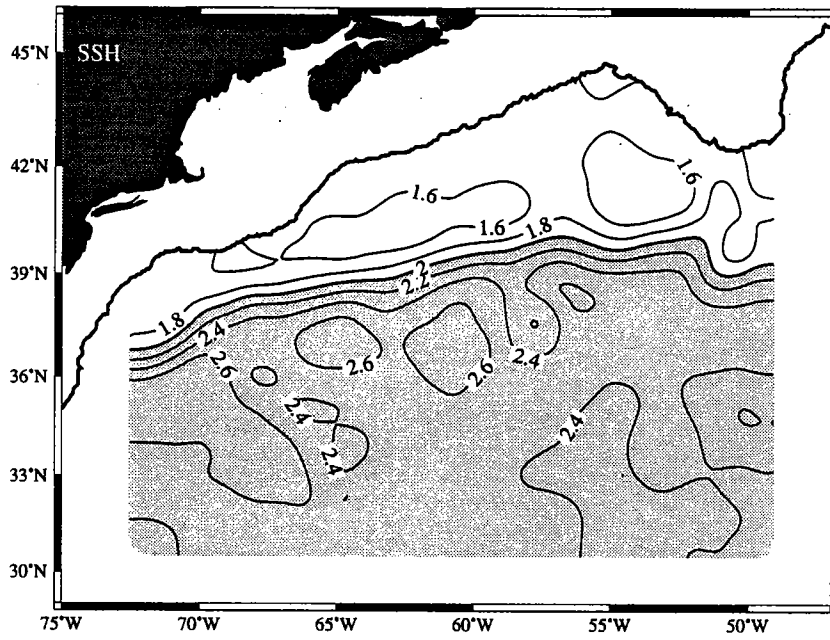


Figure 14: May 1987

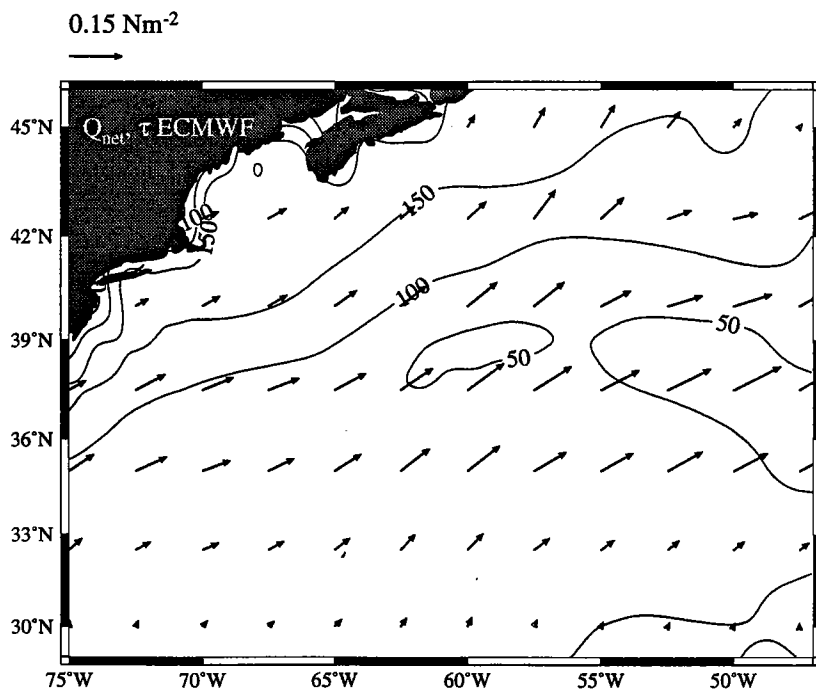
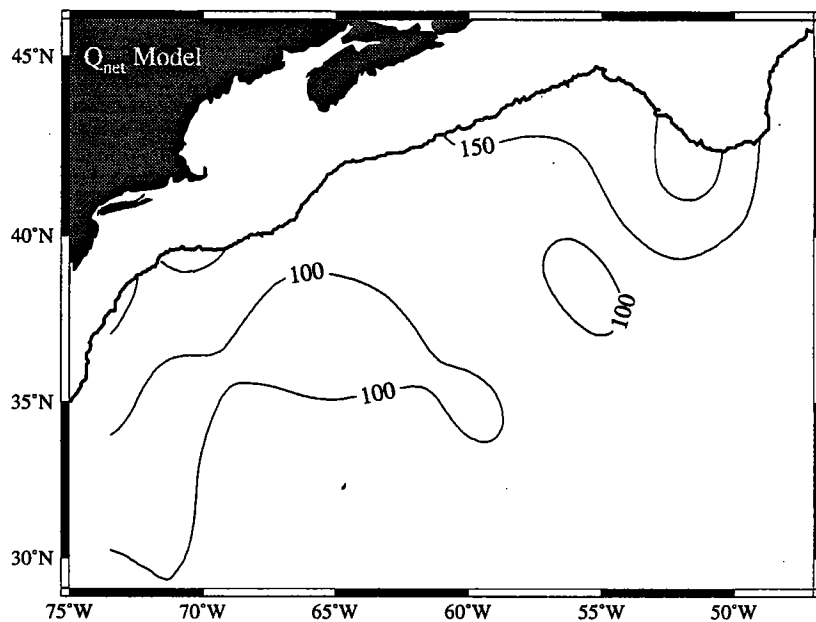


Figure 15: June 1987

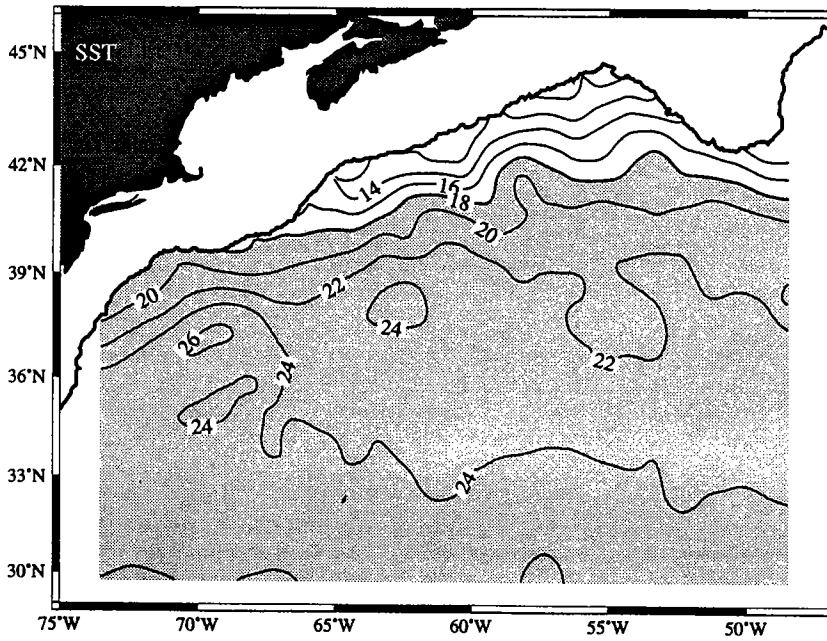
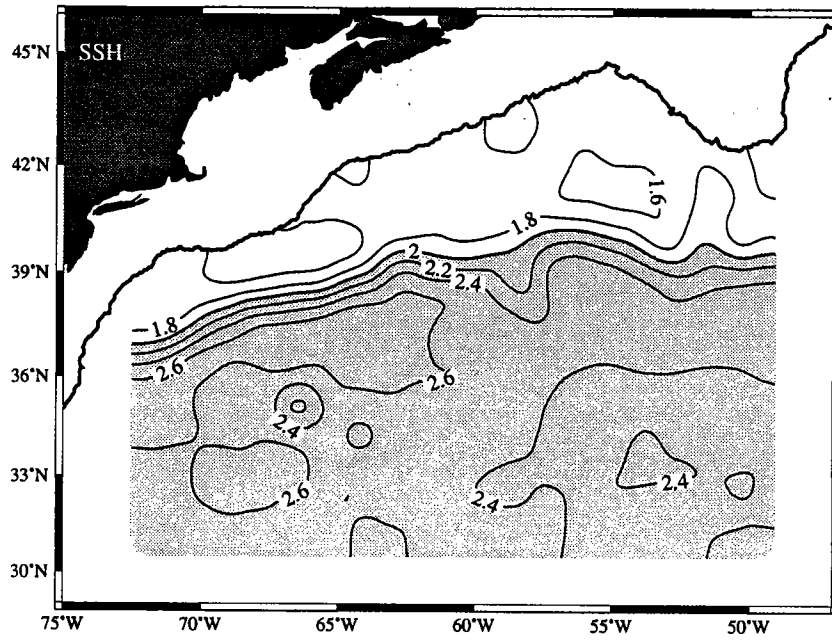


Figure 16: June 1987

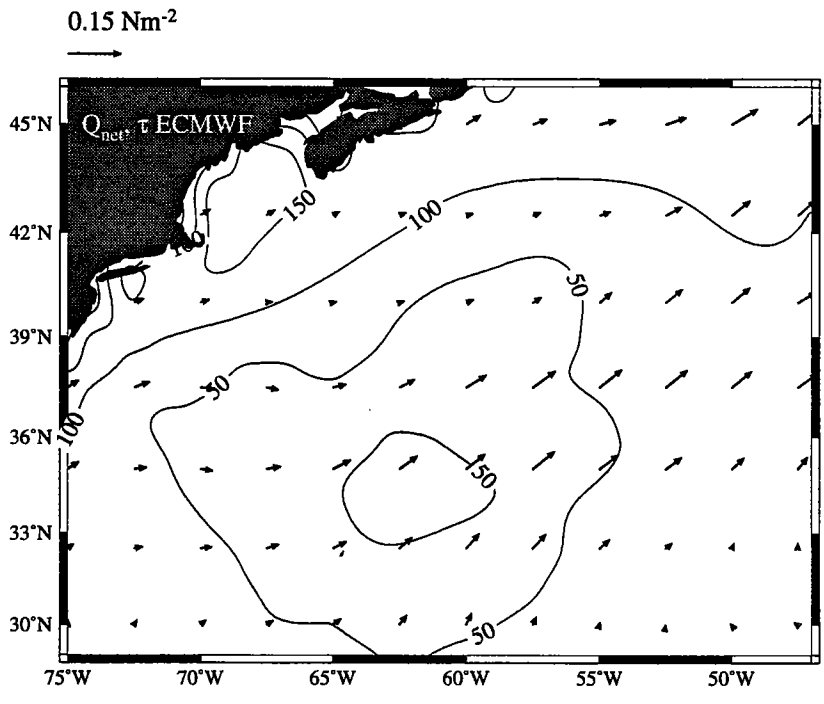
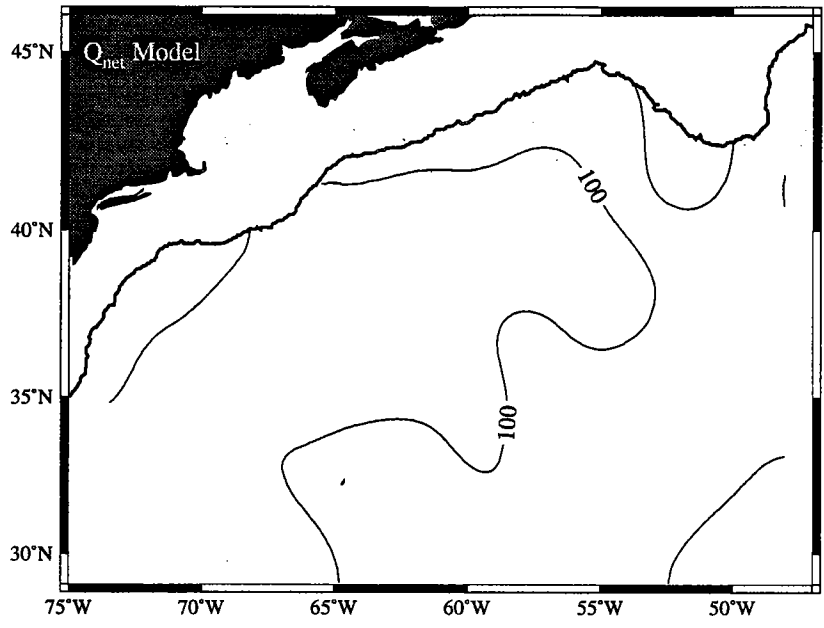


Figure 17: July 1987

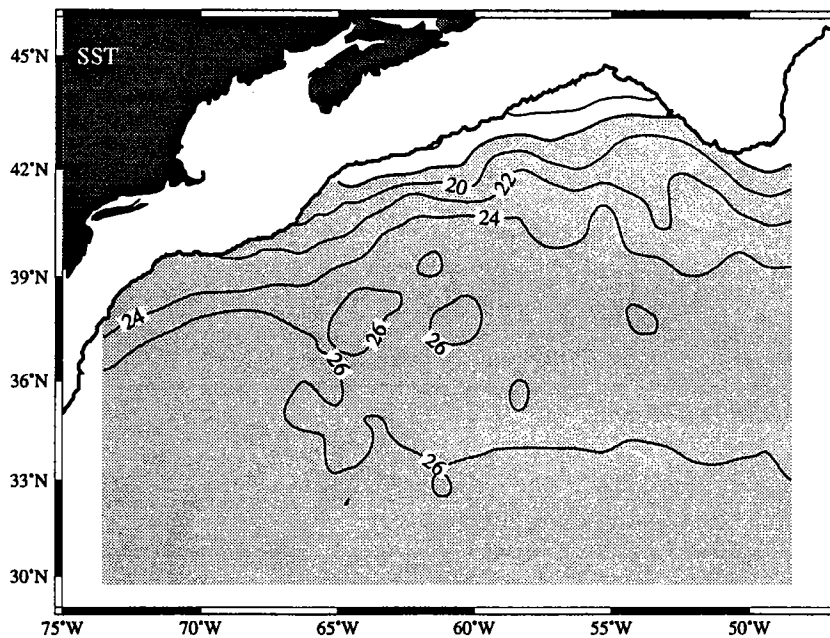
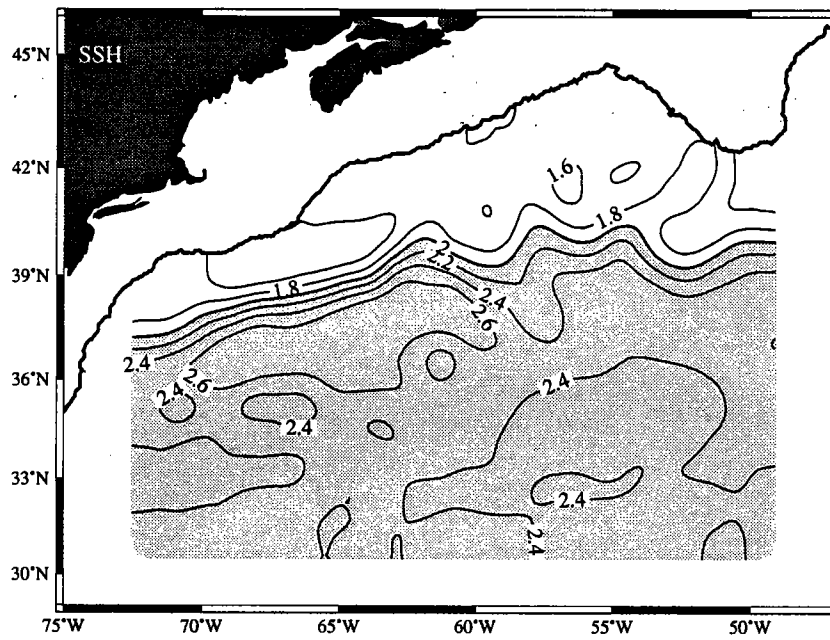


Figure 18: July 1987

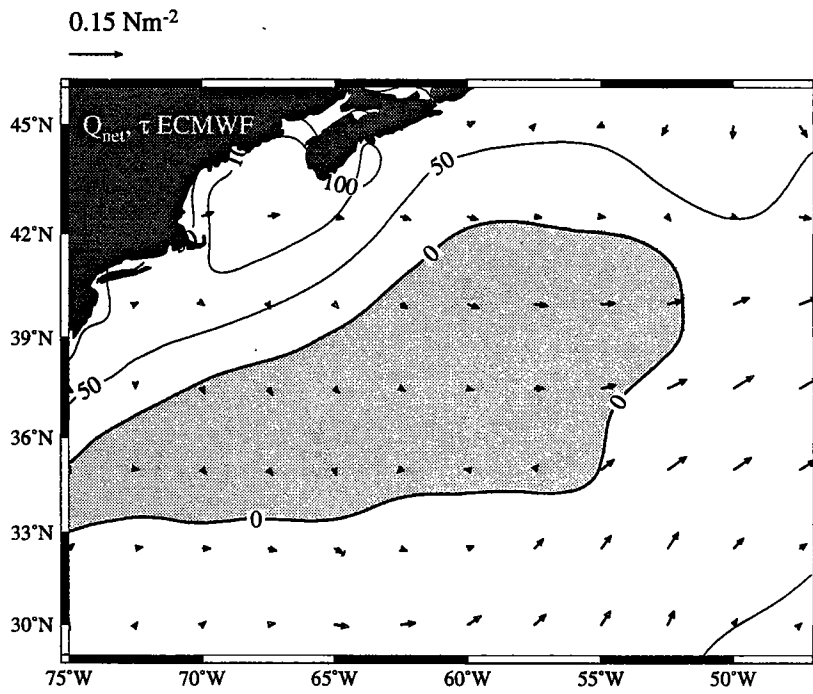
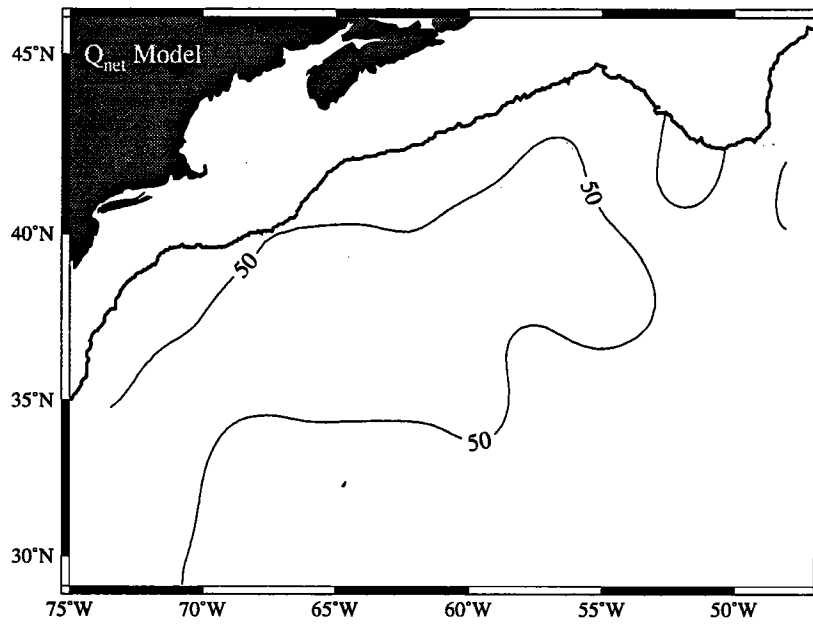


Figure 19: August 1987

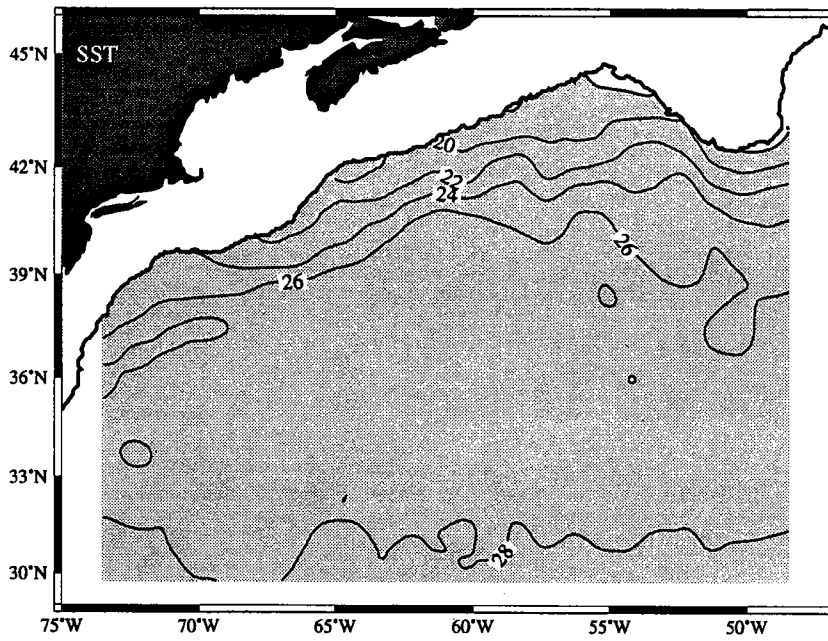
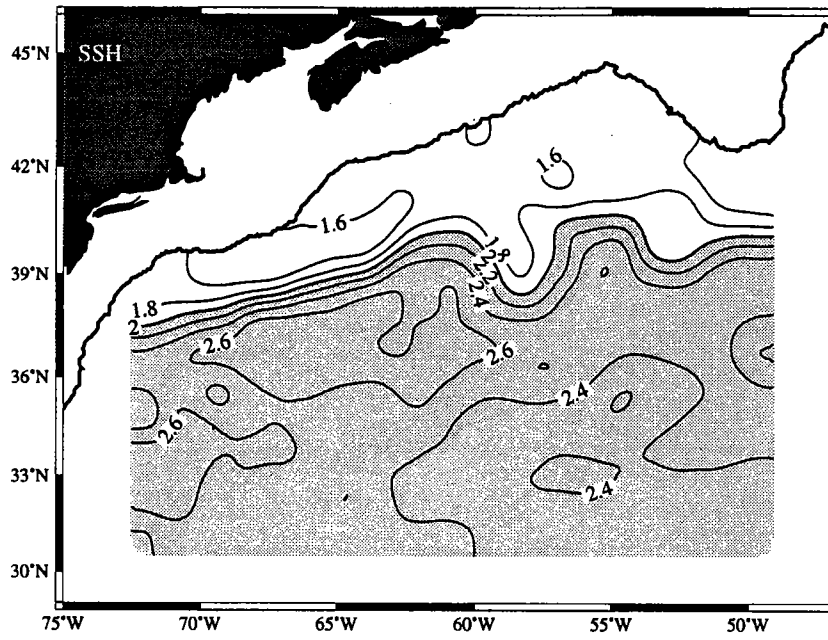


Figure 20: August 1987



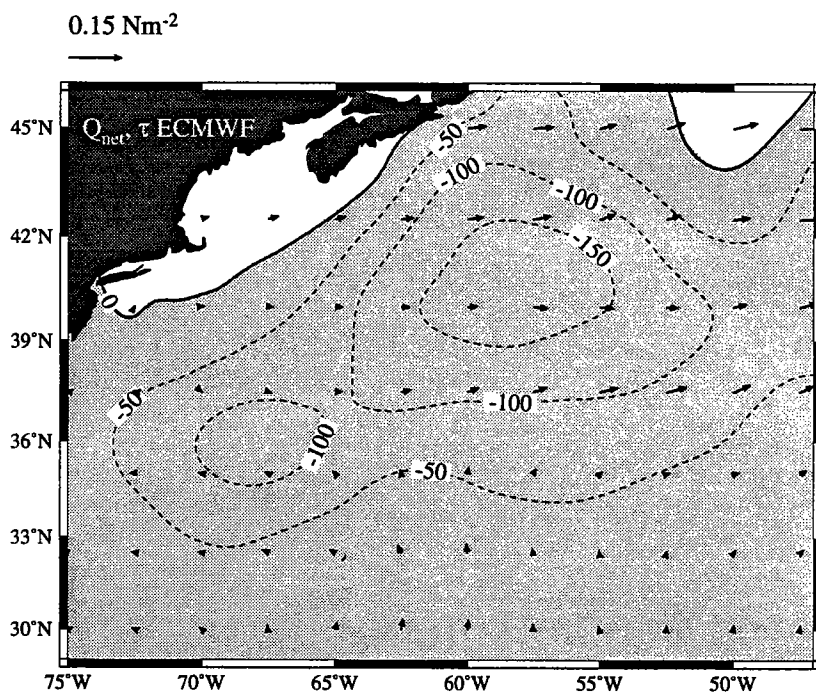
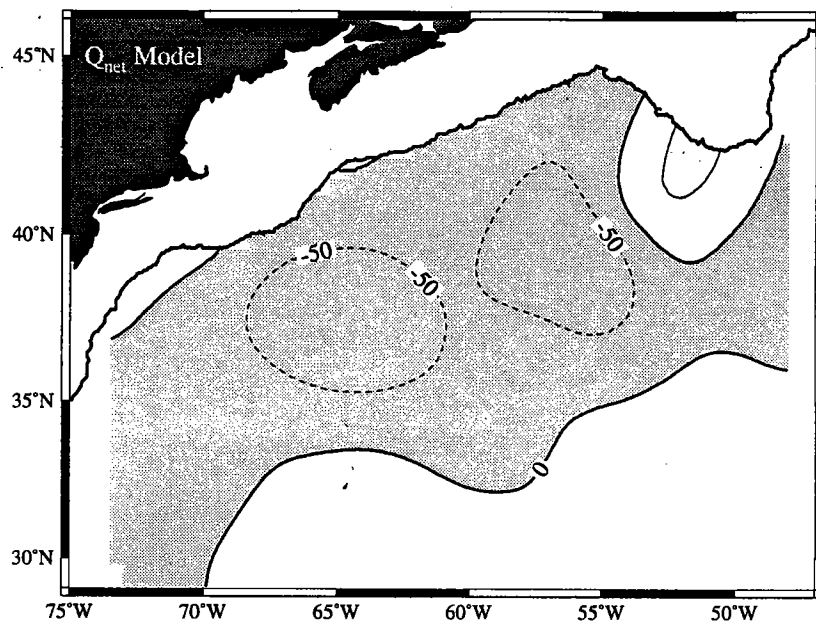


Figure 21: September 1987

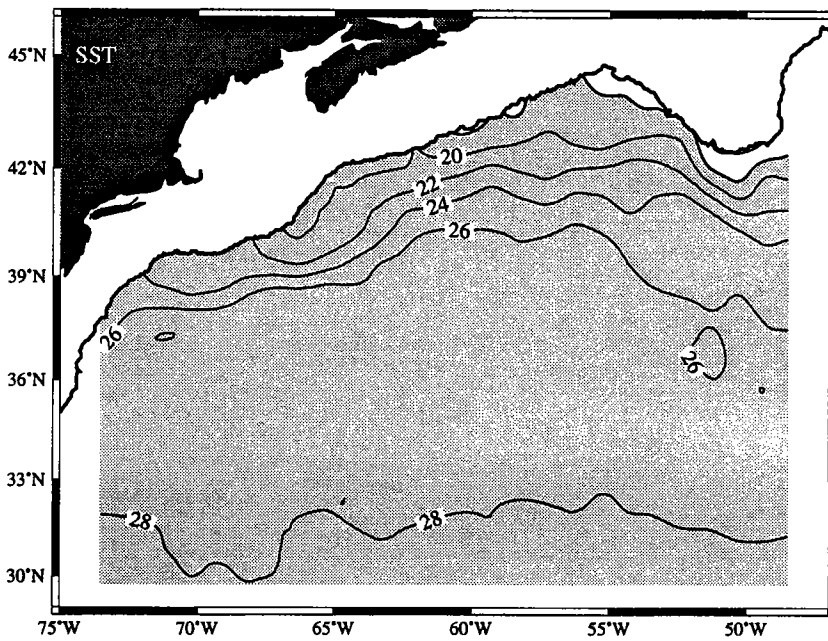
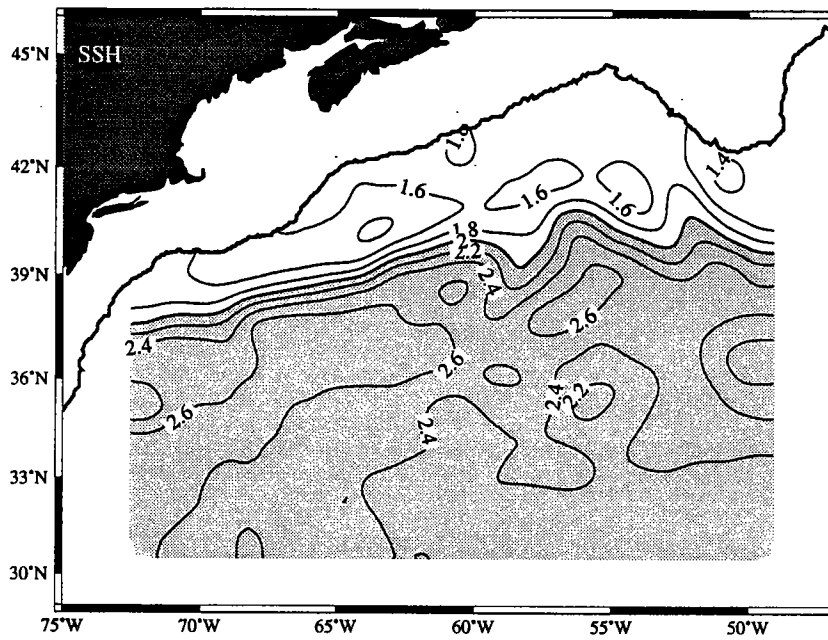


Figure 22: September 1987

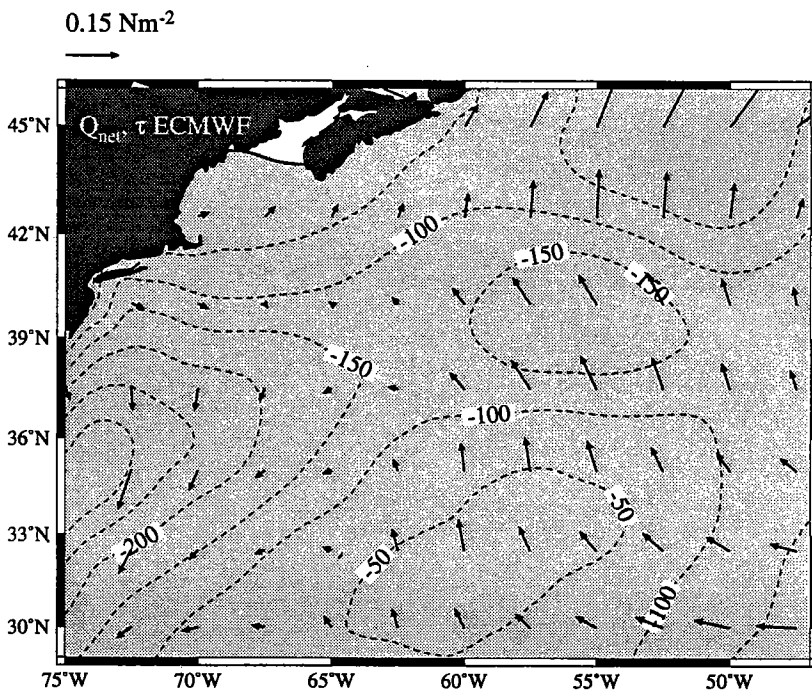
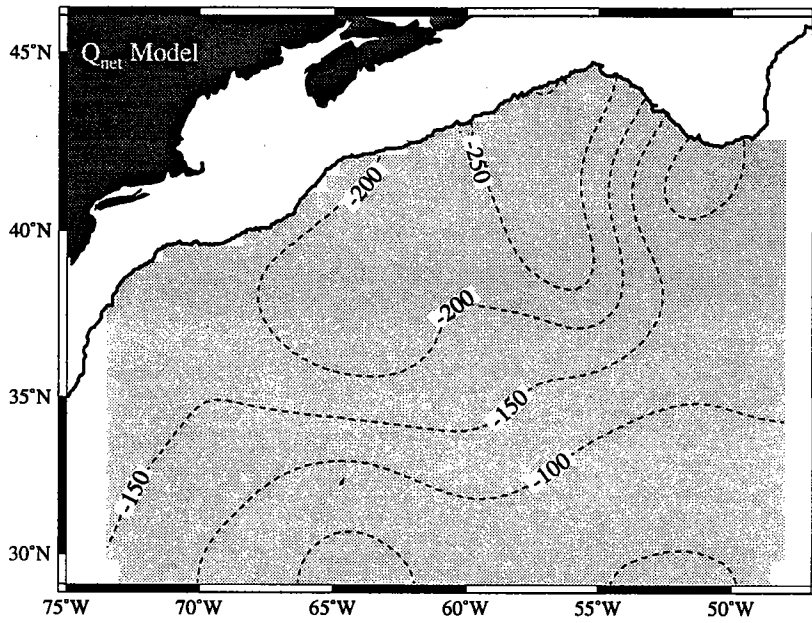


Figure 23: October 1987

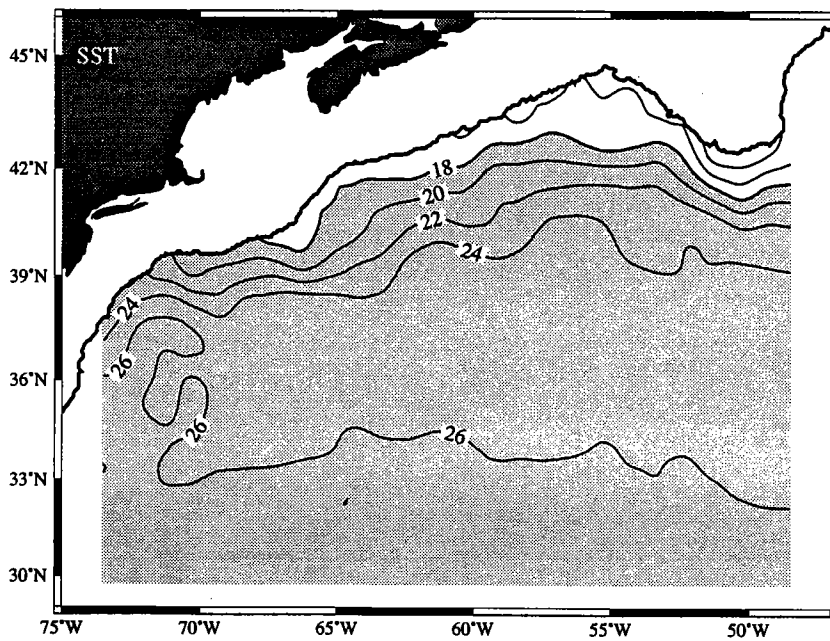
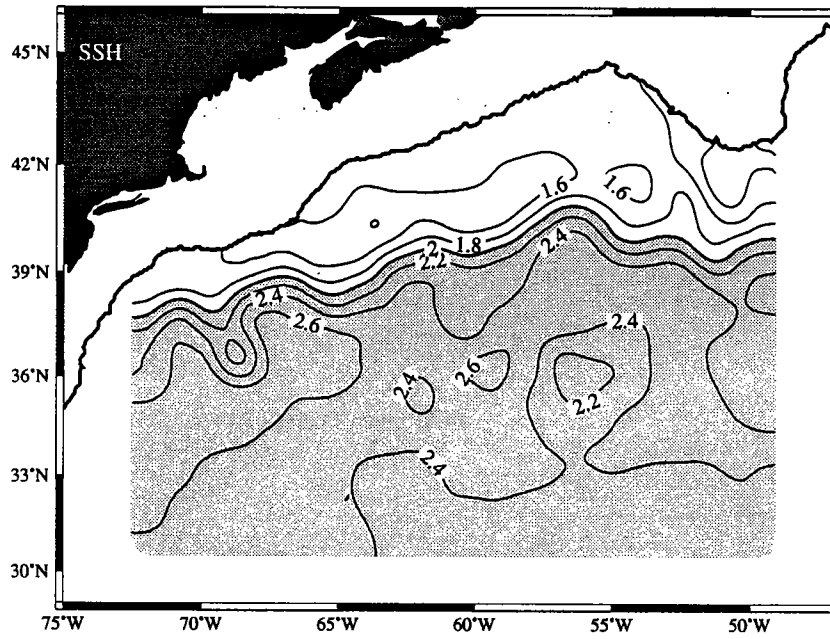


Figure 24: October 1987

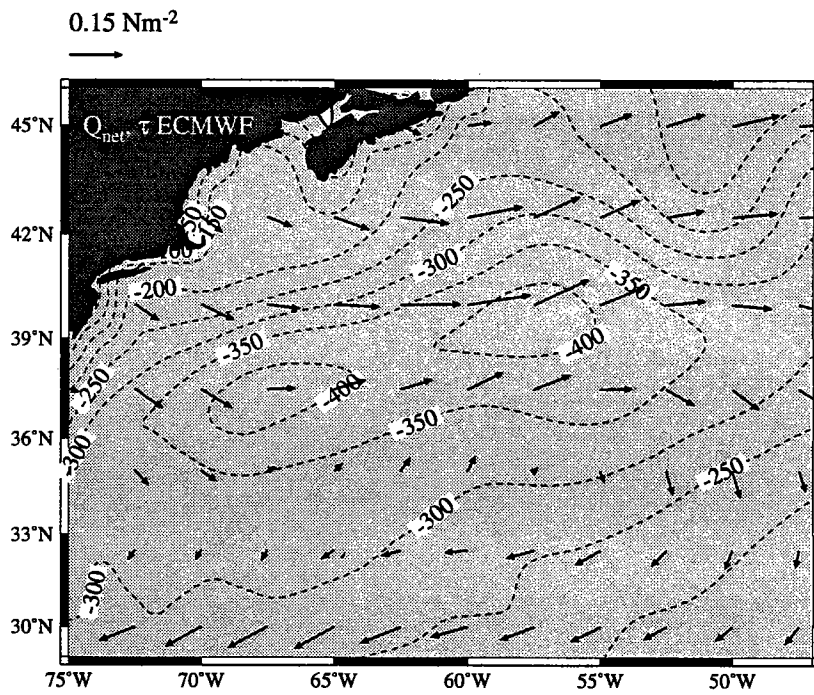
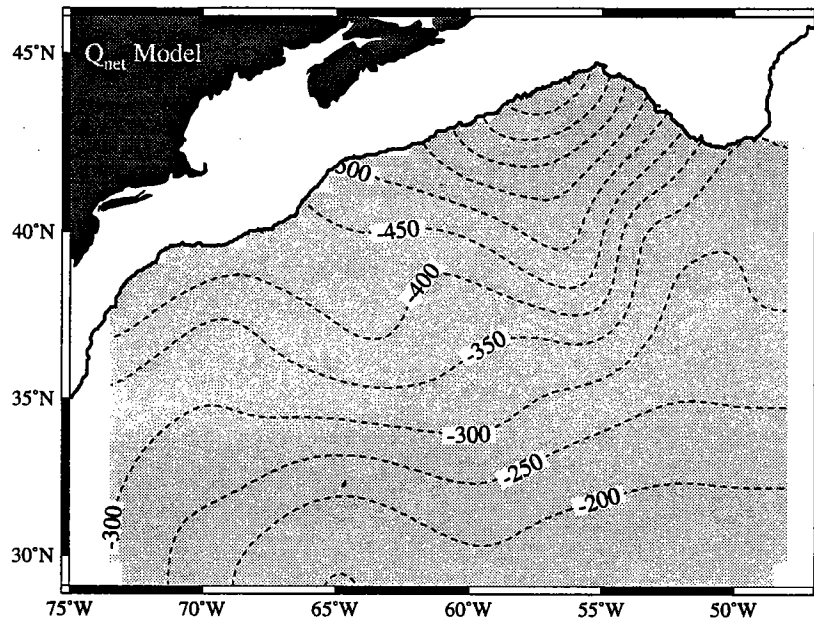


Figure 25: November 1987

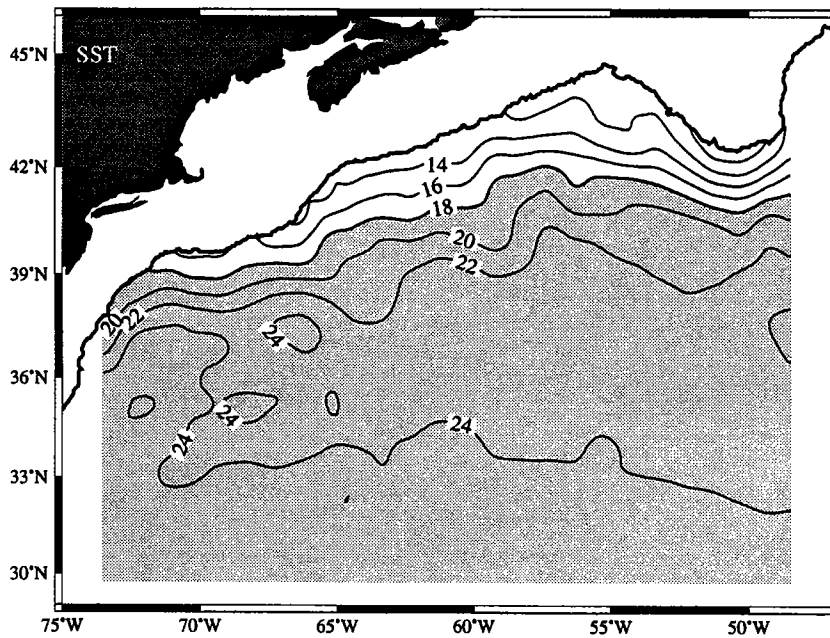
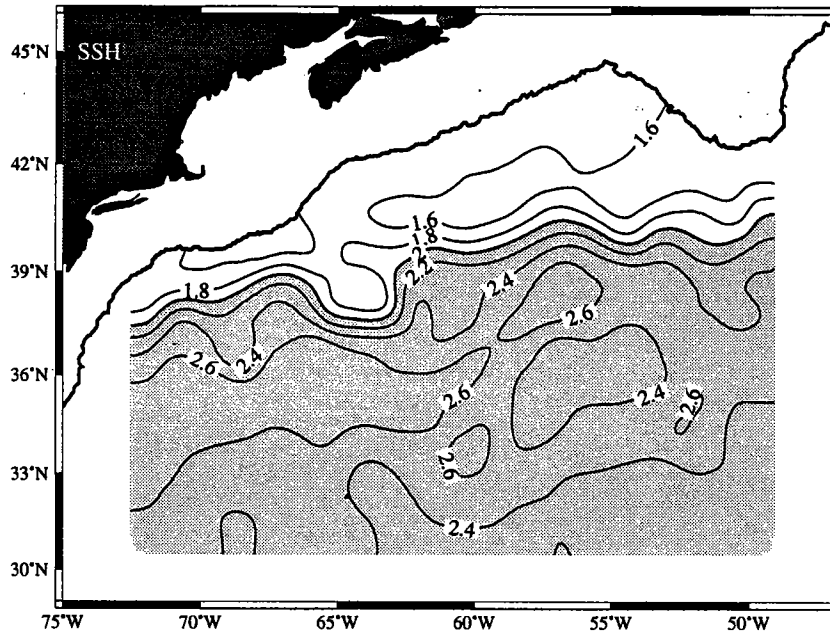


Figure 26: November 1987

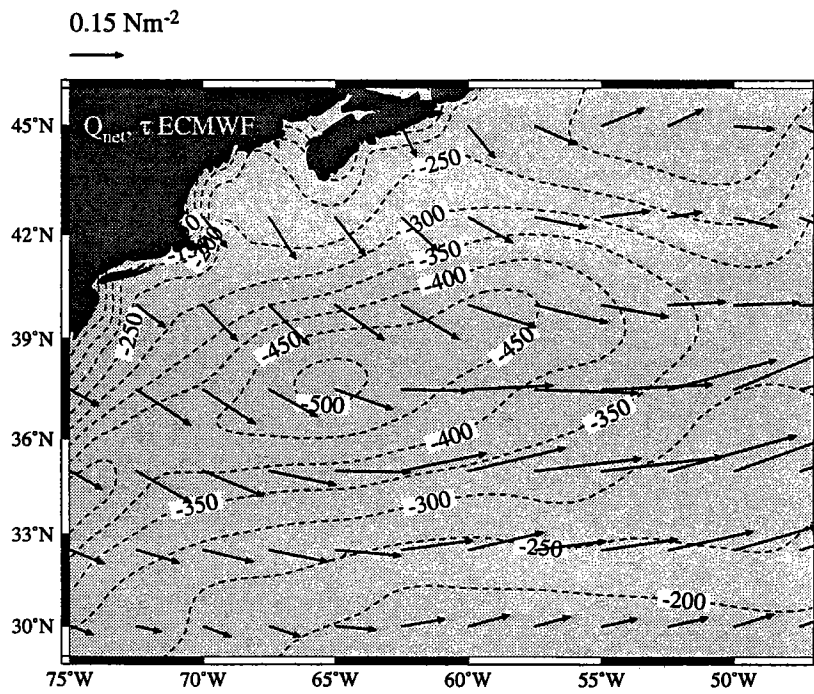
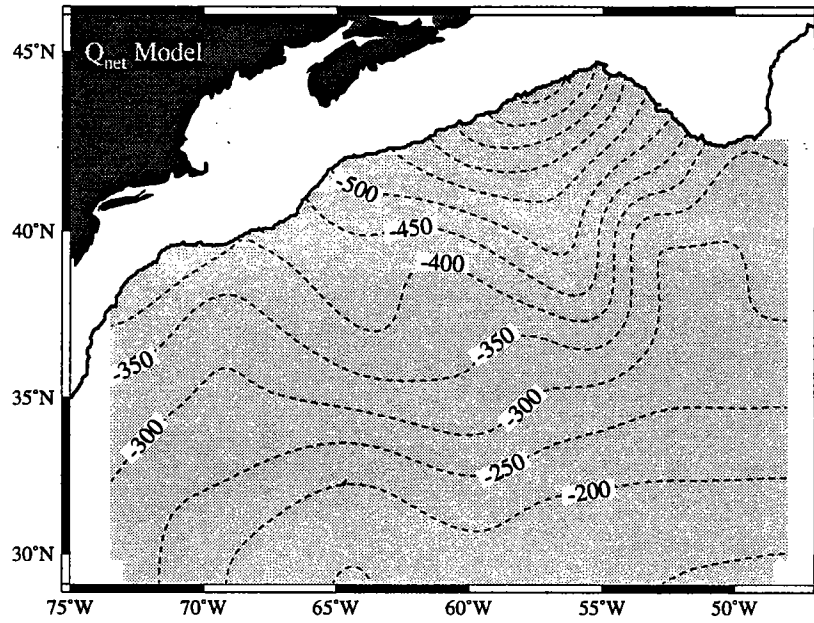


Figure 27: December 1987

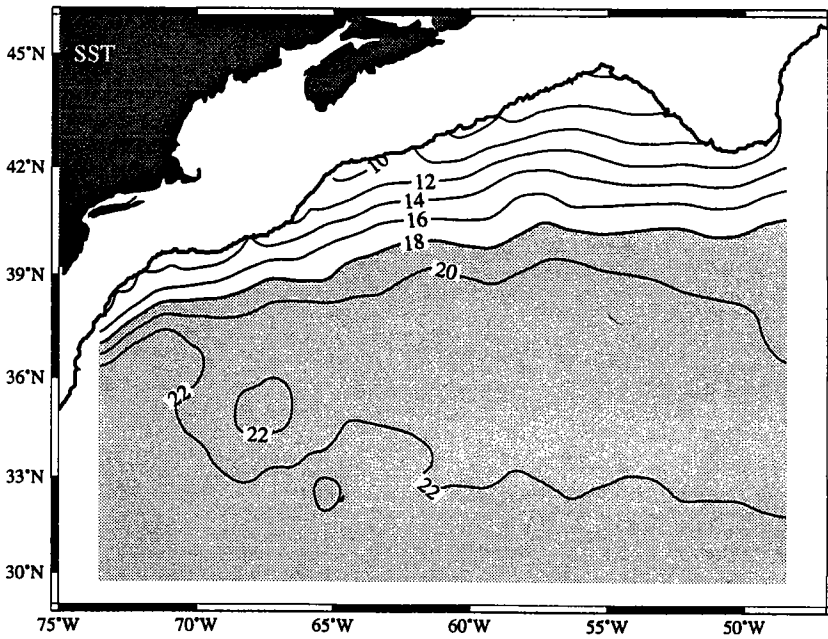
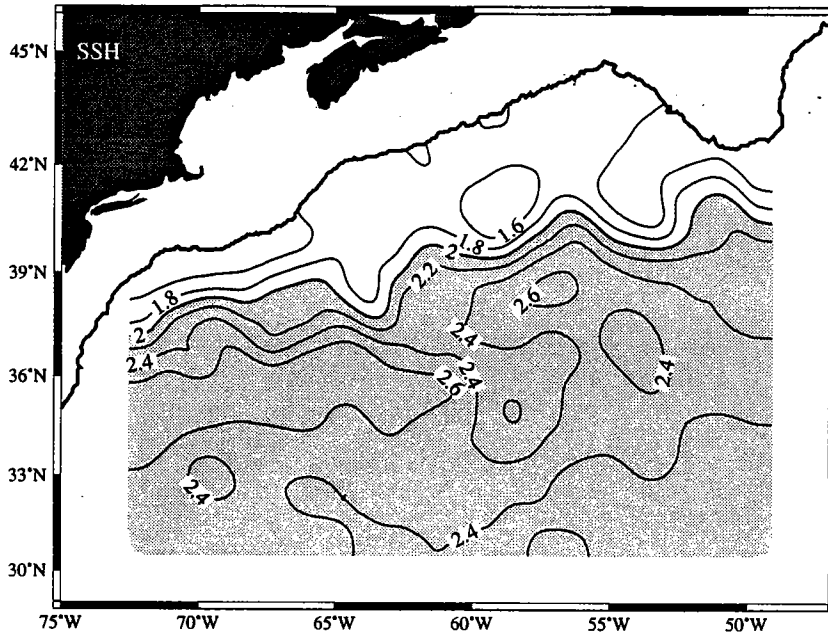


Figure 28: December 1987



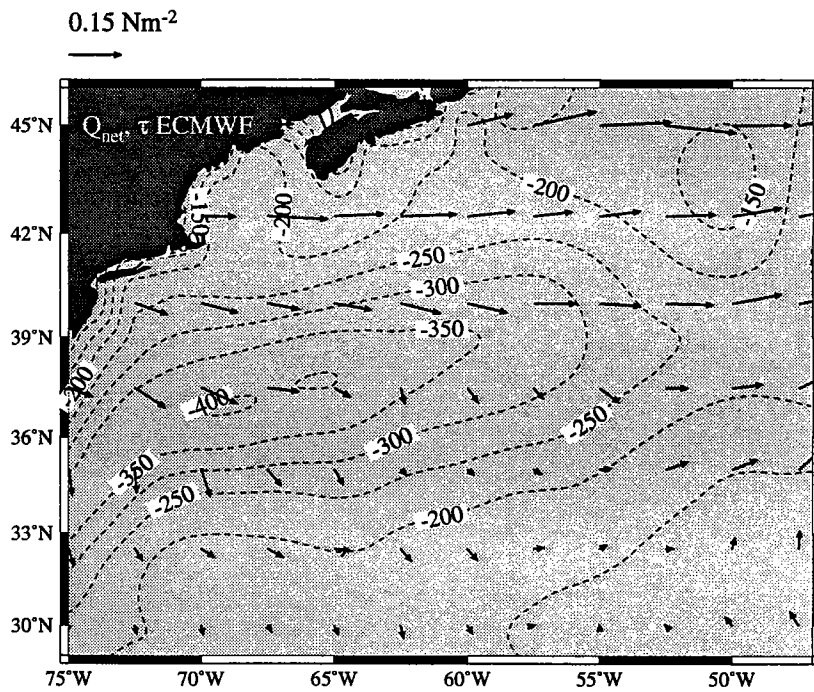
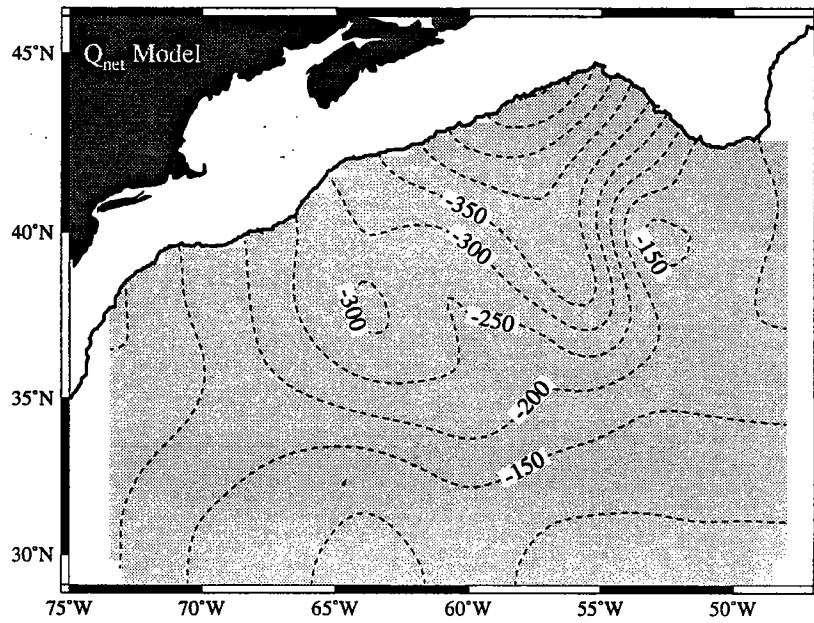


Figure 29: January 1988

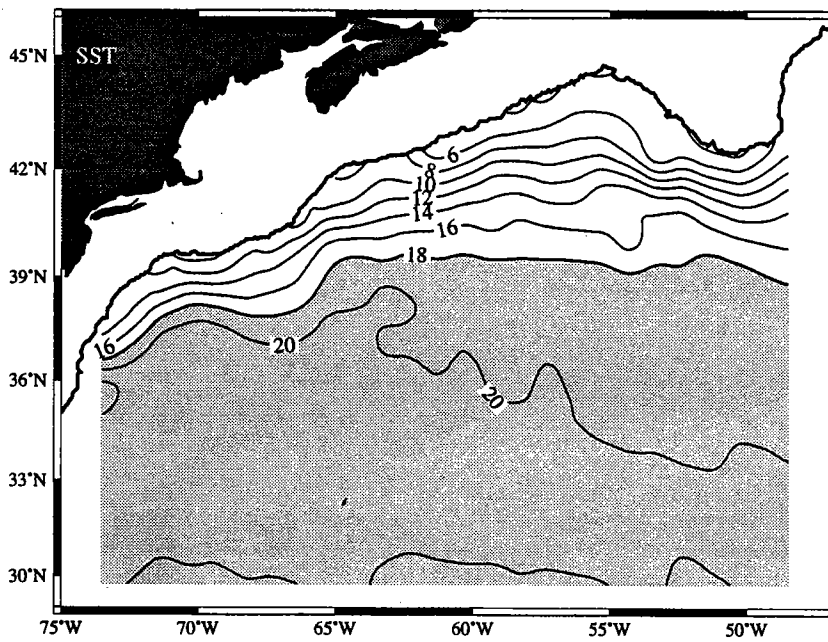
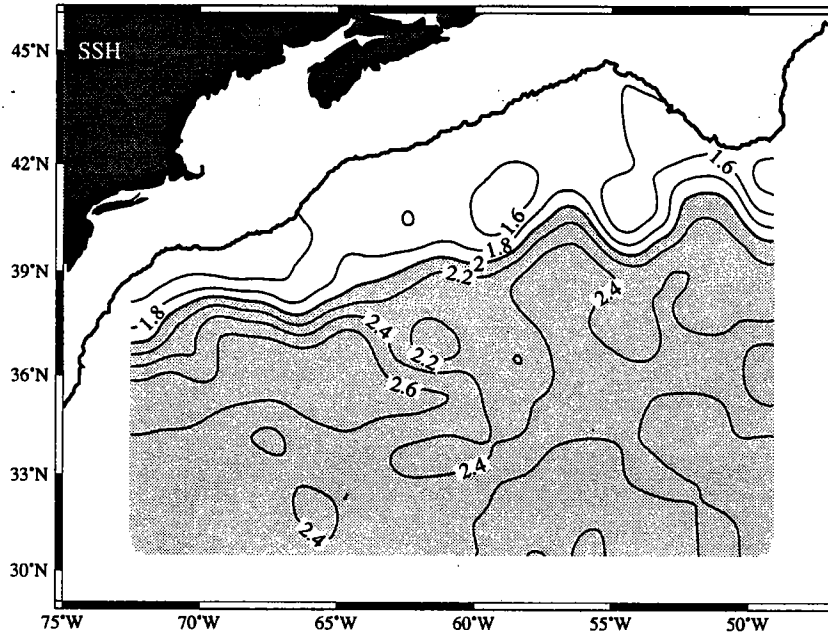


Figure 30: January 1988

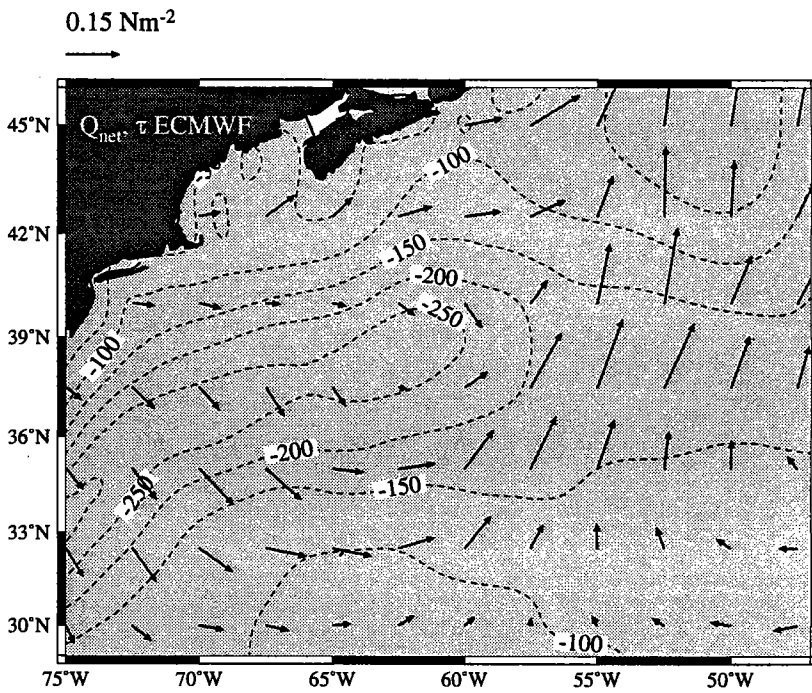
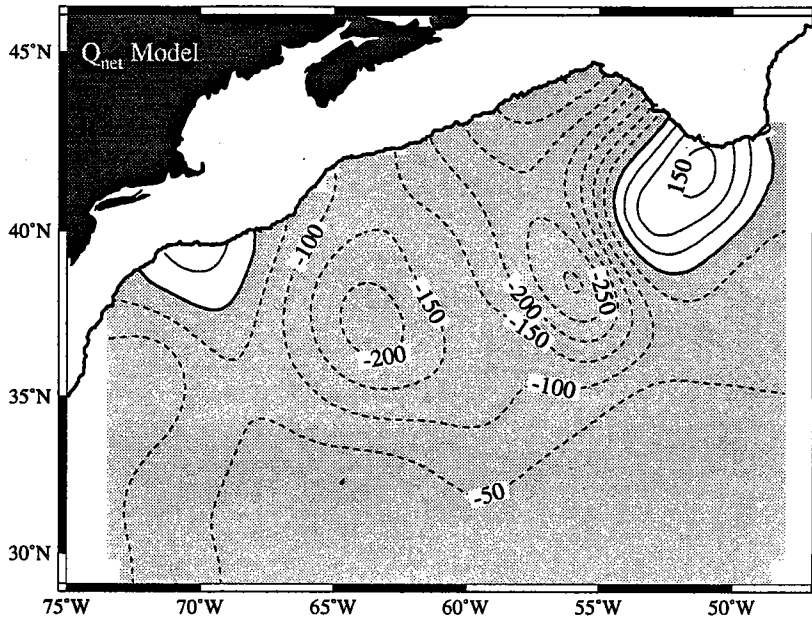


Figure 31: February 1988

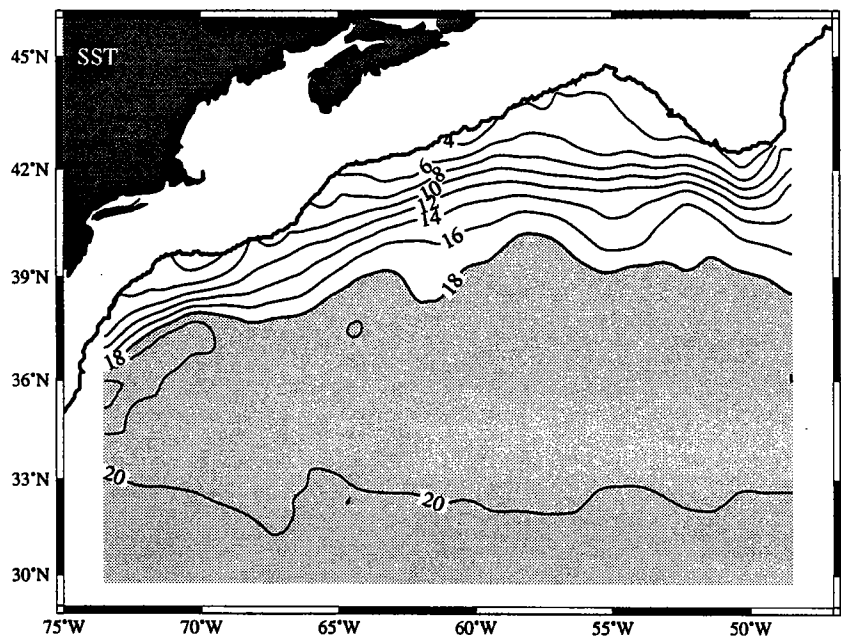
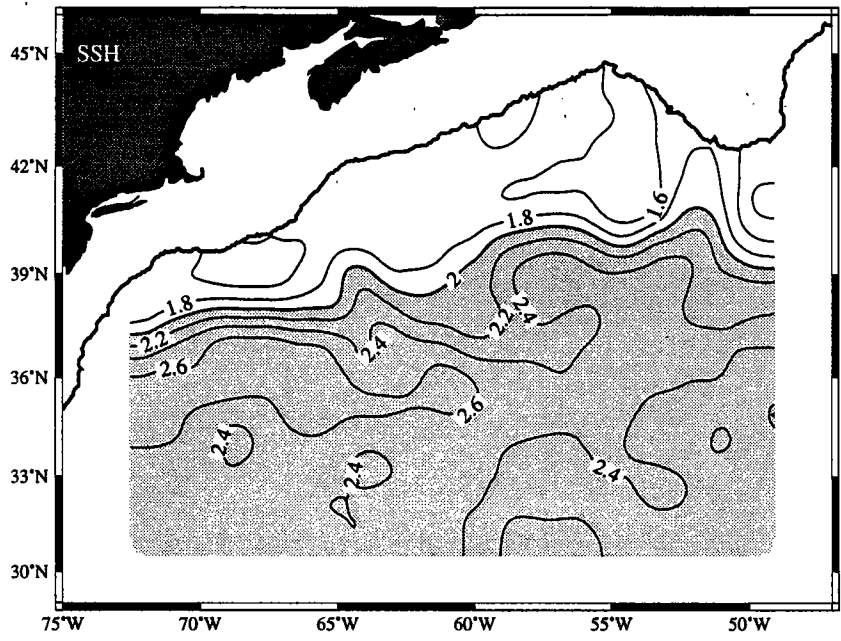


Figure 32: February 1988

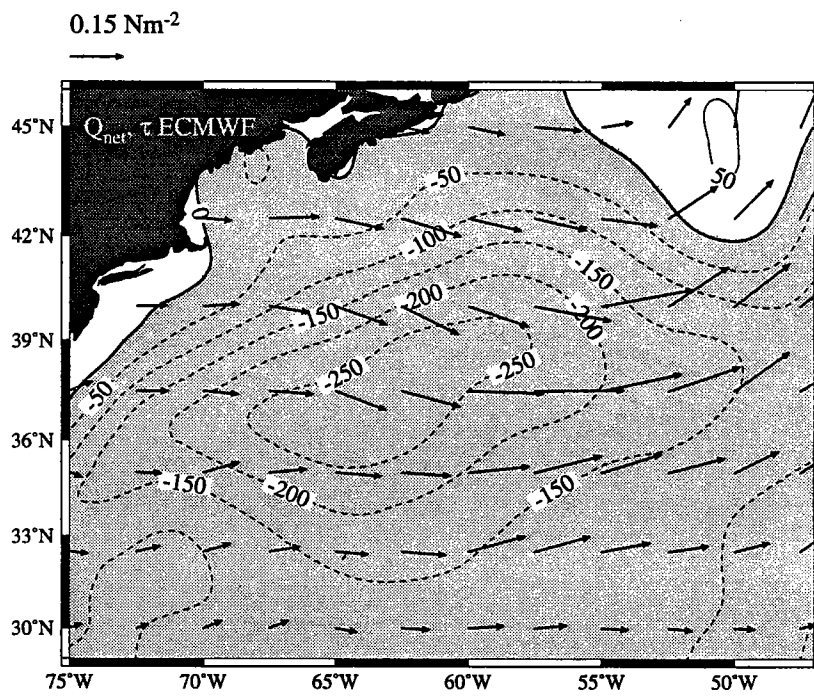
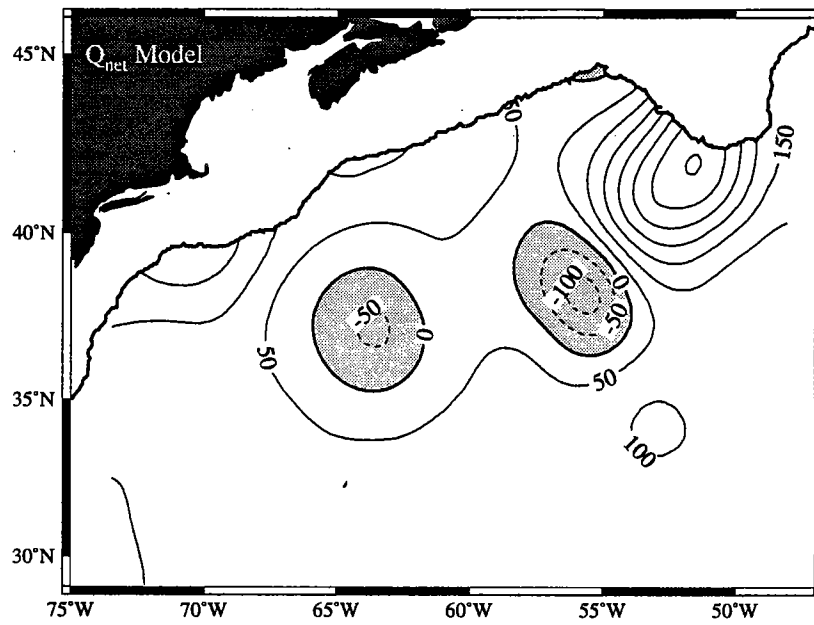


Figure 33: March 1988

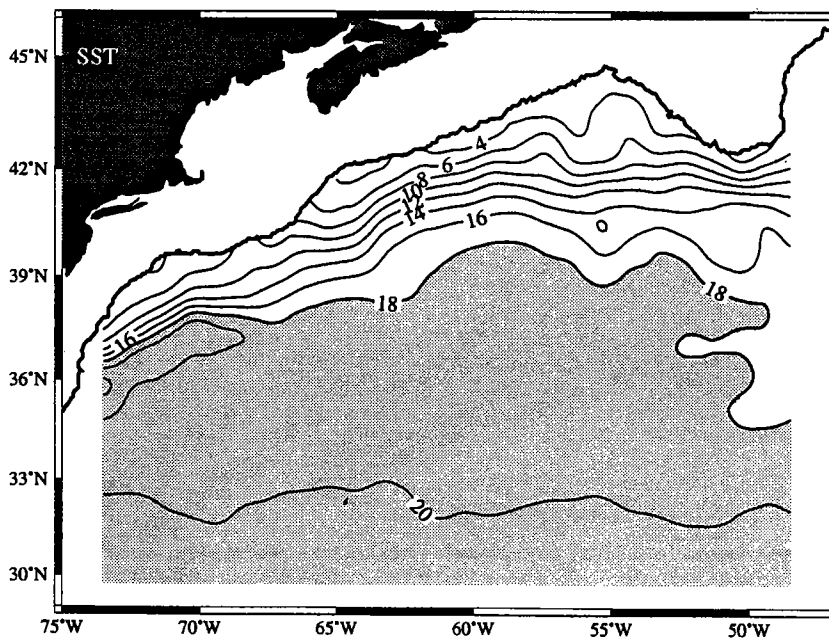
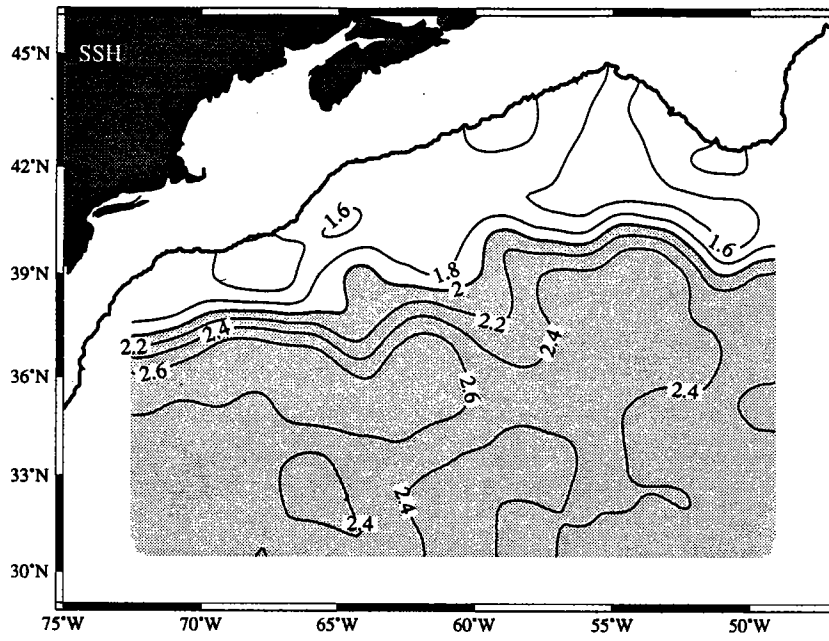


Figure 34: March 1988

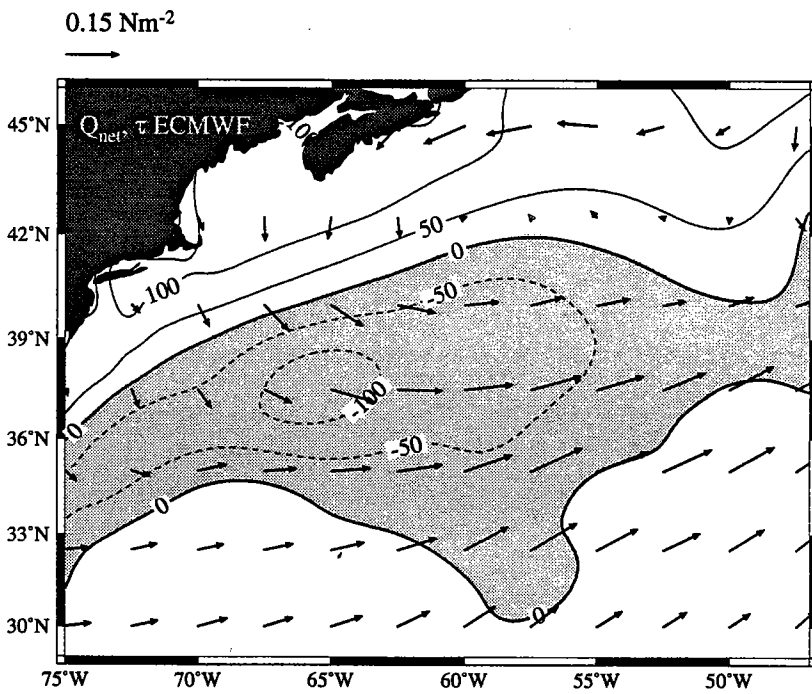
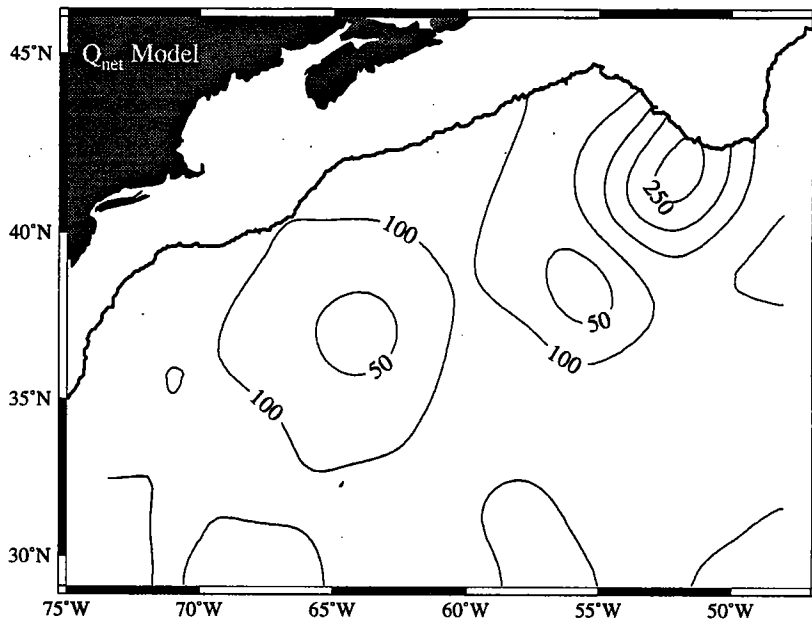


Figure 35: April 1988

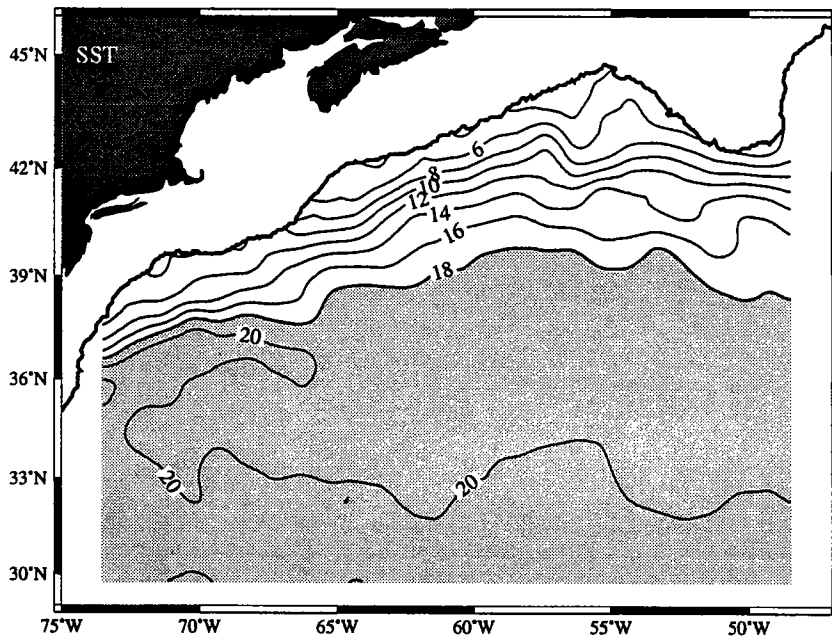
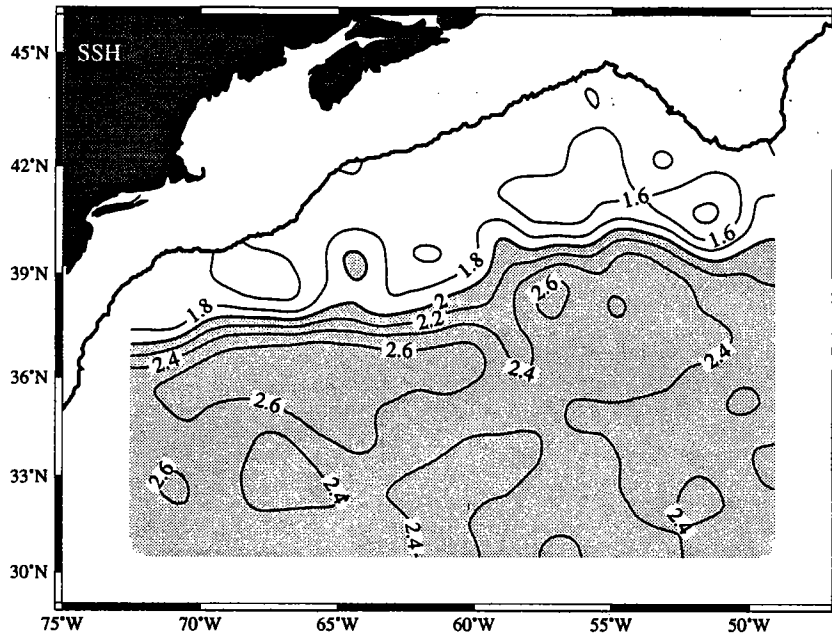


Figure 36: April 1988



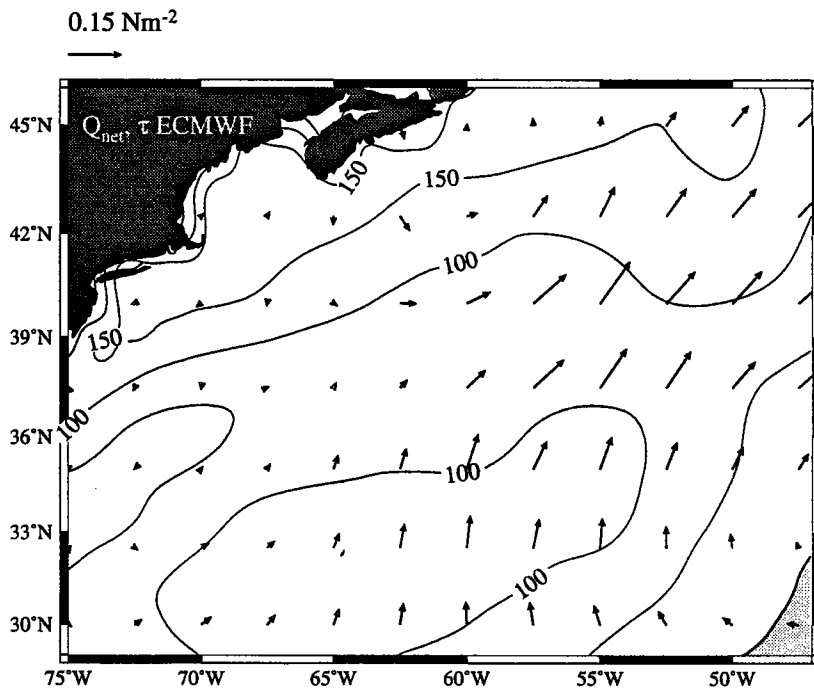
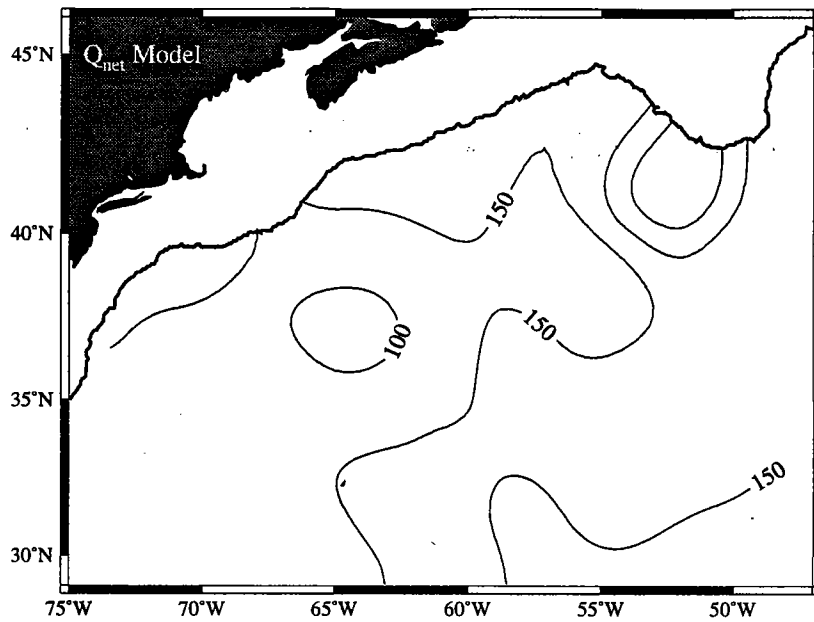


Figure 37: May 1988

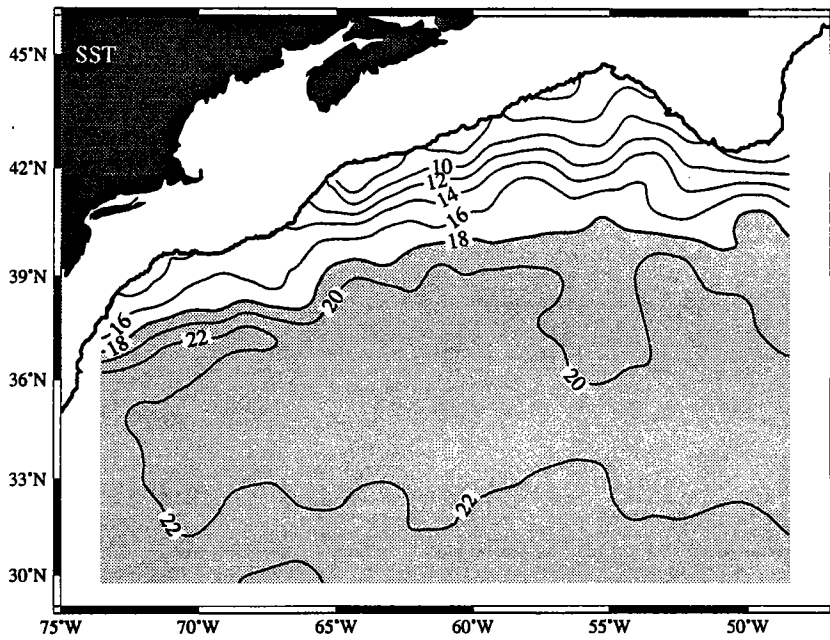
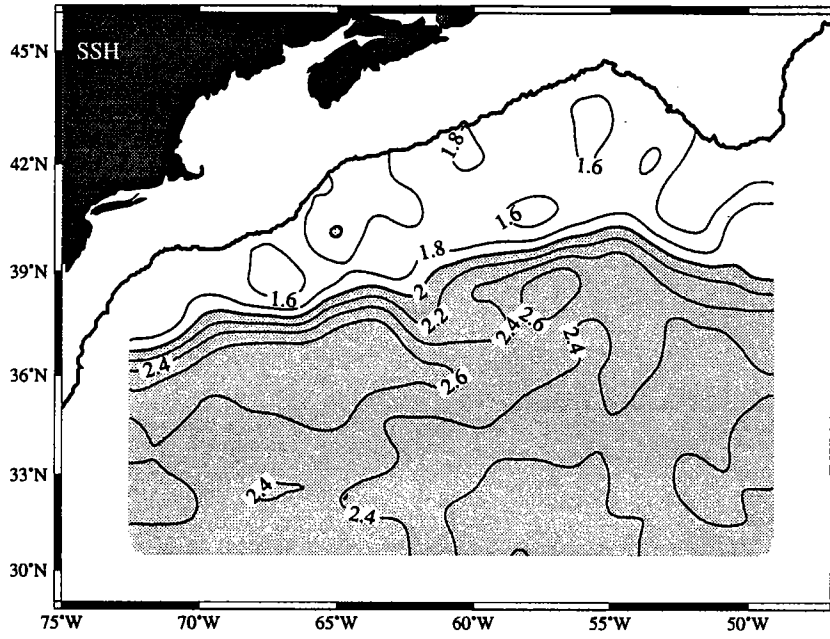


Figure 38: May 1988

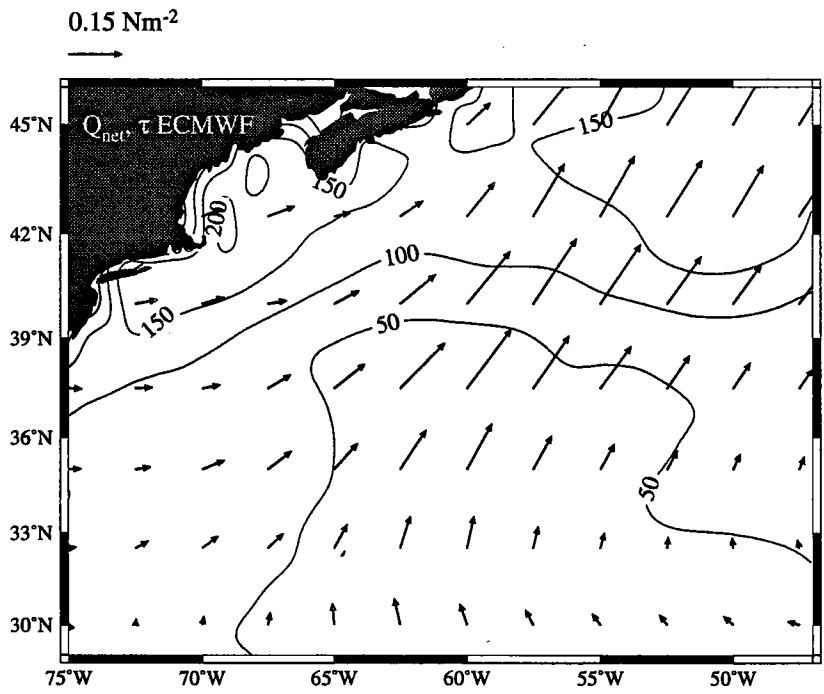
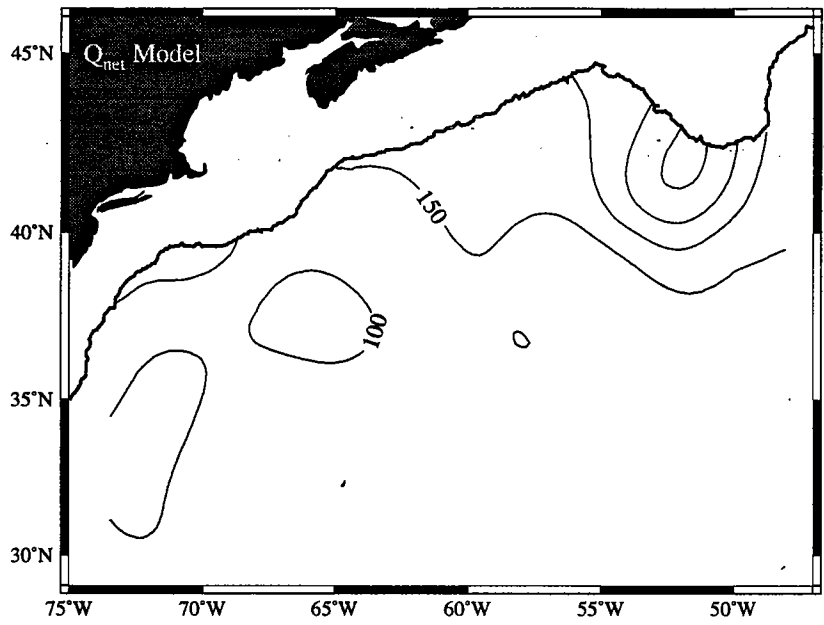


Figure 39: June 1988

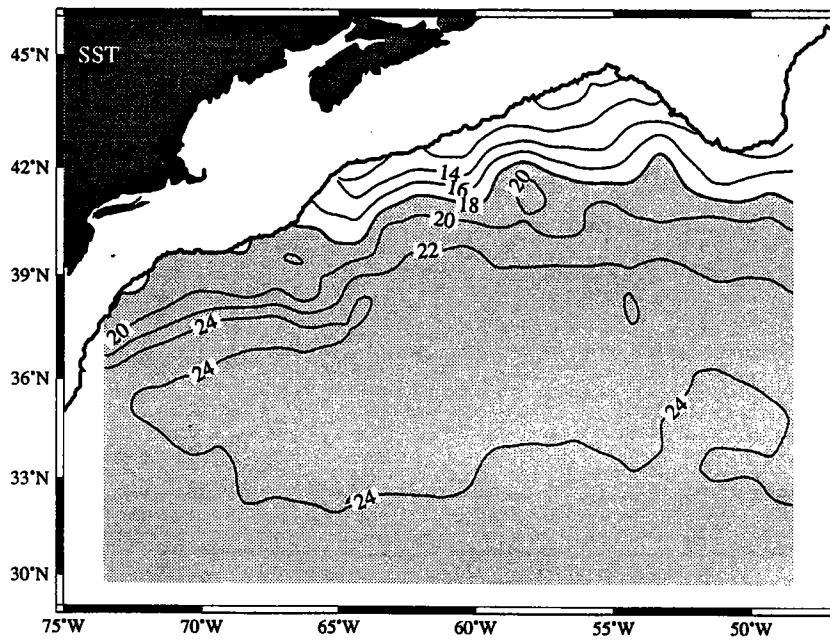
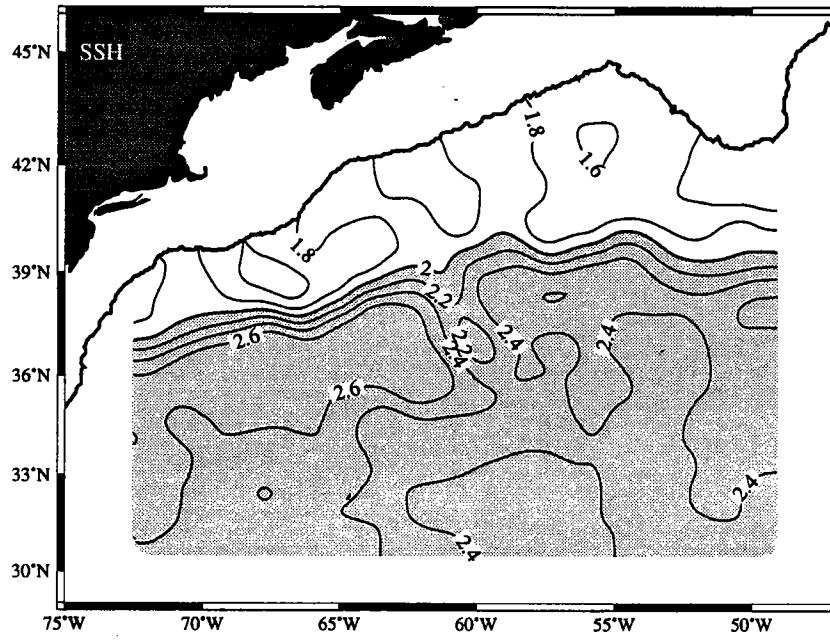


Figure 40: June 1988

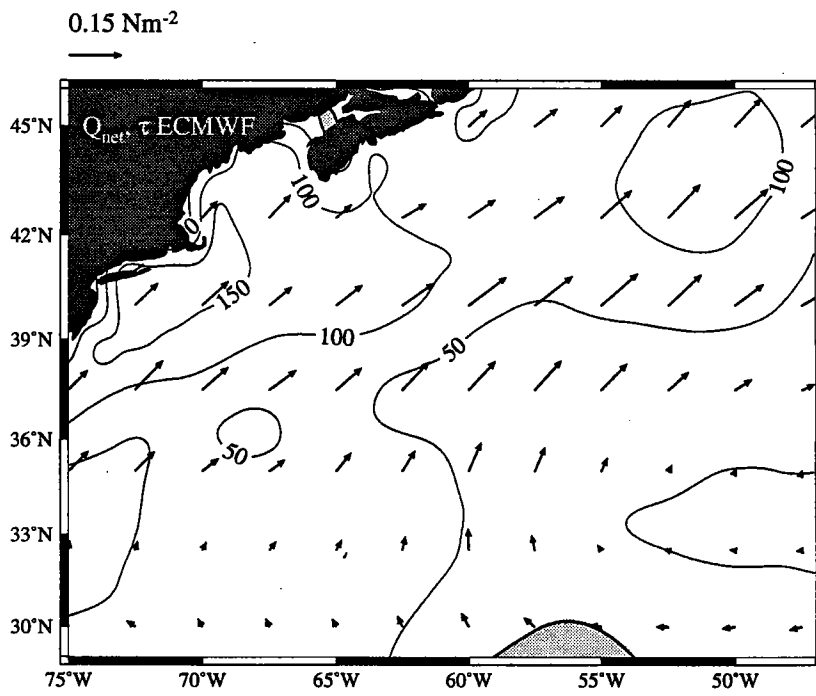
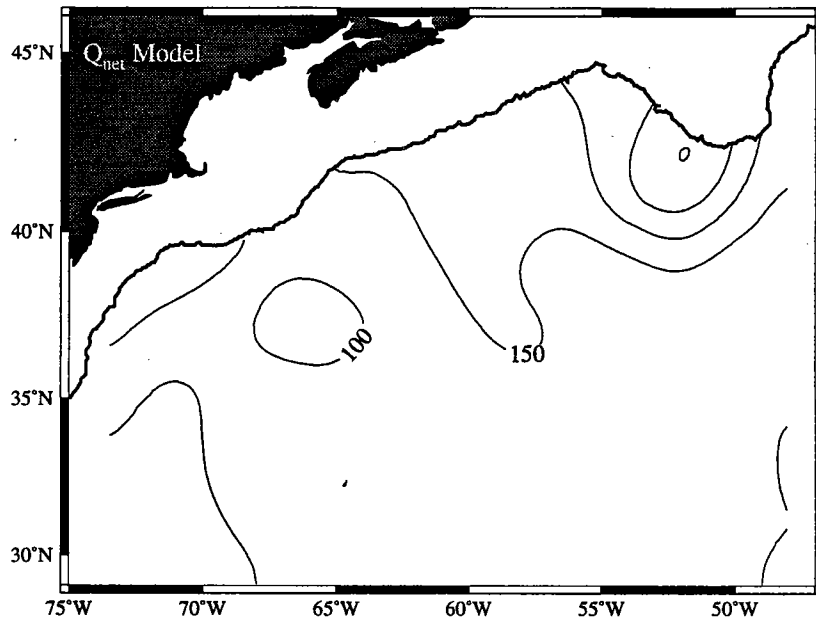


Figure 41: July 1988

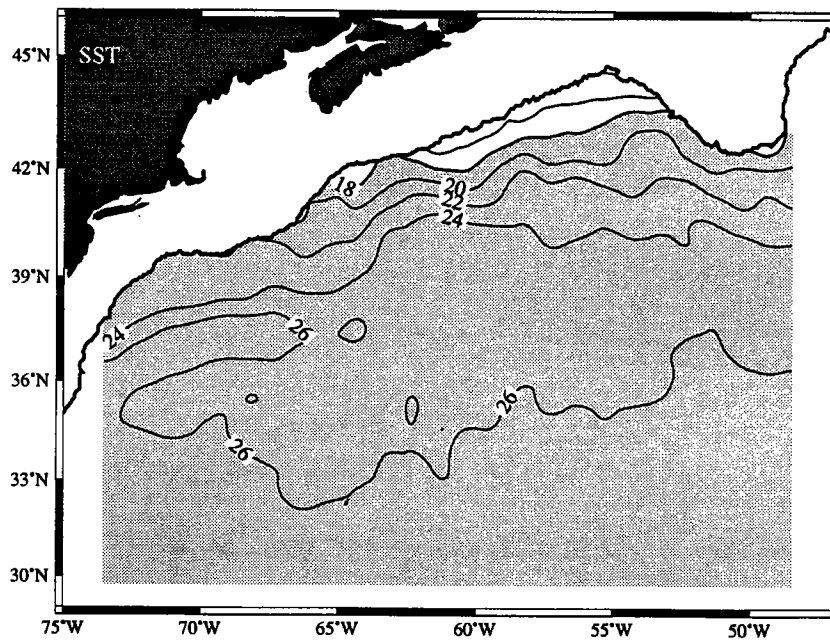
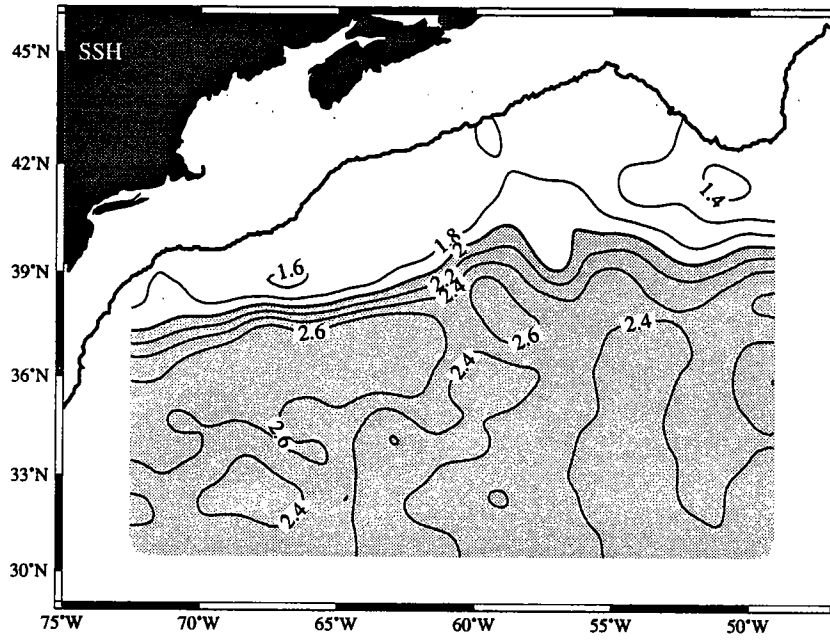


Figure 42: July 1988

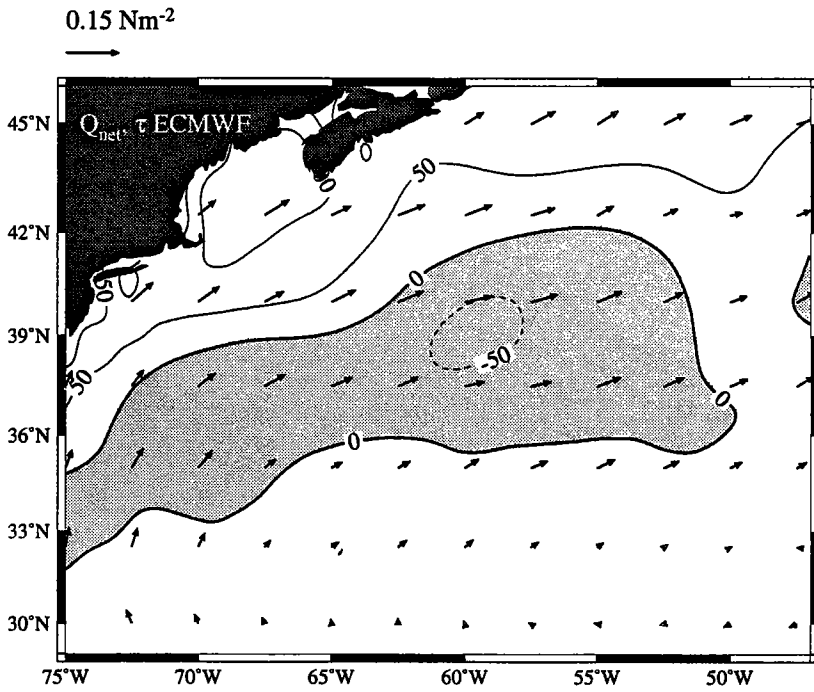
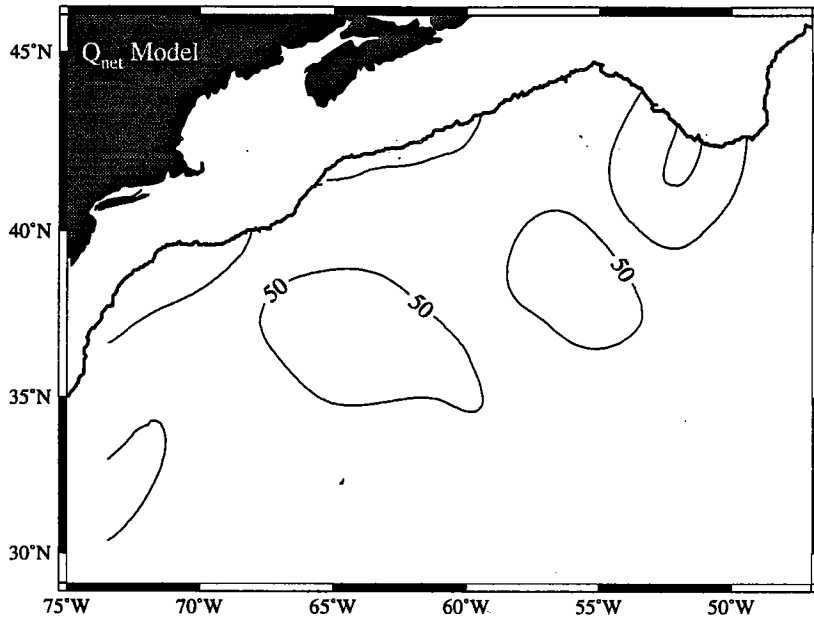


Figure 43: August 1988

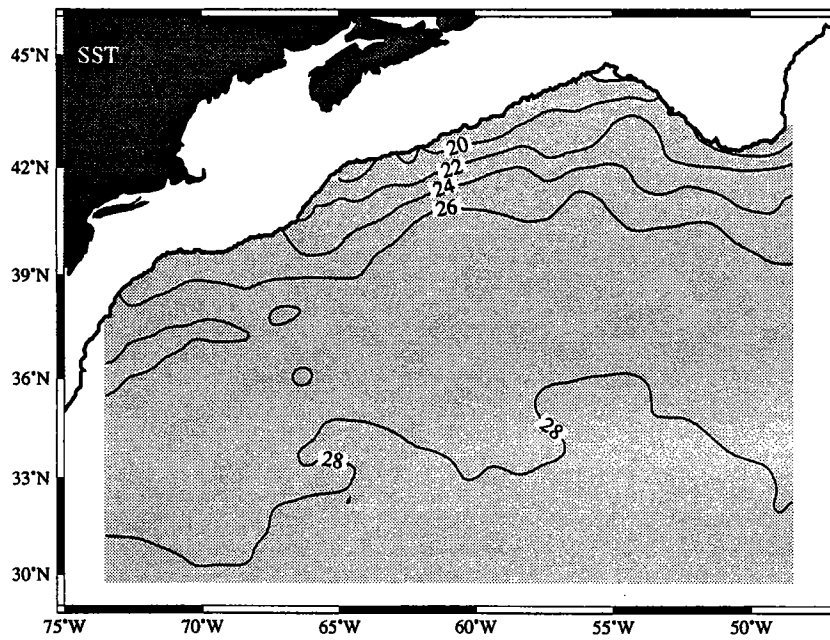
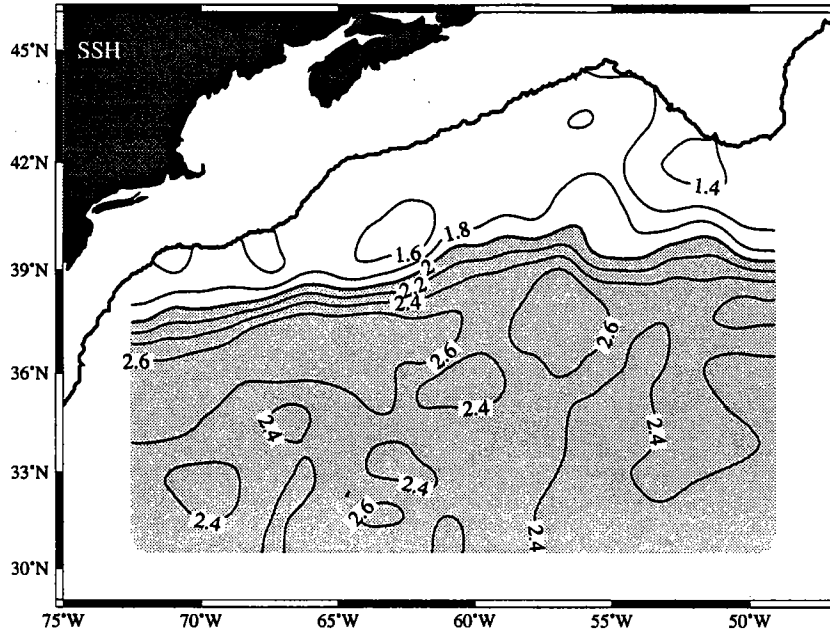


Figure 44: August 1988



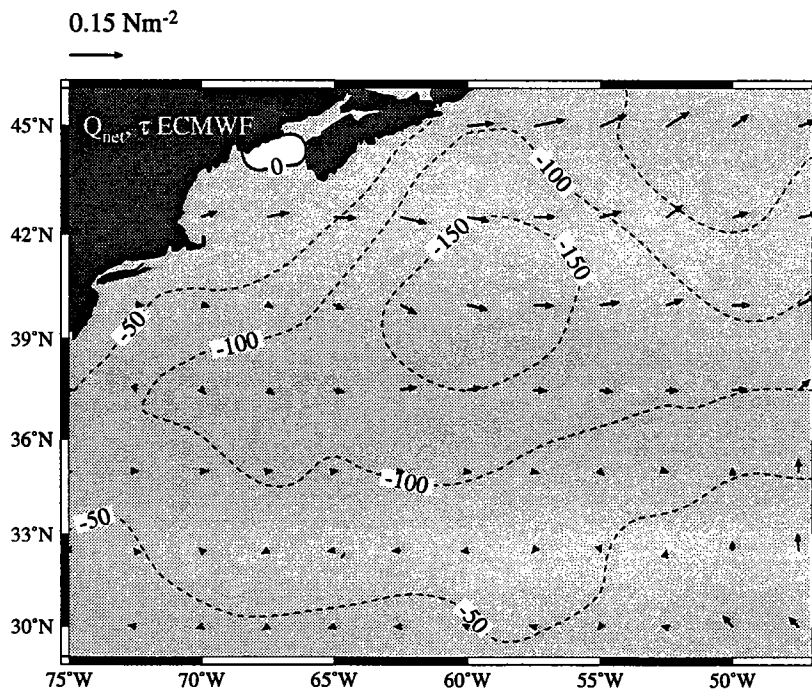
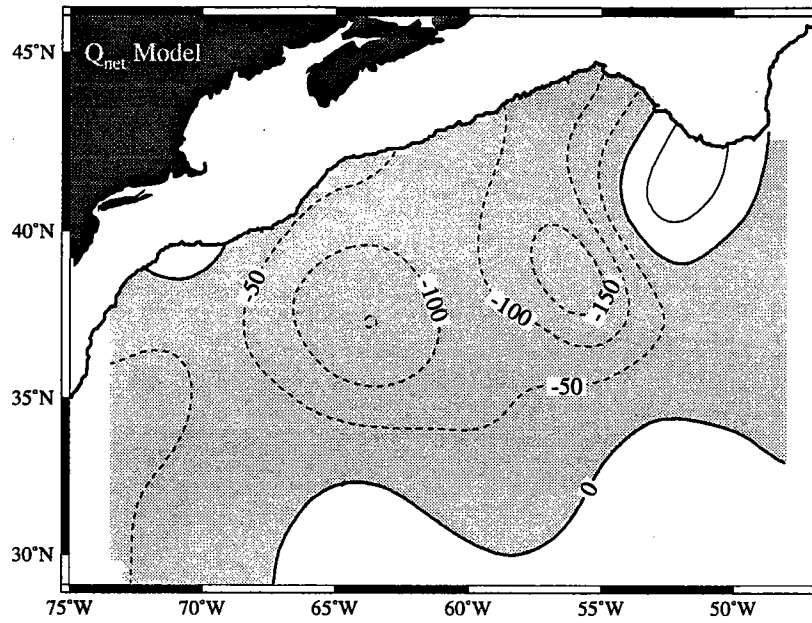


Figure 45: September 1988

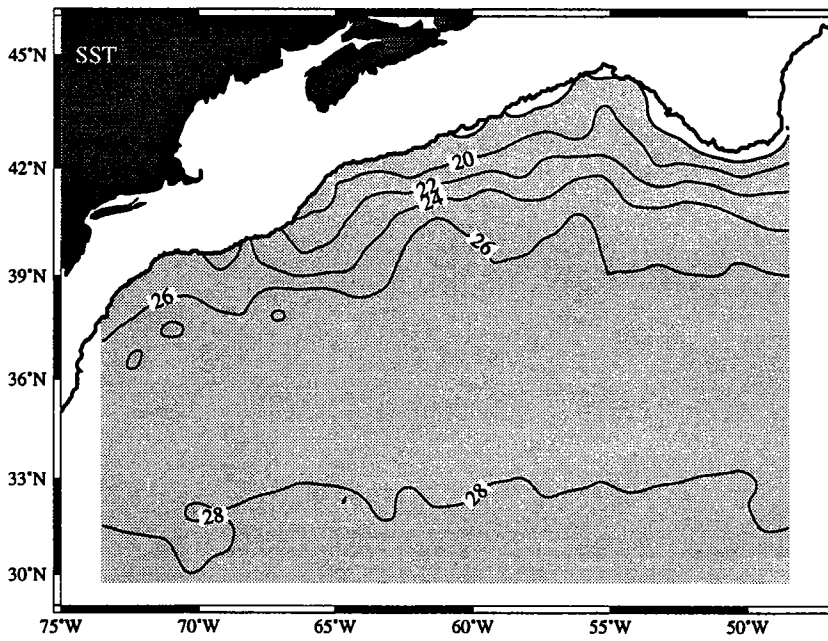
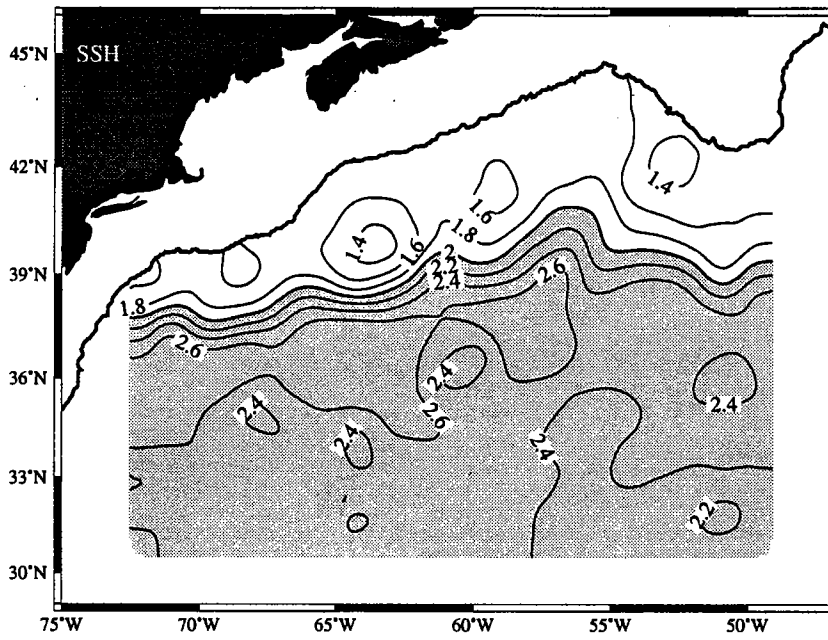


Figure 46: September 1988

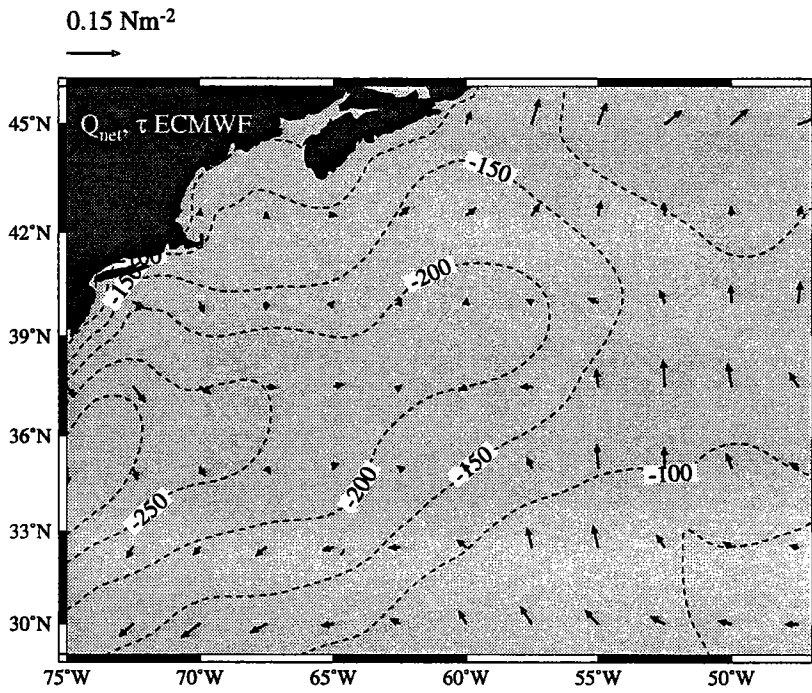
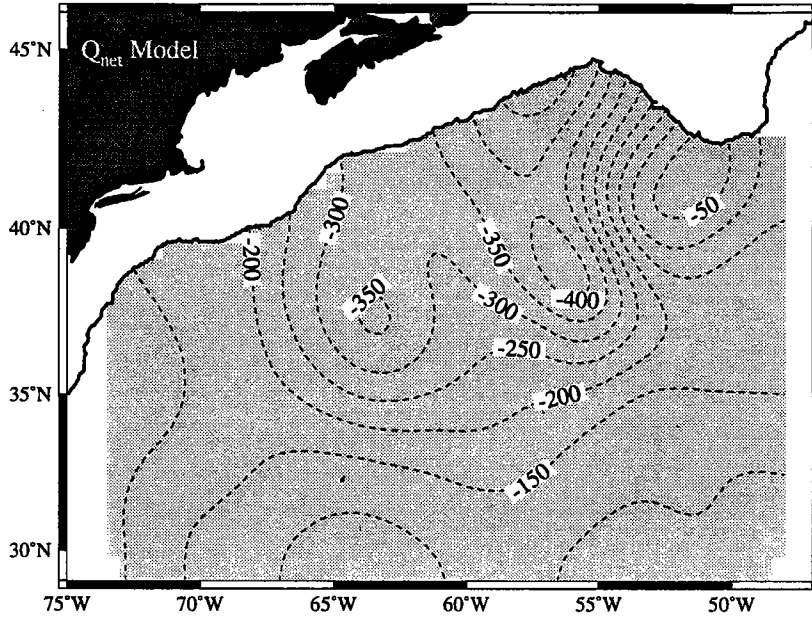


Figure 47: October 1988

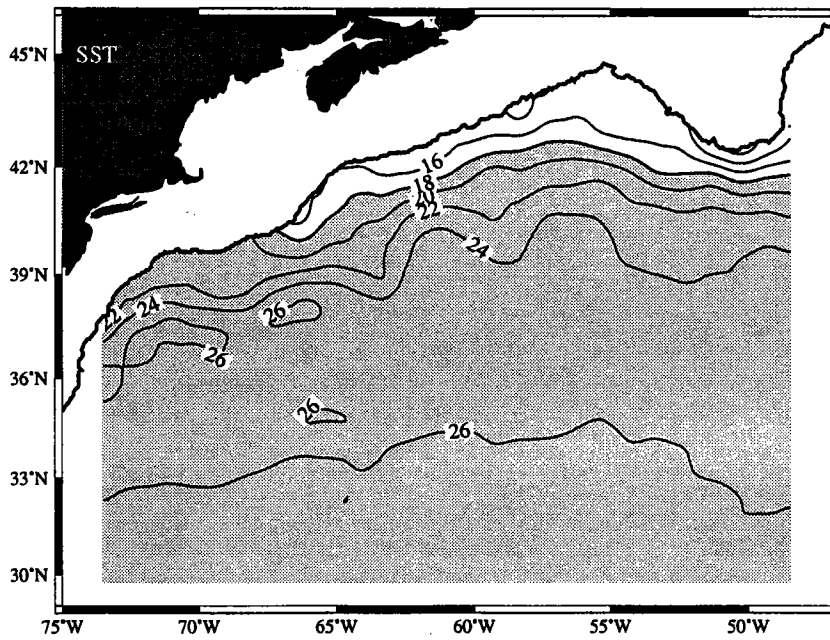
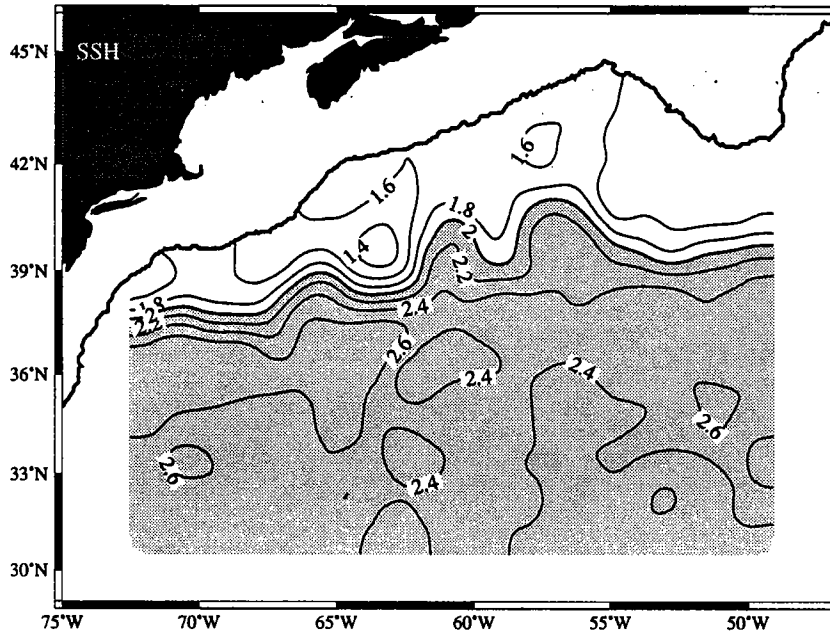


Figure 48: October 1988

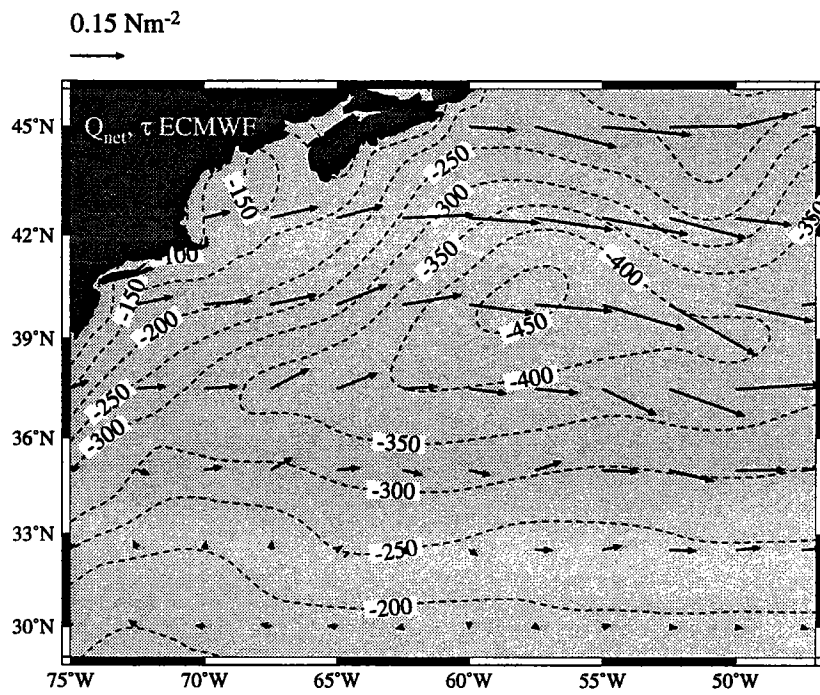
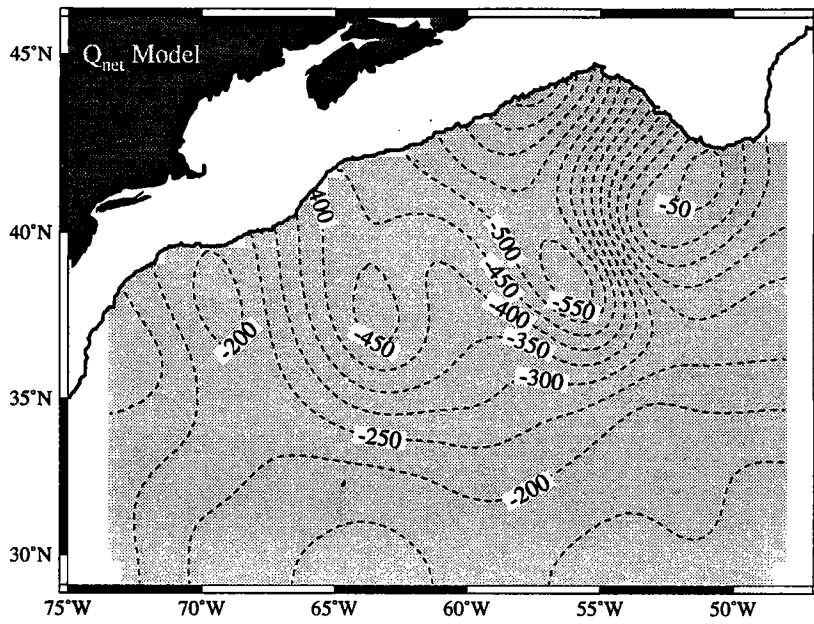


Figure 49: November 1988

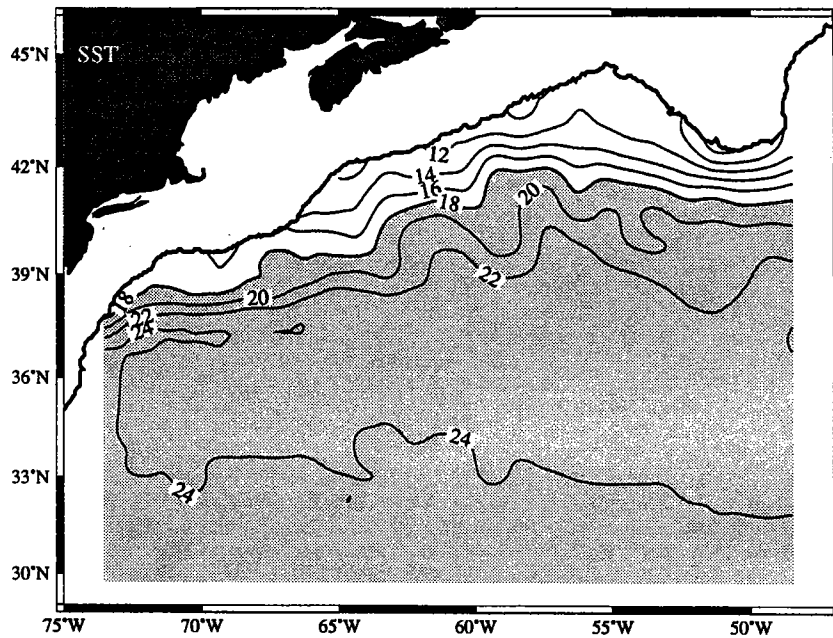
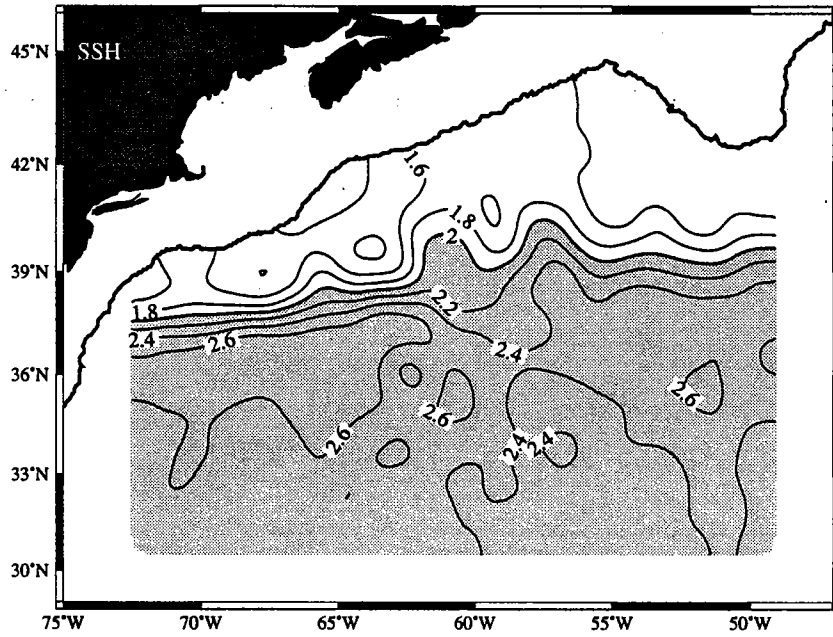


Figure 50: November 1988

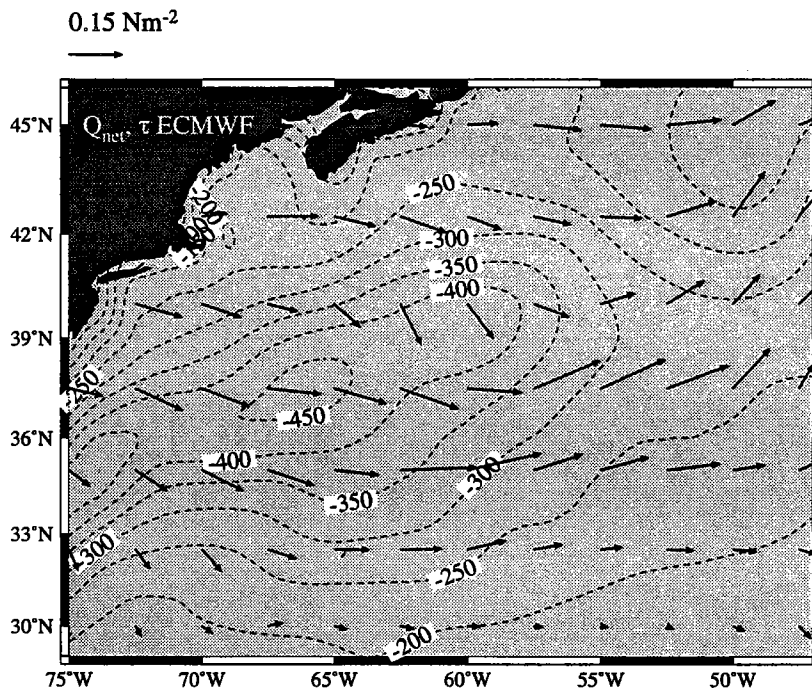
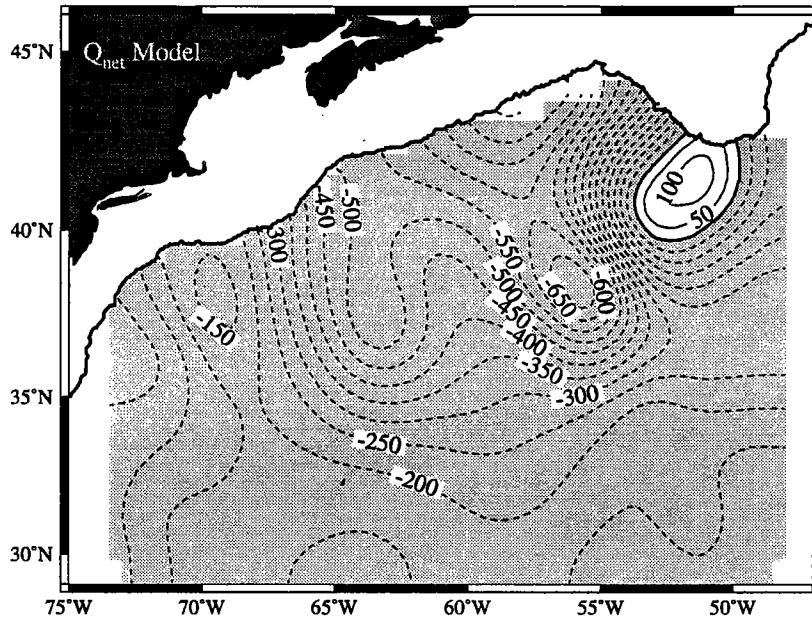


Figure 51: December 1988

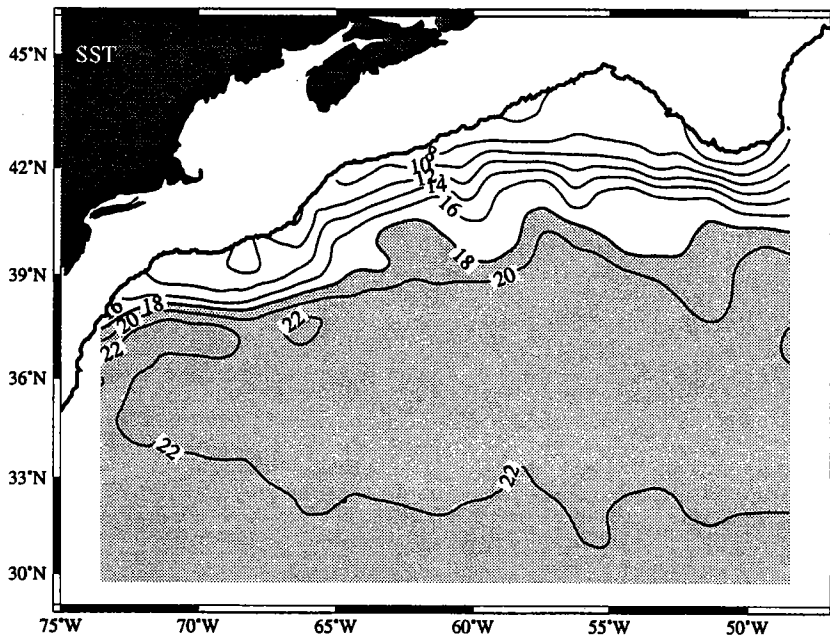
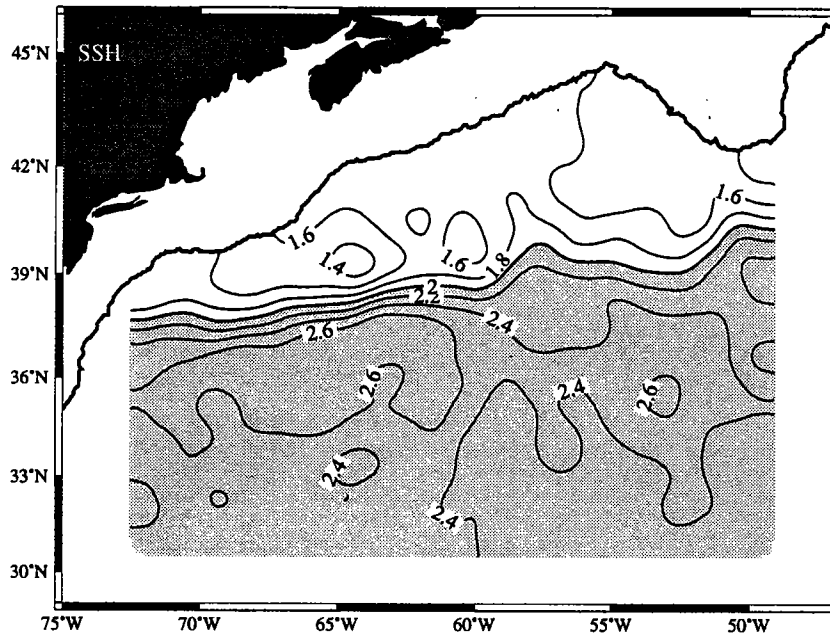


Figure 52: December 1988



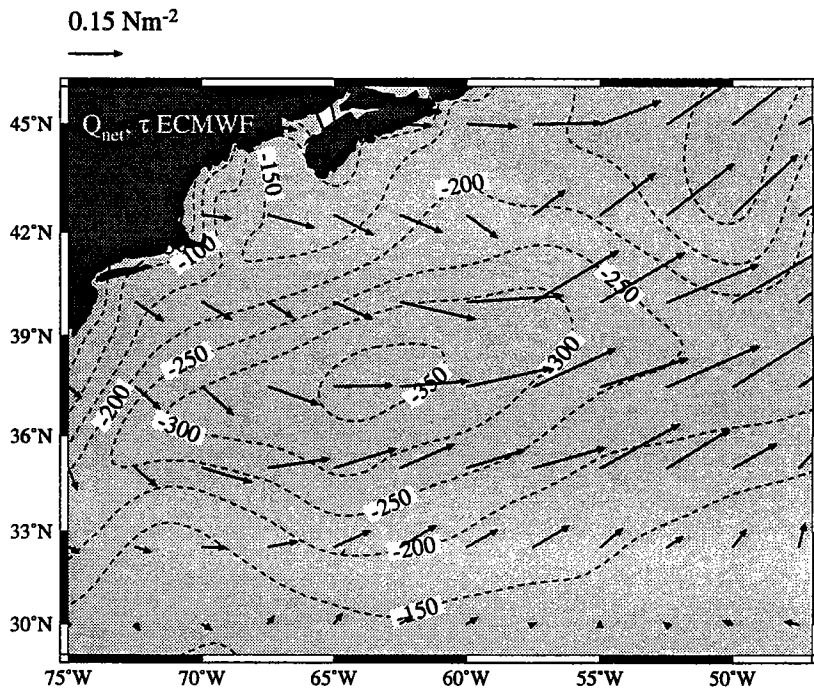
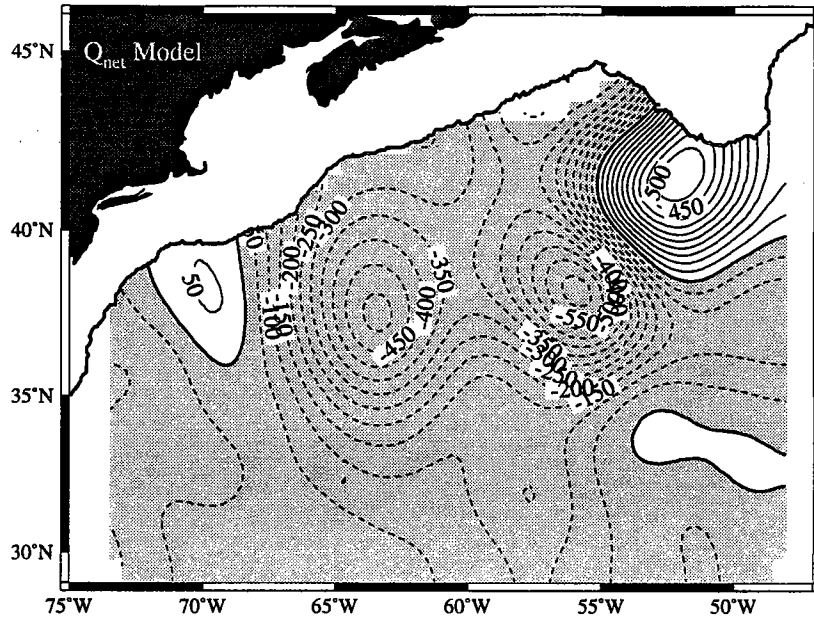


Figure 53: January 1989

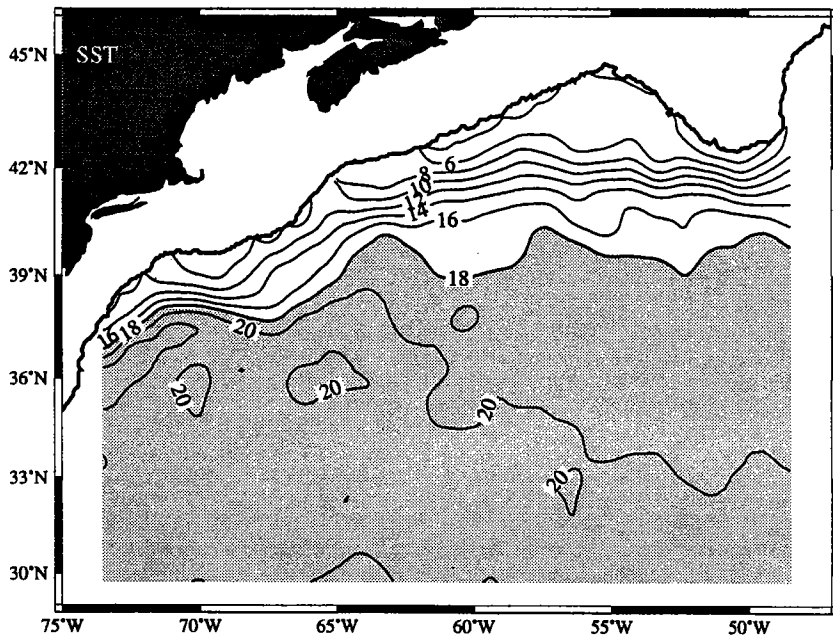
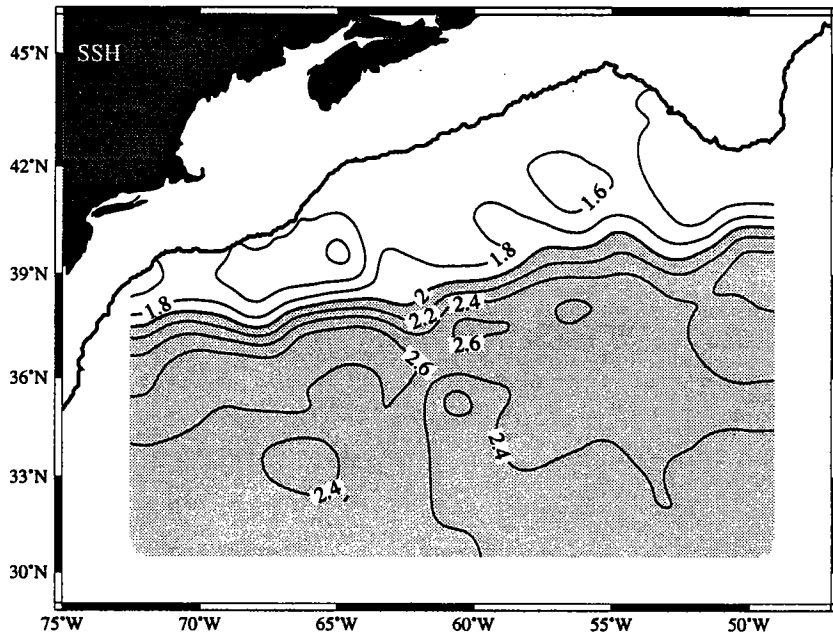


Figure 54: January 1989

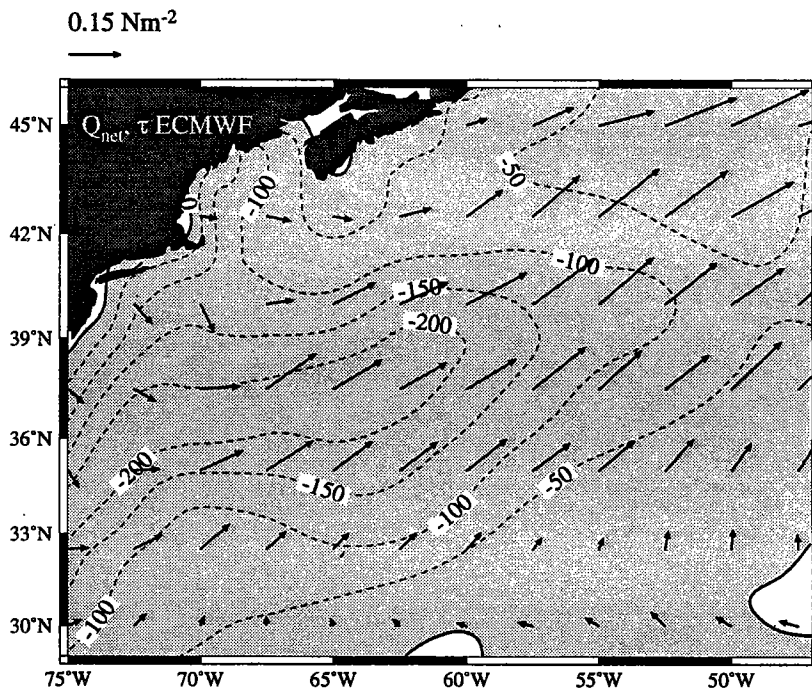
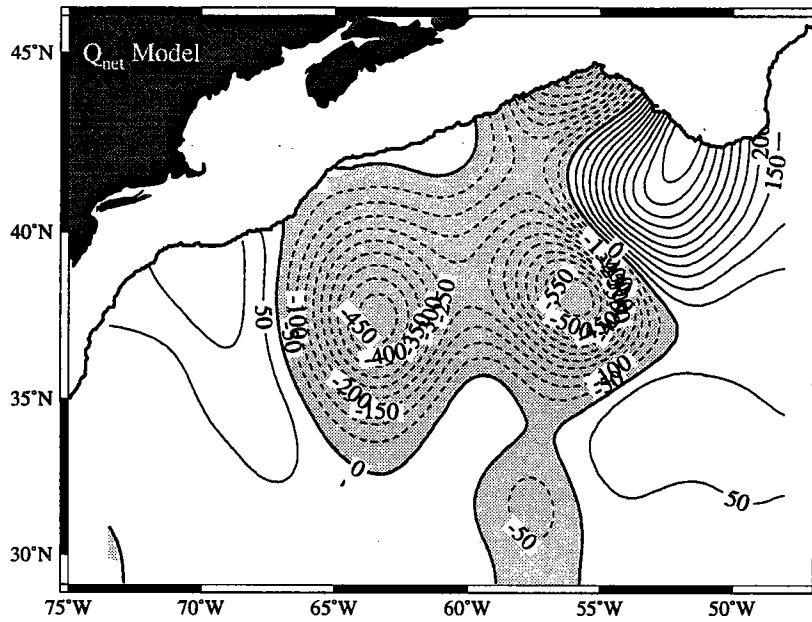


Figure 55: February 1989

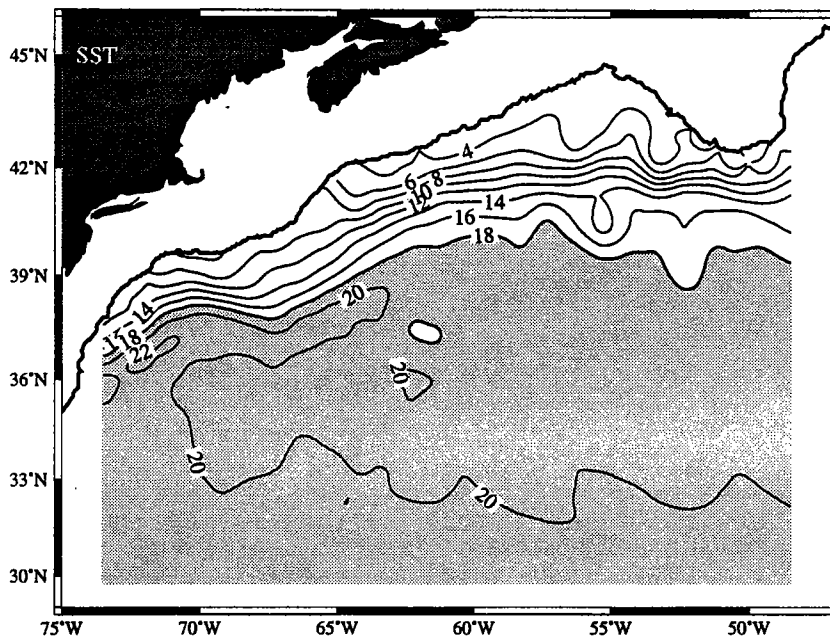
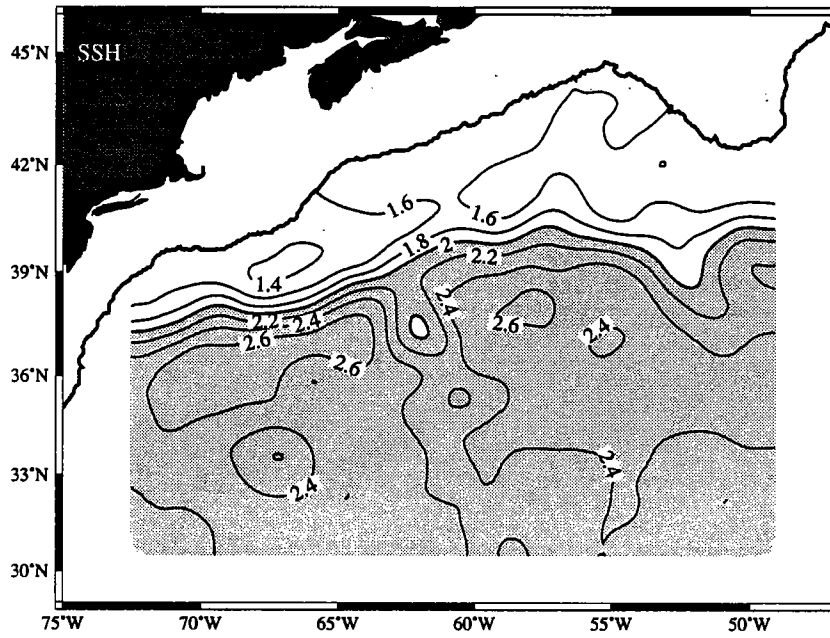


Figure 56: February 1989

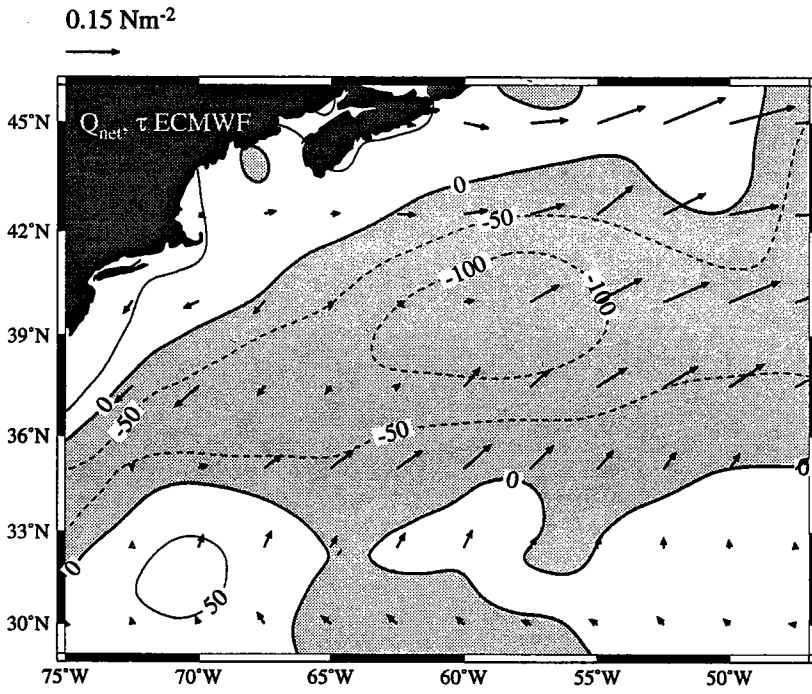
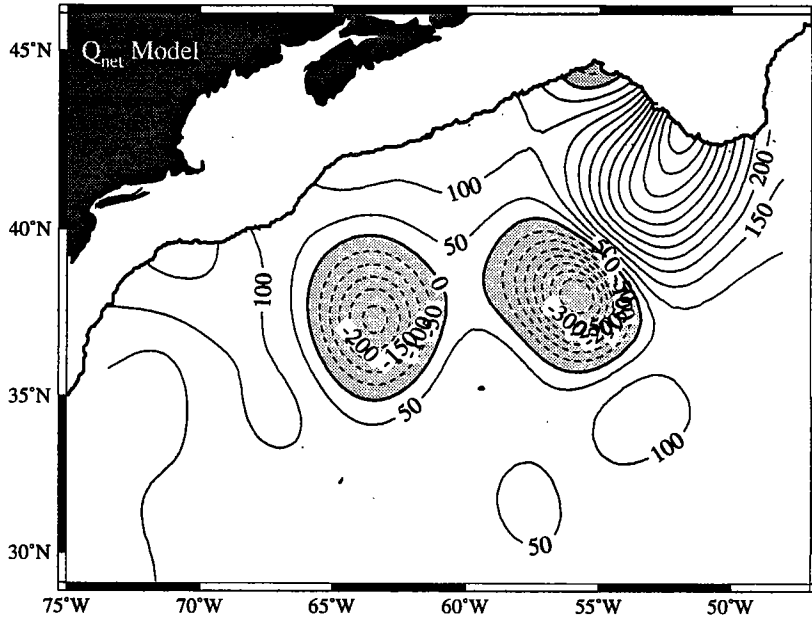


Figure 57: March 1989

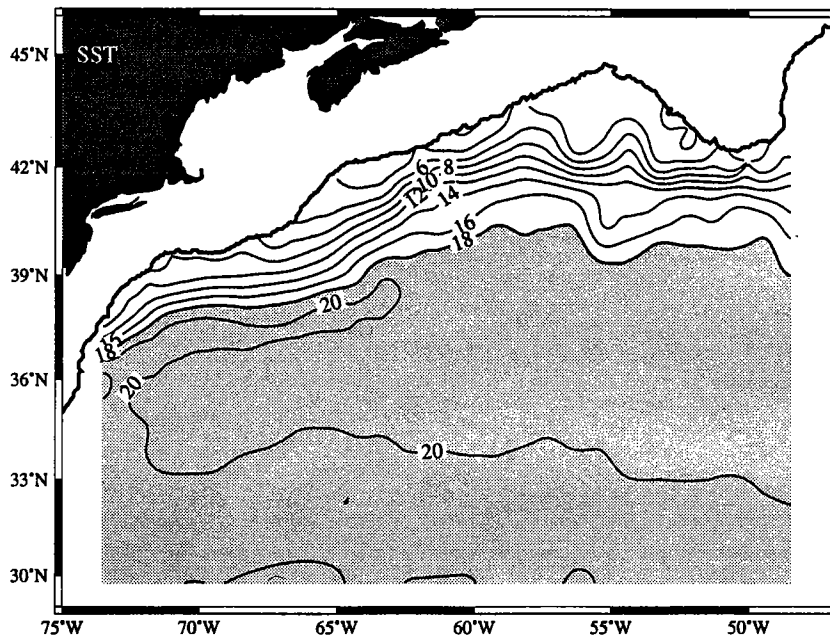
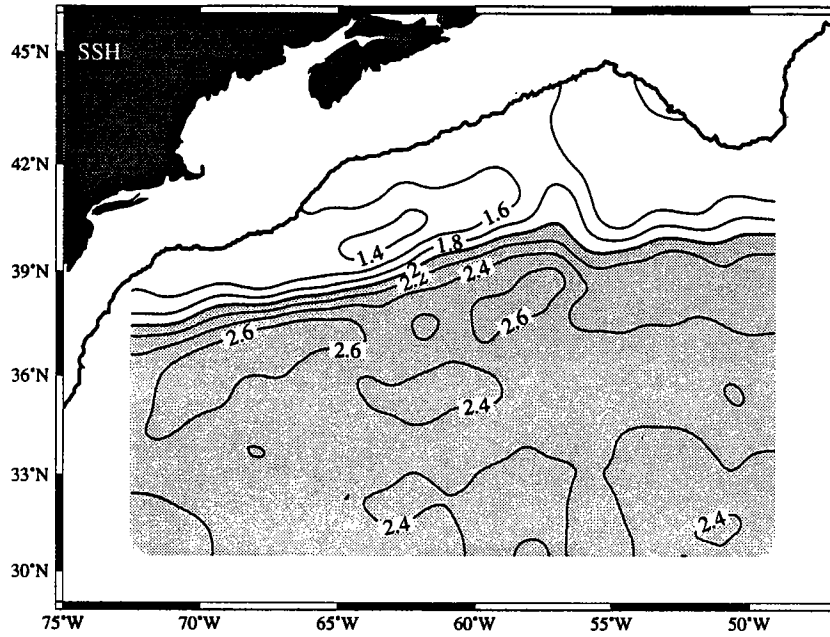


Figure 58: March 1989

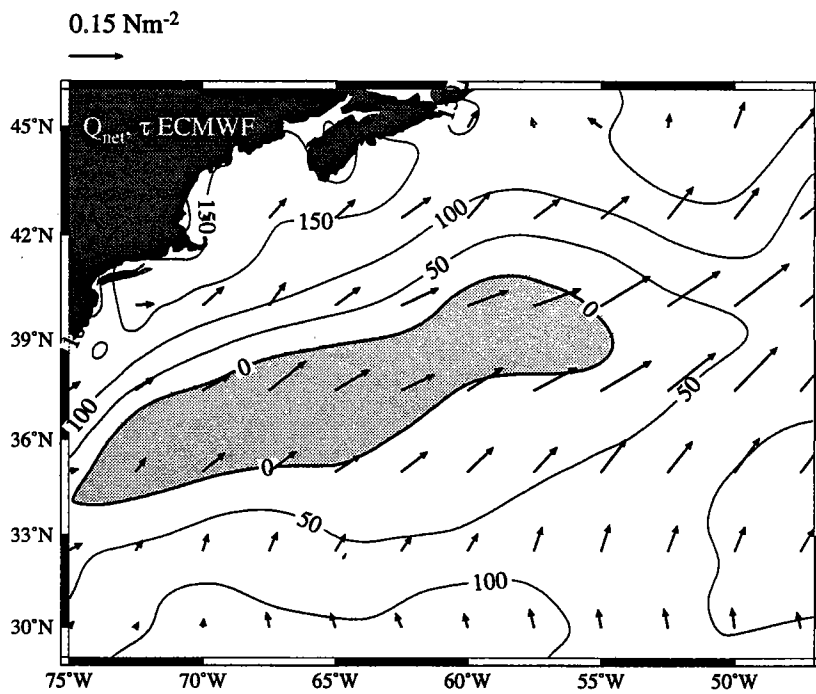
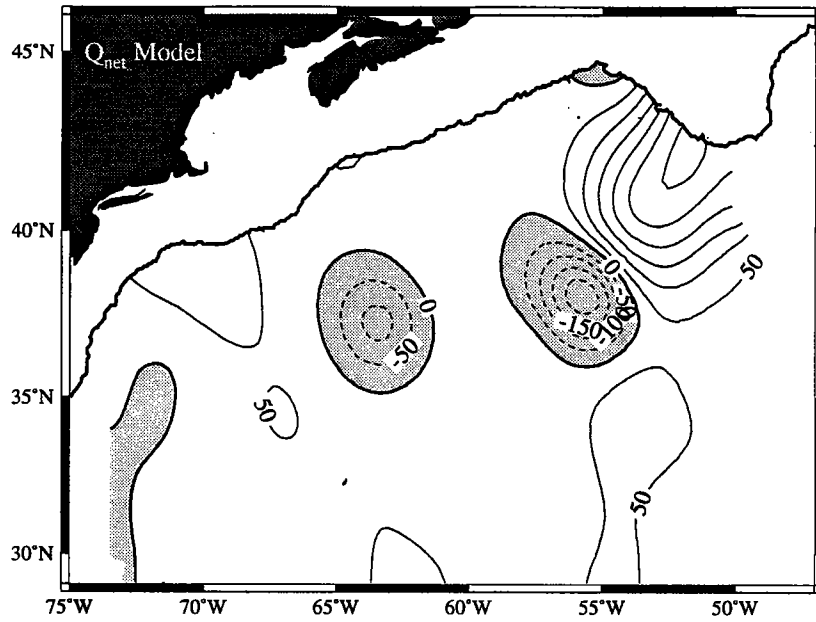


Figure 59: April 1989

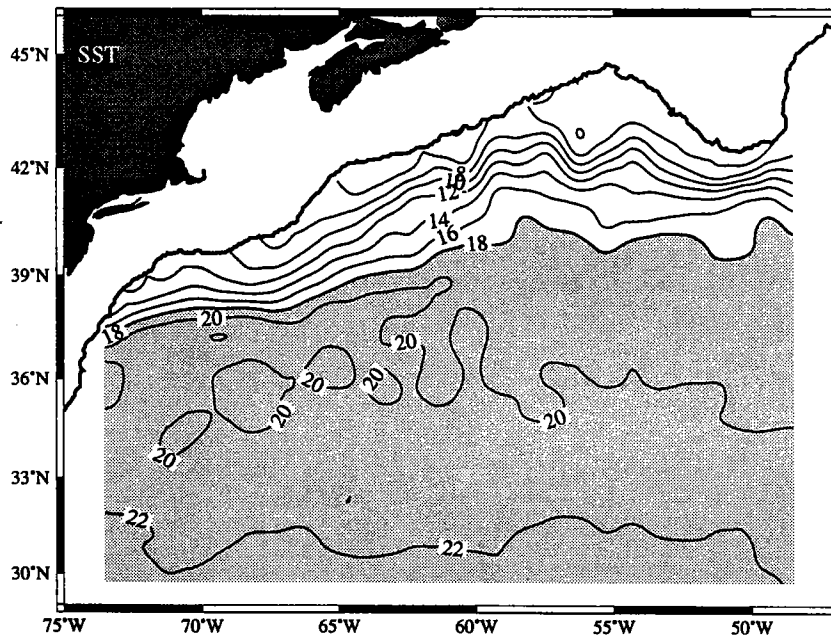
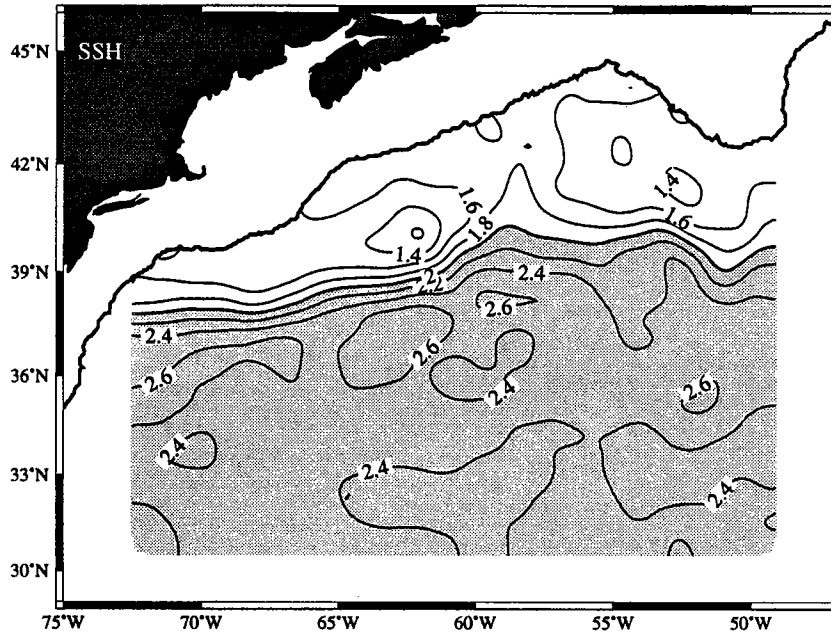


Figure 60: April 1989



## DOCUMENT LIBRARY

*Distribution List for Technical Report Exchange - May 1995*

University of California, San Diego  
SIO Library 0175C  
9500 Gilman Drive  
La Jolla, CA 92093-0175

Hancock Library of Biology & Oceanography  
Alan Hancock Laboratory  
University of Southern California  
University Park  
Los Angeles, CA 90089-0371

Gifts & Exchanges  
Library  
Bedford Institute of Oceanography  
P.O. Box 1006  
Dartmouth, NS, B2Y 4A2, CANADA

Commander  
International Ice Patrol  
1082 Shennecossett Road  
Groton, CT 06340-6095

NOAA/EDIS Miami Library Center  
4301 Rickenbacker Causeway  
Miami, FL 33149

Research Library  
U.S. Army Corps of Engineers  
Waterways Experiment Station  
3909 Halls Ferry Road  
Vicksburg, MS 39180-6199

Institute of Geophysics  
University of Hawaii  
Library Room 252  
2525 Correa Road  
Honolulu, HI 96822

Marine Resources Information Center  
Building E38-320  
MIT  
Cambridge, MA 02139

Library  
Lamont-Doherty Geological Observatory  
Columbia University  
Palisades, NY 10964

Library  
Serials Department  
Oregon State University  
Corvallis, OR 97331

Pell Marine Science Library  
University of Rhode Island  
Narragansett Bay Campus  
Narragansett, RI 02882

Working Collection  
Texas A&M University  
Dept. of Oceanography  
College Station, TX 77843

Fisheries-Oceanography Library  
151 Oceanography Teaching Bldg.  
University of Washington  
Seattle, WA 98195

Library  
R.S.M.A.S.  
University of Miami  
4600 Rickenbacker Causeway  
Miami, FL 33149

Maury Oceanographic Library  
Naval Oceanographic Office  
Building 1003 South  
1002 Balch Blvd.  
Stennis Space Center, MS, 39522-5001

Library  
Institute of Ocean Sciences  
P.O. Box 6000  
Sidney, B.C. V8L 4B2  
CANADA

Library  
Institute of Oceanographic Sciences  
Deacon Laboratory  
Wormley, Godalming  
Surrey GU8 5UB  
UNITED KINGDOM

The Librarian  
CSIRO Marine Laboratories  
G.P.O. Box 1538  
Hobart, Tasmania  
AUSTRALIA 7001

Library  
Proudman Oceanographic Laboratory  
Bidston Observatory  
Birkenhead  
Merseyside L43 7 RA  
UNITED KINGDOM

IFREMER  
Centre de Brest  
Service Documentation - Publications  
BP 70 29280 PLOUZANE  
FRANCE

<b>REPORT DOCUMENTATION PAGE</b>	<b>1. REPORT NO.</b> WHOI-95-05	<b>2</b>	<b>3. Recipient's Accession No.</b>
<b>4. Title and Subtitle</b> Monthly Atmospheric and Oceanographic Surface Fields for the Western North Atlantic: December, 1986 - April, 1989			<b>5. Report Date</b> April 1995
<b>7. Author(s)</b> Michael J. Caruso, Sandipa Singh, Kathryn A. Kelly and Bo Qiu			<b>6</b>
<b>9. Performing Organization Name and Address</b>  Woods Hole Oceanographic Institution Woods Hole, Massachusetts 02543			<b>8. Performing Organization Rept. No.</b> WHOI-95-05
<b>12. Sponsoring Organization Name and Address</b>  The National Oceanic and Atmospheric Administration and the National Aeronautic Space Administration			<b>10. Project/Task/Work Unit No.</b>
<b>15. Supplementary Notes</b> This report should be cited as: Woods Hole Oceanog. Inst. Tech. Rept., WHOI-95-05.			<b>11. Contract(C) or Grant(G) No.</b> (C) NA16RC0468-01 (NOAA) (G) NAGW-1666
<b>16. Abstract (Limit: 200 words)</b>  Monthly atmospheric and oceanographic variables for the western North Atlantic Ocean from various sources are presented as contour or vector maps. These fields were assembled for a study of the upper ocean heat budget. Atmospheric fields include the net surface heat fluxes and wind stress derived from the 1000 mb winds from the European Centre for Medium-range Weather Forecasting (ECMWF). Oceanographic fields include the sea surface height from the Geosat radar altimeter and sea surface temperature from the Advanced Very High Resolution Radiometer (AVHRR). An additional estimate of net surface heat flux is shown; this estimate was derived by assimilating winds, currents and ocean temperatures into a mixed layer model. The maps show a complex interplay of fluctuations in the winds and heat fluxes, and in the structure and temperature gradients of the Gulf Stream system. Some comments are offered on a comparison of the two heat flux estimates.			<b>13. Type of Report &amp; Period Covered</b> Technical Report
<b>17. Document Analysis</b>			<b>14.</b>
<p><b>a. Descriptors</b> heat flux sea surface height wind stress</p> <p><b>b. Identifiers/Open-Ended Terms</b></p> <p><b>c. COSATI Field/Group</b></p>			
<b>18. Availability Statement</b>  Approved for public release; distribution unlimited.		<b>19. Security Class (This Report)</b> UNCLASSIFIED	<b>21. No. of Pages</b> 75
		<b>20. Security Class (This Page)</b>	<b>22. Price</b>